Declassified and Approved For Release 2013/02/27 : CIA-RDP10-02196R000300110005-5

Russian Original Vol. 33, No. 5, November, 1972

May, 1973

SATEAZ 33(5) 1025-1108 (1972)

SOVIET ATOMIC ENERGY

АТОМНАЯ ЭНЕРГИЯ
(ATOMNAYA ÉNERGIYA)

TRANSLATED FROM RUSSIAN

CONSULTANTS BUREAU, NEW YORK

Declassified and Approved For Release 2013/02/27 : CIA-RDP10-02196R000300110005-5

Declassified and Approved For Release 2013/02/27 : CIA-RDP10-02196R000300110005-5

SOVIET ATOMIC ENERGY

Soviet Atomic Energy is a cover-to-cover translation of *Atomnaya Énergiya*, a publication of the Academy of Sciences of the USSR.

An arrangement with Mezhdunarodnaya Kniga, the Soviet book export agency, makes available both advance copies of the Russian journal and original glossy photographs and artwork. This serves to decrease the necessary time lag between publication of the original and publication of the translation and helps to improve the quality of the latter. The translation began with the first issue of the Russian journal.

Editorial Board of *Atomnaya Énergiya:*

Editor: M. D. Millionshchikov

Deputy Director
I. V. Kurchatov Institute of Atomic Energy
Academy of Sciences of the USSR
Moscow, USSR

Associate Editors: N. A. Kolokol'tsov
N. A. Vlasov

A. A. Bochvar
N. A. Dollezhal'
V. S. Fursov
I. N. Golovin
V. F. Kalinin
A. K. Krasin
A. I. Leipunskii
V. V. Matveev
M. G. Meshcheryakov
P. N. Palei
V. B. Shevchenko
D. L. Simonenko
V. I. Smirnov
A. P. Vinogradov
A. P. Zefirov

Copyright©1973 Consultants Bureau, New York, a division of Plenum Publishing Corporation, 227 West 17th Street, New York, N.Y. 10011. All rights reserved. No article contained herein may be reproduced for any purpose whatsoever without permission of the publishers.

Consultants Bureau journals appear about six months after the publication of the original Russian issue. For bibliographic accuracy, the English issue published by Consultants Bureau carries the same number and date as the original Russian from which it was translated. For example, a Russian issue published in December will appear in a Consultants Bureau English translation about the following June, but the translation issue will carry the December date. When ordering any volume or particular issue of a Consultants Bureau journal, please specify the date and, where applicable, the volume and issue numbers of the original Russian. The material you will receive will be a translation of that Russian volume or issue.

Subscription
$75.00 per volume (6 issues)
2 volumes per year
(Add $5 for orders outside the United States and Canada.)

Single Issue: $30
Single Article: $15

CONSULTANTS BUREAU, NEW YORK AND LONDON

227 West 17th Street
New York, New York 10011

Davis House
8 Scrubs Lane
Harlesden, NW10 6SE
England

Published monthly. Second-class postage paid at Jamaica, New York 11431.

Declassified and Approved For Release 2013/02/27 : CIA-RDP10-02196R000300110005-5

Declassified and Approved For Release 2013/02/27 : CIA-RDP10-02196R000300110005-5

SOVIET ATOMIC ENERGY

A translation of *Atomnaya Énergiya*

Volume 33, Number 5

May, 1973

November, 1972

CONTENTS

Declassified and Approved For Release 2013/02/27 : CIA-RDP10-02196R000300110005-5

Declassified and Approved For Release 2013/02/27 : CIA-RDP10-02196R000300110005-5

CONTENTS

(continued)

The Russian press date (podpisano k pechati) of this issue was 10/31/1972. Publication therefore did not occur prior to this date, but must be assumed to have taken place reasonably soon thereafter.

Declassified and Approved For Release 2013/02/27 : CIA-RDP10-02196R000300110005-5

Declassified and Approved For Release 2013/02/27 : CIA-RDP10-02196R000300110005-5

SOVIET ATOMIC ENERGY

A translation of *Atomnaya Énergiya*

May, 1973

Volume 33, Number 5 November, 1972

CONTENTS

Declassified and Approved For Release 2013/02/27 : CIA-RDP10-02196R000300110005-5

Declassified and Approved For Release 2013/02/27 : CIA-RDP10-02196R000300110005-5

CONTENTS

(continued)

The Russian press date (podpisano k pechati) of this issue was 10/31/1972. Publication therefore did not occur prior to this date, but must be assumed to have taken place reasonably soon thereafter.

Declassified and Approved For Release 2013/02/27 : CIA-RDP10-02196R000300110005-5

Declassified and Approved For Release 2013/02/27 : CIA-RDP10-02196R000300110005-5

ON THE OCCASION OF THE EIGHTIETH BIRTHDAY OF ACADEMICIAN DMITRII VLADIMIROVICH SKOBEL'TSYN

The editorial staff of the periodical Atomnaya Énergiya warmly greets Academician Dmitrii Vladimirovich Skobel'tsyn on the occasion of his 80th birthday, and wishes him excellent health, long years of life, and new creative successes.

Translated from Atomnaya Énergiya, Vol. 33, No. 5, p. 882, November, 1972.

© 1973 Consultants Bureau, a division of Plenum Publishing Corporation, 227 West 17th Street, New York, N. Y. 10011. All rights reserved. This article cannot be reproduced for any purpose whatsoever without permission of the publisher. A copy of this article is available from the publisher for $15.00.

Declassified and Approved For Release 2013/02/27 : CIA-RDP10-02196R000300110005-5

Declassified and Approved For Release 2013/02/27 : CIA-RDP10-02196R000300110005-5

ARTICLES

SOME TECHNICAL PRINCIPLES FOR THE INTERNATIONAL CONTROL OF NUCLEAR MATERIALS

V. M. Shmelev

UDC 621.039.54

According to the requirements of the pact reached regarding the halt to the spread of nuclear weapons and regarding the system of guarantees of the International Atomic Energy Agency (IAEA), a technical goal in the IAEA's effort to control nuclear materials is to rapidly detect the conversion of nuclear materials from peaceful uses to the construction of weapons.

This goal can be achieved by three basic guarantee and control methods: by taking inventories of nuclear materials; by conserving materials through the use of appropriate buildings and installations, containers, safes, and technical means such as those involving seals; and by monitoring the state of the materials and the operations in which they are used through the use of instruments (television, photography, etc.) or direct observation by control and inspection personnel.

The control methods are put into operation after an agreement on control is reached between the IAEA and the government. Such agreements are based on the system of guarantees of the IAEA and include four basic control elements: analysis of information about the installations; a registration system at nuclear installations; filing of reports with the IAEA; and inspection of nuclear materials inside and outside installations by the IAEA.

These four elements, which will be included in agreements on guarantees, constitute the legal basis for the application of the control methods. They furnish the basis for the IAEA's acquisition of information necessary for an independent check of nuclear materials.

Here a "check of nuclear materials" means a series of actions and decisions by which the amount and distribution of nuclear materials are determined. Since the results of the control are of considerable importance to the government, the IAEA's determination of the amount of nuclear materials must be free from procedural and arithmetic errors, as free as possible from systematic and random measurement errors, and convincing, i.e., the conclusions reached must be based on evidence which satisfies the governments participating in the control system.

The method of taking an inventory of nuclear materials establishes the quantity and distribution of nuclear materials and the accuracy with which the quantity is determined. Conservation and monitoring methods can be used to determine the location of materials and to reduce the effort and expenditure necessary for inspection, measurement, and analysis of samples. Moreover, the reliability of the inventory method can be increased appreciably by means of observation.

An effective system for controlling nuclear materials requires a judicious use of all three control methods. The current tendency is to consider the inventory method the primary one, supplemented where necessary by conservation and observation methods, particularly when the control is extended to the entire nuclear-energetics fuel cycle of one or several governments.

In the development and application of various technical methods and procedures certain other requirements and limitations, for which there is provision in the pact on the halt to the spread of nuclear weapons and in the system of guarantees of the IAEA, must be taken into account. These technical methods and procedures must not hinder the economic and technological development of industry or international cooperation

Translated from Atomnaya Énergiya, Vol. 33, No. 5, pp 883-888, November, 1972. Original article submitted May 5, 1972.

© 1973 Consultants Bureau, a division of Plenum Publishing Corporation, 227 West 17th Street, New York, N. Y. 10011. All rights reserved. This article cannot be reproduced for any purpose whatsoever without permission of the publisher. A copy of this article is available from the publisher for $15.00.

Declassified and Approved For Release 2013/02/27 : CIA-RDP10-02196R000300110005-5

Declassified and Approved For Release 2013/02/27 : CIA-RDP10-02196R000300110005-5

in the peaceful uses of atomic energy; they must provide for the protection of commercial and industrial secrets and other confidential information; they must be consistent with economic and safe operation of nuclear installations; and they must take into account technological developments which can improve the effectiveness of control methods.

In several specific cases the additional conditions limit the applicability of various technical control methods and procedures. Because of these conditions, there is increasing interest in the maximum use of devices and other technical means in positions most suitable for control.

As the IAEA performs its control function, all nuclear installations and locations at which there are nuclear materials within a country or within a group of countries are divided into "material-balance zones" (MBZ) which satisfy the following requirements:

1. The amount of nuclear material entering and leaving each MBZ must be measured (or determined by some other objective method, e.g., by counting discrete elements or by calculating the uranium consumption and plutonium production in reactions);
2. The actual amount of material in each zone can be measured by a suitable procedure (e.g., by a physical inventory of the material within the MBZ).

The MBZs can be classified into three types.

Type 1 (Production MBZ). Production processes are those in which nuclear materials undergo physical and chemical changes, in which waste products are produced and for which losses may not be determinable. In this case the "registered quantity" (RQ) of material, determined from measurements of materials entering the zone and leaving it, is periodically compared with the "actualquantity" (AQ) of material in the zone, i.e., that actually measured. The difference between the registered and actual quantities of material is called the unaccountable-material factor (UMF), and its analysis is an important element of the method for inventorying nuclear materials in the system of the IAEA guarantees. For this type of zone the material-balance equation can be written as $RQ - AQ = UMF$.

Type 2 (MBAs which Are Stockpiles of Initial Products). These zones include places at which the initial products to be used in an installation are stored, not yet having been incorporated in the production process. In this type of zone the amount of material incident is usually determined from data from the supplier. The amount of material which leaves such a zone is detected by measurements carried out by personnel at the installation (just before the beginning or at the beginning of the treatment of the material). Differences arise between the actual and detected amounts of material in this type of zone because of differences between the measurements made by the supplier and by the personnel of the given installation; the magnitude of this difference is equal to the difference between the measurements of the supplier and those of the personnal at the apparatus (DRS). Since there is generally no waste or loss in this type of zone, the unaccountable-material factor here should usually be equal to the difference between the measurements of the supplier and the recipient; i.e., $RQ - AQ = DRS$.

Type 3 (MBZs in which Finished Products Are Stored; Reactor MBZs). For these zones, the quantities of material which are received and shipped are determined either through measurement of the material received or on the basis of data from the supplier, supplemented by a calculation of the uranium consumption and plutonium production. In this type of zone the registered and actual quantities of material are indistinguishable, and the unaccountable-material factor is assumed equal to zero; i.e., $RQ - AQ = 0$.

Successful use of the inventory method depends to a large degree on the correct choice of zone, the acquisition of the pertinent information regarding the materials entering and leaving each zone (including waste, scrap, etc.) and information about the material in the zone, the possibility of checking the quality of the information received through independent measurements or other objective methods, and analysis of all the information available for each zone and the correctness of the conclusions reached on the basis of this analysis.

A procedure for carrying out the control can be worked out for each zone and for the group of all nuclear installations in a country or in a group of countries. The control process is comparatively simple for zones 2 and 3, since the possibility that large quantities of material will be unaccounted for is extremely slight; for zone 1 however, this process would be extremely difficult. The difficulty involved in this control is more serious in the case in which many zones and installations must be controlled in a country. Here

Declassified and Approved For Release 2013/02/27 : CIA-RDP10-02196R000300110005-5

Declassified and Approved For Release 2013/02/27 : CIA-RDP10-02196R000300110005-5

we will analyze the control of zones of type 1; this type of control is characteristic for treatment of fuel, production of fuel elements, and chemical treatment of the irradiated fuel. A similar sequence of control operations could be used for the other types of zones.

The control process includes four successive stages: acquisition of the raw information, corroboration, and supplementary control operations. The first stage is to acquire the raw information. As was mentioned above, in the system of IAEA guarantees this information can be acquired from data on the construction of the installations, from reports and documents supplied, and from independent checks during inspections.

Data on the construction of installations is furnished by the operator when agreement is reached on control. A list of the information which must be supplied to the IAEA on the various types is given in an appendix to the control agreement between the government and the IAEA. Operators of the installations are obliged to furnish the inspectors with documents on the amounts of nuclear materials, their use, treatment, and storage at the installation. It is expected that in all cases the records kept at the installation for operating purposes will also be adequate for guarantee and control purposes. In addition, the operators of the installations must furnish the IAEA with: 1) information on the change in the amount of material at an installation after each receipt or shipment of material; 2) information on the material balance at the installation after each physical inventory; and 3) special reports on significant deviations from normal operation of the installations which might lead to a loss of nuclear materials.

The information acquired from these reports on changes in the quantities of materials, supplied to the control organization by the operator of the installation, is used to calculate the amount of material in the MBZ and to construct a summary of the registered amounts of materials at an installation and the measurement error; the uncertainities in the determination of the amounts of these materials become control parameters until the next routine physical inventory of materials at the installation. If the uncertainty in the determination in the amount of material registered exceeds a control limit, a special physical inventory of the materials in the zone must be carried out.

The periodic summary thus is used to determine times at which physical inventories are necessary. In addition, the information included in this summary, calculated on the basis of reports filed regarding the changes in amounts of material at an installation and the reports of the inspectors, constitutes the raw data for comparison and analysis of the exchange of materials among the various MBZs.

The changes in the amounts of materials and exchange of materials will be calculated and analyzed at IAEA by a high-speed computerized system for storing, analyzing, and seeking information.

The system of reports is very important for controlling materials for developing and using an overlapping-control procedure for an interlocked system of installations. An important part of this system is a system of reports on changes in the amounts of the materials; these reports must be standardized in terms of reporting intervals and report contents. If these reports are furnished promptly, a whole series of interrelated checks on the amounts of materials shipped and received and on the amounts of materials on hand can be instituted.

Data measured by the shippers and receivers of nuclear materials can be used for running estimates of the capabilities of the measurements and to generate continuous information on the quantities of materials in being transported between installations. A comparative analysis of the information on the materials in the entire system under control will allow the controlling organization to determine when and where inspections should be carried out and which control methods should be used for the most rational and effective control of the entire system.

The data on an installation furnished in the reports can be checked during inspection by sampling the data of the operator on the basis of ordinary methods of statistical analysis. A check of the data in reports in this stage consists primarily of an arithmetic check of the calculations carried out by the personnel of the installation to verify that the final data in the reports regarding changes in the amounts of the materials actually correspond to the initial data found from the measurements. In this manner the correctness of the report system is checked; i.e., a check is made to see that there are no arithmetic or procedural errors or misprints. Analysis of these results and of the delays involved in furnishing the reports is the basic method for checking the reliability of the report system for a given installation.

Declassified and Approved For Release 2013/02/27 : CIA-RDP10-02196R000300110005-5

Declassified and Approved For Release 2013/02/27 : CIA-RDP10-02196R000300110005-5

If the report system at some installation does not meet the requirements of the control organization, it would be necessary for the control and inspection personnel to intensify their efforts in order to eliminate the errors in the reports, and it would be necessary to carry out more independent measurements at the given installation.

Control of nuclear materials based on independent measurements of the quantities of nuclear materials entering and leaving an MBZ and measurements of the actual quantities of materials in the zone, carried out by the controlling organization, is the most important element of the international system of guarantees. Two different systems of measurements can be used here.

In the first system, all quantities of materials entering and leaving an MBZ and the actual quantities on hand are measured and recorded by the personnel of the installation and reported to the controlling organization in the pertinent reports. The inspector checks these measurements by sampling measurements, calibrations, and other methods, including observation of the activities of the personnel; the inspector accepts the data furnished by the personnel of the apparatus on the balance of control materials if the repeated measurements and the checks are consistent within the measurement accuracy.

In the second system, the measuring instruments at the installation used for operational control are constantly monitored by the inspectors and are periodically calibrated either by the inspectors or at least in their presence. The same measurement results are used by the personnel of the installation and by the inspectors, so measurements are not repeated by the inspectors. In this case, however, the construction of the installation and the instruments with which it is equipped must meet the observation and calibration requirements of the controlling organization.

Both systems have certain advantages and certain disadvantages from the point of view of guarantees, and both will be used: the first to control existing installations and the second to control future installations, in which a provision should be made for instruments for both operational control and for control carried out for guarantee purposes.

The systematic errors involved in the measurement methods used and the imperfections of the calibrations will usually be the primary reasons for a large unaccountable-material factor. The development of a system of calibration standards and a program for exchanging samples for mutual checks and measurements should aid the personnel of the installation and of the controlling organization in improving calibration methods and in reducing the discrepancies in the measured results due to systematic errors.

An inspector usually checks the quantities of materials at an installation during the physical inventory by the personnel of the installation. The inspector can carry out sample measurements of the materials at the installation and compare the results with those furnished by the personnel of the installation, and the inspector can monitor the calibration of the instruments and the measurements by the installation personnel. In this manner, it is determined how much material is physically present at the installation at the given time; this result is compared with the detected amount of material, calculated from the amounts of materials shipped and received over a certain period (with losses taken into account). The difference between the actual and detected amounts yields the unaccountable-material factor, defined above. If this factor lies within an acceptable range for the given type of installation (i.e., if it does not exceed the limits of the control level set), the check is ended. If, on the other hand, the factor does exceed the control level set, additional control actions will be required to determine the reasons for the appearance of the large factor.

A large unaccountable-material factor may result from an imperfection in the measurement system used. Accordingly, the first step is to carry out a supplementary analysis of the measurement procedures and results to determine the reasons for the large errors or to carry out more accurate supplementary measurements.

If an unaccountable-material factor exceeding the set control level cannot be explained after this supplementary analysis of the measurement errors, the most probable reason is that the material is "hidden" at various points in the installation in which it is used (on the walls of vessels, pipes, etc.) and thus cannot be taken into account by ordinary measurements. In this case the equipment involved must be thoroughly washed and cleaned, or additional measurements with special instruments must be carried out to determine the amounts of hidden materials. It is thus important to acquire factual information about the tendency for hidden materials to accumulate at various types of installations and about the amounts of materials involved.

A large unaccountable-material factor, exceeding the control level set, could be caused by unmeasured material losses which could occur either during normal or abnormal operation of an installation.

Declassified and Approved For Release 2013/02/27 : CIA-RDP10-02196R000300110005-5

Declassified and Approved For Release 2013/02/27 : CIA-RDP10-02196R000300110005-5

The possible mechanisms for and the extent of these losses must be analyzed by the controlling organization when the construction of an installation is being checked before control has begun as well as periodically, during the control operations. It may be necessary to use additional control instruments for the liquid and gaseous waste and other effluents, to detect low leakage rates from the vessels and pipes, etc.

If all these checks fail to explain why the unaccountable-material factor exceeds the control level set, it can be stated that there is a large, unexplainable material loss at the installation.

It is important to note that this process of checks can only reveal the possibility of an illegal diversion of material by eliminating all other possible explanations for the material loss. There is still no direct evidence that the nuclear materials have been diverted for some illegal purpose. This conclusion could be reached only after an additional analysis of all the quantitative and qualitative factors and other information at the disposal of the controlling organization.

Conservation and observation methods are also important, in addition to the methods used to calculate and analyze the material balance

There are two ways to conserve nuclear materials. The first is based on the use of safes, seals, and other means to restrict the mobility of nuclear materials; to restrict the accessibility of these materials to the personnel at an installation; and to limit the opportunity for manipulation of materials (e. g., by means of gates, valves, samplers, etc.). These means can be used to supplement the observation method if an inspector is not available for continuous observation. In addition, these methods reduce the need for additional measurements after storage materials. The second method is to use structural features of the building, enclosures, and parts of the apparatus to minimize the number of entrances and exits; all entrances and exists are controlled in order to conserve the materials.

The primary advantage of the conservation method is that it can be used to detect attempts to divert nuclear materials. It is also more efficient than a method based on measurements or the presence of an inspector. A disadvantage of this method is that it is impossible to determine whether material has been lost when a conservation device is destroyed in the absence of an inspection (e. g., in an emergency or for some other pertinent reason). All conservation methods should thus be strengthened by provision allowing physical inventory of the material. In other words, the use of this method increases the allowable time between physical inventories, but it does not eliminate the need for these inventories.

Observation can be carried out by means of suitable instruments and by direct observation by control and inspection personnel. The use of this method improves the reliability of the determination of amounts of materials, since direct observation of the motion of these materials, direct verification of their presence, observation of the measurement procedure, etc., become possible. The result is to strengthen the conclusions reached regarding the balance of materials. Of particular importance here is direct observation by the control and inspection personnel of the calibration of scales and observation of the indications of the measuring instruments. This method also allows a more realistic evaluation of the validity of the operator's reports regarding material loss during abnormal operation and for other reasons. Experience shows that measured results can be explained and reports checked only if knowledge is available about the actual situation at the installation.

Physical guarding of the materials plays an important role in the system of guarantees and control. The measures involved here are the use of enclosures, signals, guard stations, etc., and measures designed to prevent the removal of materials from an installation, from warehouses, or in transport. Guarding the materials is the responsibility of the government. The role of the IAEA here is restricted to developing international standards for physically guarding materials and assisting the participating governments in institution of a program of scientific and technological development of IAEA guarantees, including systems and operational analysis of the guarantees, development and institution of analytic methods, instruments, and other technical means for measuring and controlling nuclear materials, will lead to the adequate control by the IAEA which is required by the agreement regarding the halt to the spread of nuclear weapons.

Declassified and Approved For Release 2013/02/27 : CIA-RDP10-02196R000300110005-5

Declassified and Approved For Release 2013/02/27 : CIA-RDP10-02196R000300110005-5

HYDRAULIC RESISTANCE WITH LONGITUDINAL STREAMLINE FLOW FOR BUNDLES OF PLAIN AND FINNED RODS

V. I. Subbotin, B. N. Gabrianovich, and A. V. Sheinina

UDC 621.039.5/6

This paper is devoted to the study of hydraulic resistances in rod bundles. Analysis of the data on the measurement of the coefficients of friction in bundles of plain rods is carried out in [1]. Upon considering the experimental results, it was observed that the course form influences the hydraulic resistance of the rod bundles. The opinion has been expressed that rod bundles, possessing a course with figured rotating pistons, have a greater resistance than tube bundles surrounded by a plane hexahedral course (with S/d = idem). It is also observed that the different hydraulic resistances for these two types of bundles increases with an increase in the bundle spacing.

For the investigation of the effect of the course forms on the friction coefficients for the rod bundles, experiments were conducted on rod bundles with S/d = 1.5. Measurements of the friction coefficients were conducted in four operating regions, in which the same lattice, rods, and tubes were used. The course and number of rods were changed in the models. The dimensions of the course were chosen in a manner such that one ensures the equality of the hydraulic diameters for the model and an "infinite" mesh ($d_\Gamma = d_{\Gamma\infty}$). The maximum difference between d_h and $d_{\Gamma\infty}$ was ~8%.

The experiments were conducted with the usual procedure in a hydraulic test bed. The maximum relative error in the measurement of the hydraulic resistance coefficients was 7-10%.

As is seen from Fig. 1, the difference in the friction coefficients for the investigated bundles with S/d = 1.5 is found within the limits of experimental accuracy. The experiments, conducted on four bundles with S/d = 1.5, having different courses, showed that the course form easily affects the value of the friction coefficient for an extended bundle when the dimensions and course are chosen so that $d_\Gamma \approx d_{\Gamma\infty}$. The

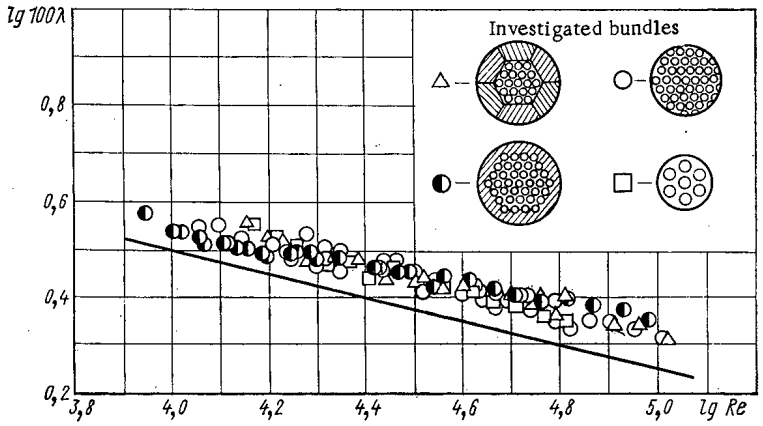

Fig. 1. Friction coefficients for bundles of plain rods with S/d = 1.5. Straight line represents calculations based on the Blasius equation ($\lambda_0 = 0.316\ Re^{-0.25}$).

Translated from Atomnaya Énergiya, Vol. 33, No. 5, pp. 889-892, November, 1972. Original article submitted December 9, 1971; revision submitted March 28, 1972.

© 1973 Consultants Bureau, a division of Plenum Publishing Corporation, 227 West 17th Street, New York, N. Y. 10011. All rights reserved. This article cannot be reproduced for any purpose whatsoever without permission of the publisher. A copy of this article is available from the publisher for $15.00.

Declassified and Approved For Release 2013/02/27 : CIA-RDP10-02196R000300110005-5

Declassified and Approved For Release 2013/02/27 : CIA-RDP10-02196R000300110005-5

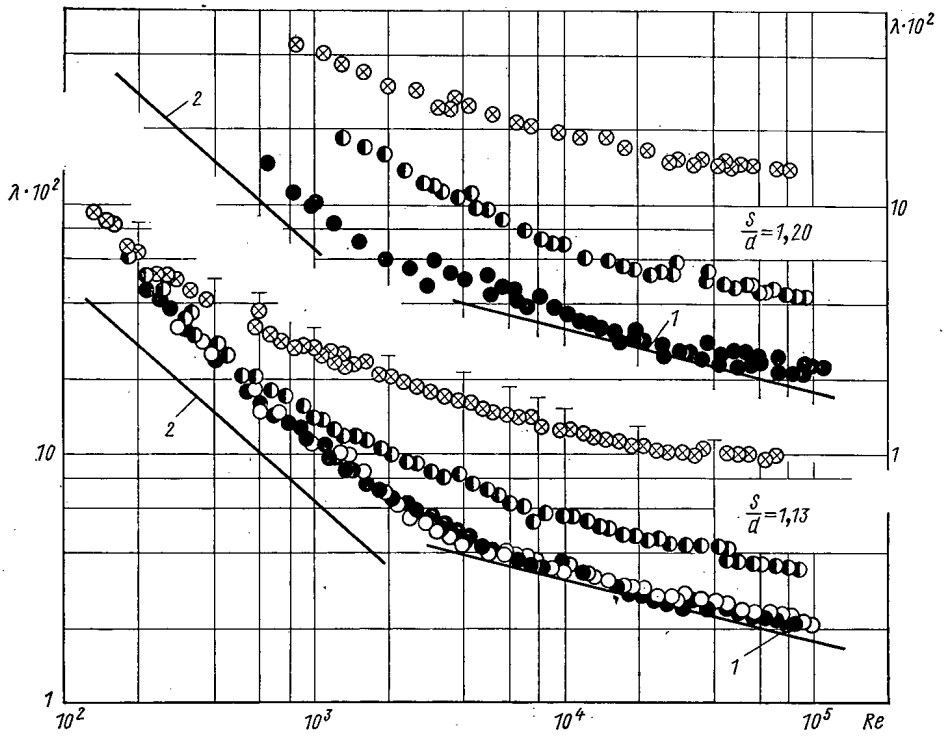

Fig. 2. Hydraulic resistance coefficients for finned bundles.

difference, noted before [1], between the friction coefficients for rod bundles with figured rotating pistons and those with a plane hexahedral course was, evidently, due to the fact that the results in [2-4], which, as more recent studies have shown, are overestimated, were used in the analysis of the experimental data. In these papers, the experiments were conducted on models with figured rotating pistons.

As a result of the analysis of the experimental data, an empirical formula for the calculation of the friction coefficients for bundles of plain rods in a triangular lattice for which $1 < S/d < 1.5$, in the presence of a turbulent liquid flow, is obtained:

$$\lambda/\lambda_0 = 0.6 + 0.6\,(S/d - 1)^{0,2}. \qquad (1)$$

This equation well approximates the results of the present paper and describes, with an accuracy of ±10%, most of the experimental data considered by other authors.

At the present time, the most common method for spacing the rods is the spiral fin. When the spiraling of the spacing fins is present on the surface of the rod, the fin length equals the minimum distance between the rods (S−d) or half of this distance (S−d)/2. In the first case, contact occurs "fin to casing," in the second, "fin to fin." In the present paper, the results of the measurements of the hydraulic resistance coefficients for finned bundles, in which the spacing of the rods is achieved by "fin to fin" contact, are considered.

Detailed studies were conducted on finned bundles with S/d = 1.05 [1]. The effect of the spacing of the spiraling of the fins and their number on the value of the hydraulic resistant coefficient for a finned bundle (λ_f) was studied. It is shown that for bundles with S/d = 1.05, the deviation of λ_f, when the spaces of the spiraling $T/d > 20$, from the friction coefficients for plain bundles occurs within the limits of experimental accuracy. With a decrease in the spacing of the fins from 20 to five, the value of the resistance coefficients increases more than two times. The experiments also confirmed that an increase in the number of fins from two to four (when $20 \leq T/d \leq 100$) does not affect the value of the hydraulic resistance coefficients.

In the present paper, the systematic studies of the hydraulic resistances for finned bundles, commenced earlier [1], are extended. The measurements of the hydraulic resistance coefficients are conducted on rod bundles with a triangular lattice spacing of 1.13 and 1.20 when the fin spacing is 21.4, 10, and 5 (Fig. 2). In this same figure, the straight lines for cylindrical tubes are cited for comparison: line 1, calculated from Blasius' formula, and line 2, calculated from the formula

Declassified and Approved For Release 2013/02/27 : CIA-RDP10-02196R000300110005-5

Declassified and Approved For Release 2013/02/27 : CIA-RDP10-02196R000300110005-5

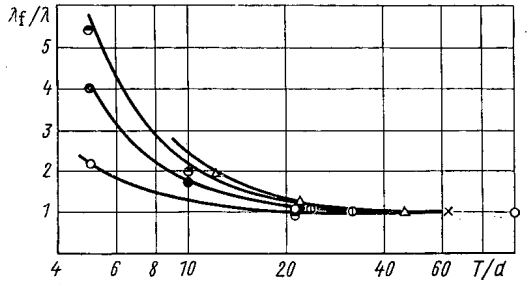

Fig. 3

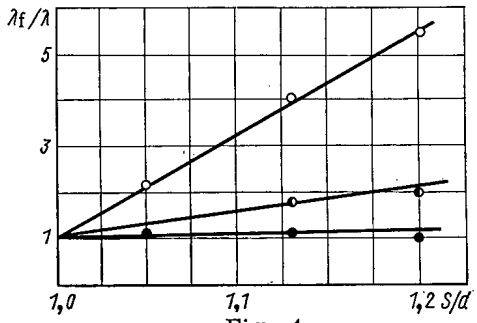

Fig. 4

Fig. 3. Dependence of the hydraulic resistance coefficients for finned bundles on the spiraling interval for the fins: ○) calculated from formula (4) for S/d = 1.05, m = 4 [1]; ●) S/d = 1.13, m = 4; ◓) S/d = 1.20, m = 4; Δ) S/d = 1.23, m = 3 [6]; ⊙) S/d = 1.10, m = 2 [1]; ×) S/d = 1.15, m = 4 [1].

Fig. 4. Dependence of hydraulic resistance coefficients for finned bundles on the bundle spacing S/d. T/d equals: ○) 5; ◐) 10; ●) 21.4.

$$\lambda = \frac{64}{\mathrm{Re}} . \qquad (2)$$

From the figure, it follows that the hydraulic resistance coefficients for a finned bundle with S/d = 1.13 and T/d = 21.4, under turbulent fluid flow conditions ($\mathrm{Re} > 10^4$), coincide, in practice, with the friction coefficients for a plain bundle with the same S/d. For a bundle with T/d = 10, the ratio $\lambda_f/\lambda \approx 1.8$ for T/d = 5, the resistance coefficients for a bundle with finned tubes are approximately four times greater than for a bundle with plain tubes.

From experimental results, the approximate critical Reynolds numbers for the bundles investigated, with S/d = 1.13, were found to be about 800, 500, and 200 for T/d equal to 21.4, 10, and 5, respectively. The passage from laminar to turbulent flow conditions in a bundle of tubes, with and without fins, when T/d = 21.4, commences at the same critical Reynolds number ($\mathrm{Re}_{cr} \approx 800$). This verifies the fact that fins with a spiraling interval greater than 20 easily agitate the fluid flow.

For the calculation of the friction coefficients in bundles of finned tubes with S/d = 1.13, under laminar fluid flow conditions, one obtains the empirical equation

$$(\lambda_f/\lambda)_l = 1 + \frac{1.7}{T/d} . \qquad (3)$$

For tube bundles with S/d = 1.2, the experiments were conducted in the intermediate and turbulent fluid flow regions (see Fig. 2). As was the case for a bundle with S/d = 1.13, along with a large spiraling interval for the fins (T/d = 21.4), the effect of the fins on the hydraulic resistance coefficients in the turbulent fluid flow region is unimportant and occurs within the limits of experimental accuracy. With a decrease in the spiraling interval for the fins, the hydraulic resistance coefficients for a finned bundle (S/d = 1.2) increase. In this case, the increase in the resistance coefficients in finned bundles, in comparison with a plain bundle, comprises $\lambda_f/\lambda \approx 1.9$, for T/d = 10 and $\lambda_f/\lambda = 5.4$ for T/d = 5. The data for a plain bundle with S/d = 1.2, obtained by us earlier [5], was used for determining λ_f/λ. Let us compare these results with the known data of other authors for finned bundles with "fin to fin" contact.

In order to analyze the experimental data for the determination of the hydraulic resistance coefficients in finned bundles, we shall examine the quantity λ_f/λ. Let us assume that λ is the friction coefficient for a plain bundle with the same S/d, but that it is the resistance coefficient for a finned bundle, with a large spiraling interval for the fins (T/d > 30), where the data for a plain bundle is not applicable.

Let us examine Fig. 3, in which the results of the measurements of the hydraulic resistance coefficients for finned bundles, obtained in [1,6], are presented, as well as the results of the present paper for turbulent fluid flow conditions. All the experimental data is represented in λ_f/λ–T/d coordinates for a fixed S/d.

From Fig. 3, it follows that the hydraulic resistance coefficients for finned bundles are slightly dependent on the spiraling interval for the fins when T/d > 30. The decrease in the spiraling interval in the

Declassified and Approved For Release 2013/02/27 : CIA-RDP10-02196R000300110005-5

Declassified and Approved For Release 2013/02/27 : CIA-RDP10-02196R000300110005-5

$T/d < 30$ region results in a marked increase in the resistance coefficients for finned bundles. With an increase in S/d, the degree of the effect of the spiraling interval for the fins on the value of the hydraulic resistance coefficient is increased. From an analysis of the experimental results, it is established that with a constant relative interval of spiraling for the fins, a linear dependence of λ_f/λ on the bundle spacing or, what amounts to the same, on the fin length, is observed (Fig. 4).

As a result of the processing of the experimental data, there was obtained the empirical formula

$$\frac{\lambda_p}{\lambda} = 1 + \frac{600}{(T/d)^2}(S/d - 1), \tag{4}$$

from which one can calculate the hydraulic resistance coefficients for finned bundles under turbulent fluid flow conditions ($10{,}000 \leq Re \leq 100{,}000$). Equation (4) reproduces well the experimental data in the present paper (S/d equals 1.13 and 1.2) and the results in [1,5] for S/d equal to 1.05 and 1.23, respectively.

LITERATURE CITED

1. A. V. Sheinina, in: Liquid Metals [in Russian], Atomizdat, Moscow (1967), p. 210.
2. P. Miller et al., AIChE J., 2, No. 2, 226 (1956).
3. V. I. Subbotin et al., At. Énerg., 9, 308 (1960).
4. E. V. Firsova, Inf.-Fiz. Zh., No. 5, 17 (1963).
5. V. I. Subbotin et al., Symposium of the Economical Mutual Aid Council, "Status and outlook for the production of mobile power plants with fast neutron reactors" [in Russian], Vol. 2, Obninsk (1967), p. 529.
6. P. I. Puchkov and O. S. Vinogradov, Trudy TsKTI, No. 82, 135 (1968).

Declassified and Approved For Release 2013/02/27 : CIA-RDP10-02196R000300110005-5

Declassified and Approved For Release 2013/02/27 : CIA-RDP10-02196R000300110005-5

EXPERIMENTAL INVESTIGATION OF AVERAGED CHARACTERISTICS OF TURBULENT FLOW IN CELLS OF ROD PACKS

Yu. D. Levchenko, V. I. Subbotin, and P. A. Ushakov

UDC 621.039.5/6:532.517.4

Most of the known experimental studies of the fluid dynamics in packs of rods are carried out in order to obtain data on the coefficients of friction [1]. Only some isolated investigations are devoted to the measurement of local characteristics of the flow. For example, hydraulic losses and the velocity field in a channel, simulating a cell of a triangular lattice of rods with s/d = 1.015, have been measured in [2]. Rather overestimated values of the coefficients of friction and limited information on the velocity distribution make it difficult to use these data in practice. While conducting the experiments the authors came to know of [3], in which the velocity profiles in packs with s/d equal to 1.05, 1.1, 1.15 have been measured.

Considering the importance of the knowledge of local hydrodynamic characteristics in packs of rods for the development of computational methods and for direct use in the development of reactors with rod-type fuel elements the authors continued the investigations, the first stage of which (dense packing of rods) was discussed in [4,5]. The profiles of the tangential stresses on the rods and the velocity fields in channels, representing two adjacent cells of triangular lattice of rods with s/d equal to 1.05, 1.1, 1.2 (Fig. 1), were measured in experiments with air. In contrast to the cells of an infinite lattice the channels are closed along the perimeter. Thick-walled stainless steel tubes, which had been heat-treated beforehand, were used for preparing these channels. Sections of these tubes were separated by four plates which were welded in a discontinuous joint. Quick-drying plastic (butacryl) was used for the final hermetic sealing. With this technology of preparation of the area of the transverse sections of the channels the departure from the computed values at different lengths was less than 1%, which was disregarded in the analysis of the experimental data. The basic dimensions of the channels are given in Table 1. In contrast to the data of [3] these channels had 4-6.5 times larger flow cross sections. This made it possible to measure the local characteristics of the air flow in greater detail and more accurately.

TABLE 1. Basic Dimensions of Experimental Channels and Some Results of Measurements

s/d	1,05	1,1	1,2
$R=\frac{d}{2}$, mm	$51^{-0,025}$	$51^{-0,025}$	$40,1^{-0,025}$
$d_{l.c.}$, mm	20,68	30,23	37,57
$d_{h\infty}$, mm	22,00	34,02	47,13
L/d_{LC}	164	113	91
$\bar{u}_C$, m/sec	29,56	21,32	13,35
$\bar{u}_I$, m/sec	30,78	21,79	13,93
$\bar{u}_\infty$, m/sec	30,96	22,16	14,07
u_C^m, m/sec	38,33	27,12	16,30
u_∞^m, m/sec	40,21	27,82	17,00
$Re_C \cdot 10^{-3}$	41,8	42,7	34,8
$Re_\infty \cdot 10^{-3}$	46,6	50,7	44,7
λ_C/λ_{tu}	0,890	0,946	0,985
$\lambda_\infty/\lambda_{tu}$	0,920	0,995	1,085

Note: R = d/2) the radius of curvature of the perimeter; d) the equivalent hydraulic diameter; L) the length of the channel; $\bar{u}$) the average velocity; u^m) maximum velocity; λ) coefficient of friction; $Re = ud_h/\nu$) Reynolds number; Subscripts c) channel; i) i^{th} cell(i = I, II, III); ∞) infinite lattice of rods; φ) a given angle; tu) tube.

Cells of type I in Fig. 1 correspond to those of a regular infinite lattice of rods. In order to estimate the effect of the separating plates on the velocity field in these cells the problem of laminar flow of a fluid was solved by electrical analog method using an electrically conducting paper. It was found that this effect is practically nonexistent.

The experiments were conducted on an equipment with air flow up to 10,000 m^3/h at a thrust up to 1000 mm H_2O col. The flow of air was regulated by throttling. The

Translated from Atomnaya Énergiya, Vol. 33, No. 5, pp. 893-899, November, 1972. Original article submitted December 9, 1971.

© 1973 Consultants Bureau, a division of Plenum Publishing Corporation, 227 West 17th Street, New York, N. Y. 10011. All rights reserved. This article cannot be reproduced for any purpose whatsoever without permission of the publisher. A copy of this article is available from the publisher for $15.00.

Declassified and Approved For Release 2013/02/27 : CIA-RDP10-02196R000300110005-5

Declassified and Approved For Release 2013/02/27 : CIA-RDP10-02196R000300110005-5

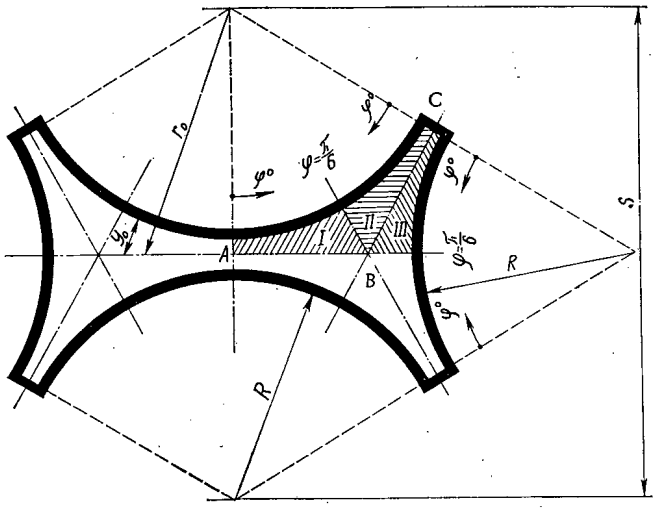

Fig. 1. Diagram of the experimental channel.

temperature and the excess pressure of air were measured at the points of installation of the throttle flow meter and the experimental channel, and also in the place of the equipment. The entrance section of the channels having sharp edges was introduced inside a pipe up to 400 mm. Thus conditions of input close to those for input from a large volume were obtained.

The local tangential stresses at the wall were determined by Preston's method [6] with the use of the calibration relation obtained by the authors in [5]. Preston tubes had outer diameter of 0.6-1.2 mm and the ratio of the inner to outer diameter ~0.6. The coefficients of friction of the channels were determined both from the tangential stresses on the wall and from the pressure gradients along the channel measured with 13 bleeds 0.6 mm in diameter. The first bleed was made at a distance of 1035 mm from the entrance; the distance between the bleeds was 180 mm.

The local velocities of air were measured by Pitot glass tubes of 0.2-0.3 mm diameter, which were displaced by a coordinate device along the normal to the walls into the section recessed to 5 mm from the exit end of the channel. The Pitot tubes were connected to glass differential manometers with spirit filling. One elbow of the differential manometers opened into the atmosphere. Thus the tubes measured the dynamic head with an accuracy up to the pressure drop over a length of 5 mm, which was taken into consideration in the analysis. The local averaged velocity of air was thus determined as:

$$u = \frac{1}{1+0.5\sum_{1}^{3}\sigma_j^2}\sqrt{2gh\,\frac{\gamma_{sp}-\gamma}{\gamma}},$$

where h is the dynamic head, γ_{sp} and γ are specific weights of spirit and air, g is acceleration due to gravity, and $\sigma_j = \sqrt{\overline{(u'_j)^2}}/u$ is the intensity of the velocity fluctuations computed according to the procedure of Bobkov et al. [7] for the main section of the air flow and from the data of Laufer [8] for boundary layers. The corrections for turbulence reached 2-3% near the wall and decreased with the increase of the distance from the wall. Corrections smaller than 0.5% were disregarded.

The effect due to the compressibility of air was negligibly small (+ 0.2%). The effect of the nonuniformity of the static pressure along the cross section of the channels was also insignificant [$\Delta p/(0.5\rho u^2) \approx 0.005$, where ΔP is the difference of pressures at the wall and in the air flow, ρ is the density of air]. The disregarding of these two effects is all the more justified, as they are of opposite sign. Close to the wall the "effect of displacement" of the geometrical center of Pitot tube was taken into consideration and for the true distance from the wall the value

$$y_{true} \approx (y_{meas} + 0.15 d_{tu}),$$

where d_{tu} is the external diameter of the tube, was used.

Due to the symmetry of the air flow, which was checked by measurements of the velocity profiles at the the axes of symmetry of the channels, the main investigations were carried out for a quarter of the cross section of each channel (for cells I, II, III). Some results of the measurements are given in Table 1.

Declassified and Approved For Release 2013/02/27 : CIA-RDP10-02196R000300110005-5

Declassified and Approved For Release 2013/02/27 : CIA-RDP10-02196R000300110005-5

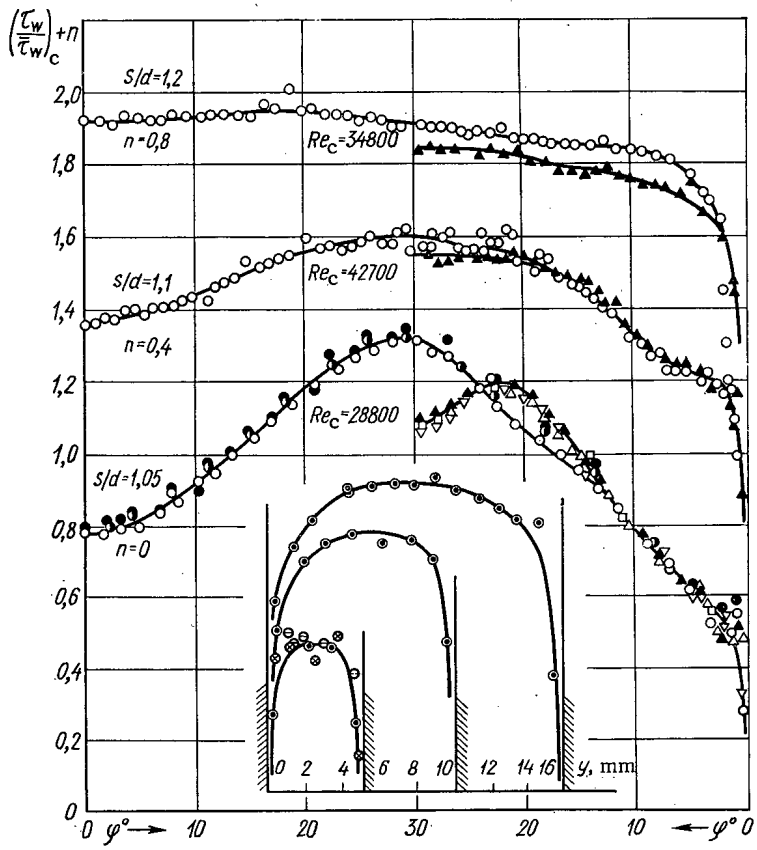

Fig. 2. Distributions of tangential stresses along the perimeter of the channels: ○, ◑, ●) for cells of type I and II; ▽, △, □, ▲) for cells of type III; ⊖, ⊗, ⊙) for separating plates.

The distributions of the relative tangential stresses at the walls of the channels are shown in Fig. 2. In the present case $(\tau_w)_c$ is the tangential stress averaged over the entire perimeter of the channel. For cells of type I a displacement of the coordinates of the maximum tangential stress is observed. A still larger displacement is noticed in type III cell, especially for s/d = 1.05. In order to eliminate doubts about the correctness of the obtained results the tangential stresses were measured over a larger part of the entire perimeter of the channel with s/d = 1.05. In Fig. 2 the values of $(\tau_w/\bar{\tau}_w)_c$, obtained for the symmetric parts of the perimeter, are denoted by different points. The agreement of the data for different, but symmetric parts of the perimeter indicates the reliability of the effect of deformation of the tangential stress profiles at the walls of the channels. As will be shown later, the reason for this effect lies in the specific behavior of the secondary flow, caused by the presence of the longitudinal separating plates.

The profiles of tangential stresses in cell I for different Reynolds numbers are compared in Fig. 3. In this case $(\bar{\tau}_w)_I$ is the mean-interval value of the tangential stress on the wall of cell I. As in [5], the profiles of the nondimensional tangential stresses have a relatively weak dependence on Reynolds number. The distributions of the tangential stresses for an infinite lattice of rods $(\tau_w/\bar{\tau}_w)_\infty$ are obtained by extrapolation of the data for cell I taking into consideration the condition $d/d\varphi(\tau_w/\bar{\tau}_w)_I = 0$ for $\varphi = 30^\circ$. This method is based on the following arguments. Experiments with densely packed rods gave a monotonic variation of the tangential stress along the perimeter of the cell [5], although the conditions of appearance of secondary flows in the fluid were more favorable than in regular cells of separated packs of rods [9, 10]. It can be assumed that in separated packs the tangential stress profiles must be all the more monotonic. Thus the extrapolation presented in Fig. 3 is essentially a method for eliminating the effect of separating plates in the channels used here. The data for regular cells were computed from the formula

$$\Psi = \left(\frac{\tau_w}{\bar{\tau}_w}\right)_\infty \frac{(\tau_w/\bar{\tau}_w)_{I,e}}{\frac{6}{\pi}\int_0^{\pi/6}(\tau_w/\bar{\tau}_w)_{I,e}\,d\varphi},$$

Declassified and Approved For Release 2013/02/27 : CIA-RDP10-02196R000300110005-5

Declassified and Approved For Release 2013/02/27 : CIA-RDP10-02196R000300110005-5

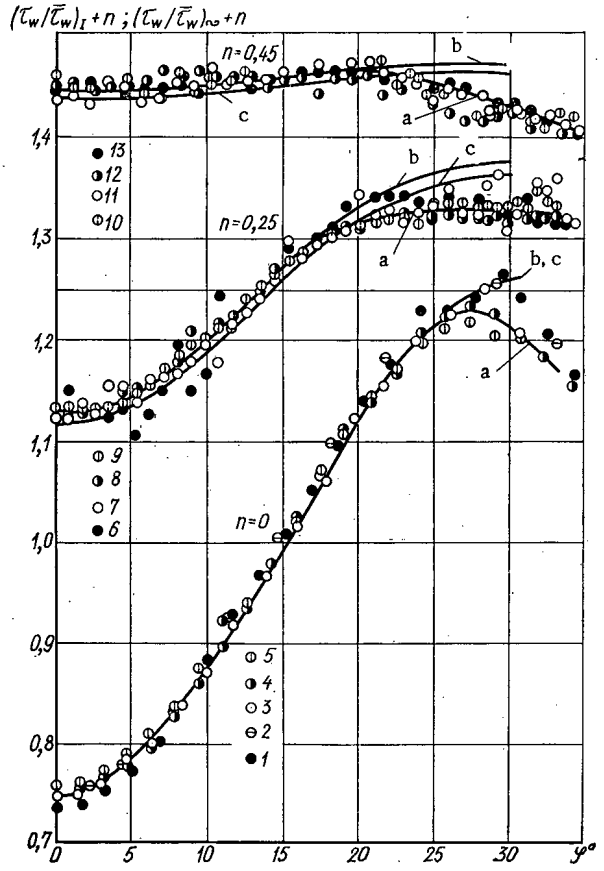

Fig. 3. Distribution of tangential stresses for type I cells and cells of an infinite pack of rods: 1-13) experimental values of $(\tau_W/\bar{\tau}_W)_I$ for $Re_c \cdot 10^{-3}$, equal to 15.0, 28.8, 41.8, 58.6, 63.3, 18.8, 43.8, 67.8, 81.6, 25.0 34.8, 81.9, and 115 respectively; a) approximating dependences; b) extrapolated dependences; c) values of relative tangential stresses in infinite packs of rods $(\tau_W/\bar{\tau}_W)_\infty$ for $Re \cdot 10^{-3}$ equal to 46.6 (s/d = 1.05), 50.7 (s/d = 1.1) and 44.7 (s/d = 1.2).

where the subscript e denotes extrapolated quantities. The distributions of the tangential stresses for regular cells are approximated by formulas that are valid for 15,000 < Re < 100,000: for s/d = 1.05 $\Psi = 1 - 0.2522 \cos 6\varphi + 0.0043 \cos 12\varphi - 0.0041 \cos 18\varphi - 0.0002 \cos 24\varphi$; for s/d = 1.10 $\Psi = 1 - 0.1277 \cos 6\varphi - 0.0098 \cos 12\varphi + 0.0028 \cos 18\varphi + 0.0014 \cos 24\varphi$; for s/d = 1.20 $\Psi = 1 - 0.0143 \cos 6\varphi$.

The nondimensional velocity profiles are plotted in Fig. 4 on the basis of the relationships obtained in the experiments:

$$\frac{u}{u_\varphi^m} = f_1\left(\frac{y}{y_0}\right) \text{ and } \frac{u_\varphi^m}{u^m} = f_2(\varphi)$$

and consequently

$$\bar{u}_\varphi = \frac{u^m}{m(1+0.5 \cdot m)}\Phi;$$

$$\bar{u}_i = \frac{12u^m}{\pi\left(\frac{2\sqrt{3}}{\pi}x^2 - 1\right)} \int_0^{\pi/6} \Phi \, d\varphi;$$

$$i = \text{I, II, III};$$

$$\bar{u} = \frac{1}{3}(\bar{u}_I + \bar{u}_{II} + \bar{u}_{III});$$

$$\Phi = m \frac{u_\varphi^m}{u^m} \int_0^1 \frac{u}{u_\varphi^m}\left(1 + m\frac{y}{y_0}\right) d\left(\frac{y}{y_0}\right),$$

where u^m is the maximum velocity of air in the channel and is taken equal to the velocity at the geometrical center of the cell (at the point B, see Fig. 1); $\bar{u}_\varphi$ is the velocity of air for a given angle φ averaged over the radius; y/y_0 is the relative distance from the wall to the axis of symmetry; $m = y_0/R = (x/\cos\varphi - 1)$; $x \equiv s/d$.

Declassified and Approved For Release 2013/02/27 : CIA-RDP10-02196R000300110005-5

Declassified and Approved For Release 2013/02/27 : CIA-RDP10-02196R000300110005-5

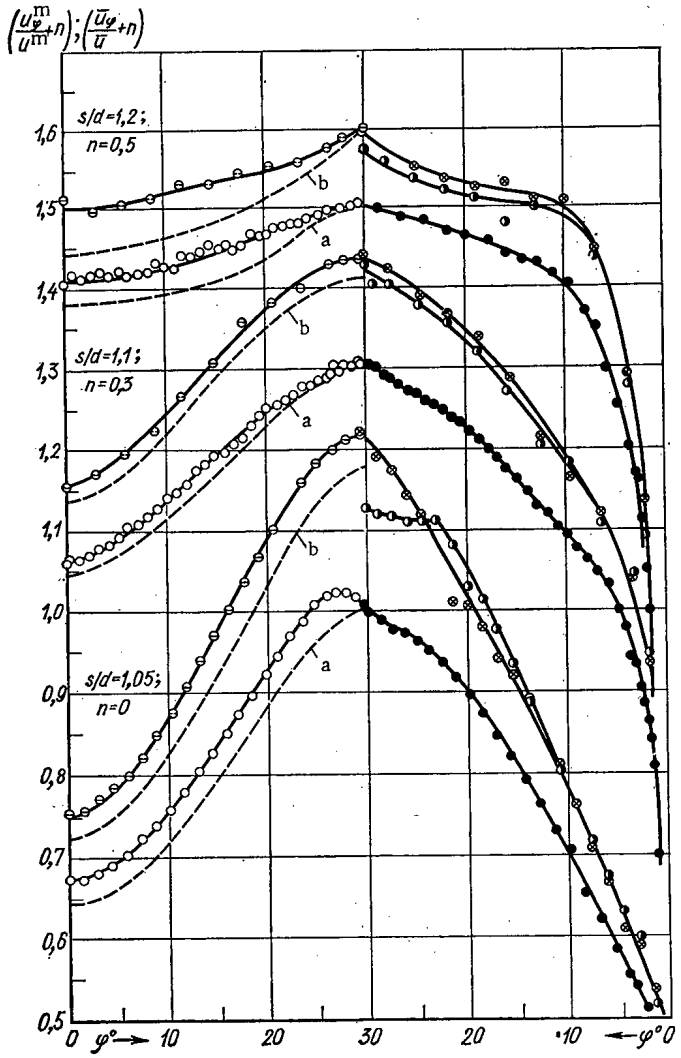

Fig. 4. Velocity profiles in channels and regular cells of infinite packs of rods: ○, ●) values of u_φ^m/u^m at the axes AB and BC (see Fig. 1); ⊖, ⊗, ◑) values of $\bar{u}_\varphi/\bar{u}$ for I, II, III cells respectively; a, b) extrapolated values of u_φ^m/u^m and $\bar{u}_\varphi/\bar{u}$ respectively for infinite packs.

For the channel with s/d = 1.05 a displacement of the coordinate of the maximum velocity by 1.5-2° is observed, analogous to the displacement of the maximum of tangential stress. For other channels this effect practically does not occur.

The experiments confirmed that the relative velocity (u/u_φ^m) profile has a very weak dependence on the tangential stress at the wall and this dependence can be disregarded. Using the empirical velocity profile along the normal to the wall $u^+ = f(\eta)$, where $\eta = (y/\nu)\sqrt{(\tau_w/\rho)}$, $u^+ = u/\sqrt{(\tau_w/\rho)}$, it is not difficult to find the extrapolated values of the velocity from the initial and extrapolated tangential stresses, shown in Fig. 3:

$$(u_\varphi^m)_\infty \approx (u_\varphi^m)_I \frac{u^+(\eta c)}{u^+(\eta)} \sqrt{c},$$

where

$$c = \left(\frac{\tau_w}{\bar{\tau}_w}\right)_{I,e} \Big/ \left(\frac{\tau_w}{\bar{\tau}_w}\right)_I.$$

From here the values of $(u_\varphi^m/u^m)_\infty$ for the infinite lattice of rods are obtained directly. The values of $(\bar{u}_\varphi/\bar{u})_\infty$ are determined with the use of the relations given earlier.

In the channel with s/d = 1.05 a clearly defined bending of the isotachs (lines of constant velocity) is observed as a result of the influence of secondary flows (Fig. 5). A similar pattern was observed for noncircular cross sections, for example, in [11]. For channels with s/d equal to 1.1 and 1.2 the bending of the isotachs was not detected. However, the secondary flows can change the form of the isotachs without causing clear bendings in them. In this case the existence of secondary flows cannot be inferred from

Declassified and Approved For Release 2013/02/27 : CIA-RDP10-02196R000300110005-5

Declassified and Approved For Release 2013/02/27 : CIA-RDP10-02196R000300110005-5

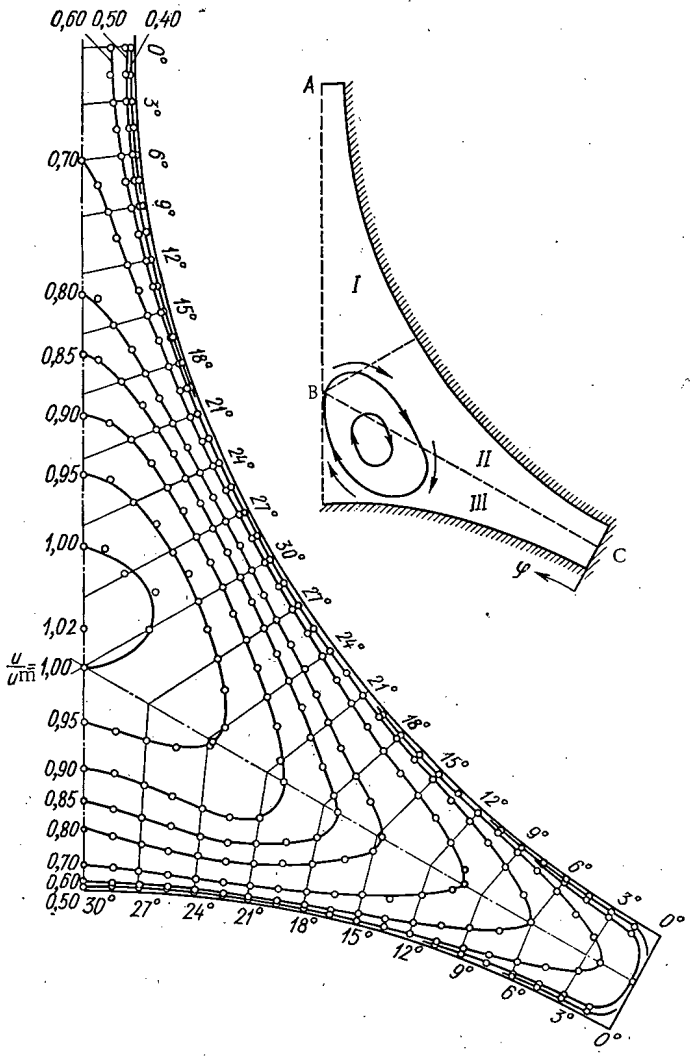

Fig. 5. Distributions of lines of constant velocity (isotachs) in the channel for s/d = 1.05; Re_c = 41,800; u_c = 29.6 m/sec; u^m = 38.3 m/sec; u/u^m = 0.771.

the form of the isotachs. An analysis of Figs. 3 and 5 shows that for φ = 14-24° the mass and momentum fluxes are directed across the axis BC from cell II into cell III, while for φ = 24-30° there is a reverse flow from cell III to cells II and I. The displacement of the velocity maxima is caused by the above-mentioned secondary flows.

In the construction of the velocity profiles along the normals to the walls in generalized coordinates (Fig. 6) the local values of tangential stresses measured in the experiments were used. Figure 6 also shows the results of [5] for a dense pack of rods. The experimental data, including those for cell III with strongly deformed profile of the tangential stresses, agree with Karman velocity profile for circular tubes roughly to the same extent as the experimental data for circular tubes obtained in [8,11,12]. Thus the hypothesis of approximate universal character of the velocity profiles along the normals to the walls of channels with not too large curvature of the perimeter is experimentally substantiated. This hypothesis is widely used in computational-theoretical investigations, for example, in [13-15].

The coefficients of friction of the channels, computated from the measured pressure gradient along the channels and the tangential stresses at the wall coincide. The graphical dependences $\lambda = f(Re)$ are equidistant to the dependences constructed from the Blasius formula for a circular tube. The coefficients of friction in regular triangular cells are approximated by the formula

$$\frac{\lambda}{\lambda_{tu}} = 0.57 + x\left[1 - e^{-1.12(x-1)}\right](\lg x)^{0.27x}$$

$$x \equiv \frac{s}{d};\ 1.0 \leqslant x \leqslant 1.2;\ 1.5 \cdot 10^3 \leqslant Re \leqslant 10^5.$$

Declassified and Approved For Release 2013/02/27 : CIA-RDP10-02196R000300110005-5

Declassified and Approved For Release 2013/02/27 : CIA-RDP10-02196R000300110005-5

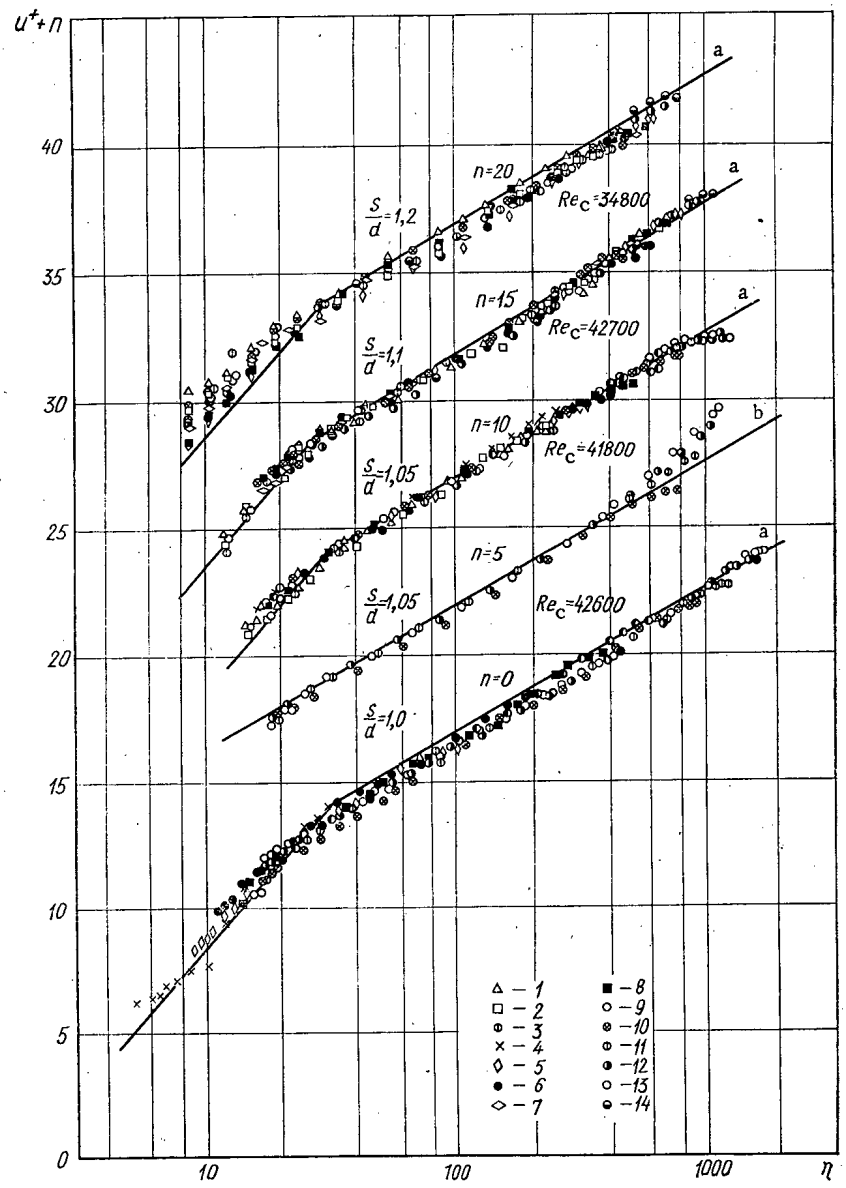

Fig. 6. Nondimensional velocity profiles along the normals to the wall of the channels: a, b) for cells I and III respectively; s/d = 1.0 and 1.05; 1 and 13) for $\varphi = 0^\circ$ and 30° respectively; 2-6, 8-12) for φ from 1.5° to 28.5° with step of three degrees; s/d = 1.1 and 1.2; 1-3, 13, 10, 6-8, 5, 12, 14) for φ from 0° to 30° with step of three degrees.

This formula is derived on the basis of experimental data on hydraulic losses in channels and computations carried out with the use of Karman velocity profile along the normals to the walls of the cells and interpolation of the tangential stress profiles to intermediate values of the rod lattice.

Engineer A. M. Aleksandrov participated in the experiments.

LITERATURE CITED

1. A. V. Sheinina, in: Liquid Metals [in Russian], Atomizdat, Moscow (1967), p. 210.
2. L. Palmer and L. Swanson, "Intern. developments of heat transfer," ASME, No. 7 (1962), p. 535.
3. W. Eifler and R. Nijsing, Nucl. Engng. Design, 5, No. 1, 22 (1967).
4. Yu. D. Levchenko et al., in: Liquid Metals [in Russian], Atomizdat, Moscow (1967), p. 223.
5. Yu. D. Levchenko, V. I. Subbotin, and P. A. Ushkov, Atomnaya Énergiya, 22, 218 (1967).

Declassified and Approved For Release 2013/02/27 : CIA-RDP10-02196R000300110005-5

Declassified and Approved For Release 2013/02/27 : CIA-RDP10-02196R000300110005-5

6. Preston, Mekhanika [Coll. of translations and reviews of foreign literature], No. 6 (1955), p. 34.
7. V. P. Bobkov et al., Izv. AN SSSR, Mekhanika Zhidkosti i Gaza, No. 3, 162 (1968).
8. J. Laufer, NASA TN 1174, 1953.
9. L. Schiller, Motion of Liquids in Tubes [in Russian], ONTI, Moscow–Leningrad (1936).
10. A. S. Ofitserov, Secondary Flow [in Russian], Gosstroiizdat, Moscow (1959).
11. I. Nikuradze, Ingenier-Archiv, 1, 306 (1930).
12. R. Deissler, NASA TN 2138, 1950.
13. R. Deissler and M. Faylor, Reactor Heat Transfer Conf. of 1958, TID-7529, Part 1, Book 2, 416 (1957).
14. L. S. Kokorev et al., in: Problems of Thermal Physics of Nuclear Reactors [in Russian], Atomizdat, Moscow (1968).
15. V. I. Subbotin et al., SEV Symposium, State and Prospects of Work on the Development of Fast Neutron Reactors [in Russian], Vol. 2, Obninsk (1967), p. 529.

Declassified and Approved For Release 2013/02/27 : CIA-RDP10-02196R000300110005-5

Declassified and Approved For Release 2013/02/27 : CIA-RDP10-02196R000300110005-5

BOOK REVIEWS

V. A. Artsybachev

NUCLEAR GEOPHYSICAL PROSPECTING*

Reviewed by V. L. Shashkin, K. I. Yakubson, and A. D. Kozhevnikov

This book is designed as a textbook aid in nuclear geophysical prospecting work. The fifteen chapters of the book are grouped under three major headings: γ-techniques, neutron techniques, and applications of nuclear techniques in prospecting for mineral occurrences.

The prospective author of a survey of nuclear geophysical prospecting is faced with serious difficulties stemming, on the one hand, from the swift growth of scientific information in that area, and on the other hand, from the inadequacy of some of the methods used in the field. Moreover, in attempting to compile a textbook, the author must present the basic material on each technique while maintaining reasonable proportions so as to get around major discrepancies in the amount of detail in the descriptions of the various techniques. Artsybashev has been able to overcome all of those difficulties, for the most part. He wields unquestionable pedagogic skill in encompassing very extensive material in a fairly detailed presentation of both the theoretical fundamentals of each method and approaches employed in practical utilization of the results, as well as the principles underlying the interpretation of the results.

To date, the only review work on nuclear geophysical prospecting has been E. M. Filippov's book Applied Nuclear Geophysics [in Russian] (Izd. AN SSSR, Moscow, 1962). Artsybashev's book includes material that appeared after the book by Filippov was published, and is distinguished by its more consistent and more compact presentation.

The presentation of the applications of nuclear geophysical techniques in a separate section, which enabled the author, wherever possible, to consider combined applications of the techniques in the light of specific examples, is a quite successful and entirely valid approach.

Naturally, it would be difficult to conduct a survey of a large amount of material on such a new area as nuclear geophysical prospecting without some errors. The basic problems in nuclear geophysical prospecting should have been placed at the beginning of the text, and the methods for solving the problems (analytical solutions, mathematical and physical simultation and analogs) should have been clearly characterized. It would have been convenient to indicate applications of the theory of similitude to the solution of those problems, since the author relies heavily on the method of similitude. That approach would have enabled the author to deal with the effect of a large number of factors on the measurement results in a concise form. But the absence of an overall characterization of the theory of similitude in the text necessitated repetitions of that theory in applications and specific examples.

The uneven state of the art in the development of nuclear geophysical techniques should have been properly characterized. That would have provided the readers with a better understanding of the unequal amount of attention given to some methods. The radiation sources employed are also characterized inadequately. The spectral characteristics of neutron sources are given little attention in the literature, but they exert a marked effect on the neutron distribution in rocks, and are also utilized directly in some methods ("two-source methods").

The detailed presentation of the theory of neutron methods of investigation is at variance with the limited use made of the theory in the description of particular methods.

*Atomizdat, Moscow, 1972.

Translated from Atomnaya Énergiya, Vol. 33, No. 5, p. 900, November, 1972.

© 1973 Consultants Bureau, a division of Plenum Publishing Corporation, 227 West 17th Street, New York, N. Y. 10011. All rights reserved. This article cannot be reproduced for any purpose whatsoever without permission of the publisher. A copy of this article is available from the publisher for $15.00.

Declassified and Approved For Release 2013/02/27 : CIA-RDP10-02196R000300110005-5

Declassified and Approved For Release 2013/02/27 : CIA-RDP10-02196R000300110005-5

In some cases, the overall characteristics of the effect of measurement conditions on the results are replaced by concrete data obtained in particular instances.

The chapter dealing with costs estimates for nuclear geophysical methods could not be acknowledged as a successful treatment. Here the author bases his inquiry on the already totally obsolete contribution by G. F. Mikheev and N. G. Feitel'man Cost Aspects of Radiometric Techniques in the Mining industries [in Russian] (Gosatomizdat, Moscow, 1962).

The author holds the view that the "principal component in the calculations is determination of cost effectiveness resulting from the acceptance of a particular instrument or method in regular production work." That approach can lead to erroneous conclusions. It would be more correct to treat cost effects resulting from the application of nuclear geophysical methods in combination with other measures taken with regard to applications of that method. There may be cases where utilization of a particular instrument or method without due attention to a set of accompanying measures would not result in savings. That is particularly the case when nuclear geophysical techniques are applied in mining work. Moreover, the use of nuclear geophysical techniques combined with other techniques and organizational measures still does not make it possible to estimate cost savings due to the individual components of the combination. The inadequate level of development of methods for calculating cost savings still hinders our ability to fully clarify this problem at the textbook level.

The terminology of nuclear geophysical prospecting has been grouping up in the field and has to be put into order. That job is currently under way, and it would be difficult to fault the author for imprecision in terminology at this point. For example, we note the use of some unsuccessful or unfortunate choices of terminology: "neutron properties of rock," "mass thickness," "γ-ray properties," and so forth. In some cases the author makes use of concepts which are defined only later on in the text. For example, the effective atomic number is invoked in the definition of the similitude criterion for γ-ray fields, but is not defined beforehand; the concept of an "inversion probe" is employed before the term is defined. Some of the terms, e.g., "depth of penetration of the method," are not defined anywhere, even though frequent use is made of them.

The list of inadequacies and errors in the text could be continued further, but should not be taken to connote a negative impression of the book as a whole.

The author has done a lot of work in reviewing widely scattered material and data, and the reader will have the opportunity to become familiarized with the present status of nuclear geophysical prospecting work in a compact and skilled presentation. The book will be a valuable aid in the training of specialists for nuclear geophysical prospecting work.

There will be a need for a new edition of the book in several years. That will afford the author an opportunity to correct the deficiencies noted, and to supplement the text with new and fresh data, in particular foreign data, which are used only sparingly in the text.

Declassified and Approved For Release 2013/02/27 : CIA-RDP10-02196R000300110005-5

Declassified and Approved For Release 2013/02/27 : CIA-RDP10-02196R000300110005-5

ARTICLES

AVERAGE NUMBER OF PROMPT NEUTRONS IN Pu^{239} FISSION

K. E. Bolodin, V. F. Kuznetsov,
V. G. Nesterov, B. Nurpeisov,
L. I. Prokhorova, Yu. M. Turchin,
and G. N. Smirenkin

UDC 546.799.4

The quantity $\bar{\nu}$ (the average number of neutrons emitted per fission) is one of the most important nuclear physics constants determining neutron multiplication in reactors. Knowledge of the dependence of $\bar{\nu}$ on the energy E_n of neutrons producing fission is important for fast reactors. The isotope Pu^{239} plays the main role in breeder reactors. The present work is devoted to a study of this isotope. The measurements were made on electrostatic and cascade generators with the E_{max} of accelerated particles being 2.5 MeV. The reaction T(p, n), which was produced in solid tritium targets, served as the neutron source. Two methods were used to study the energy dependence $\bar{\nu}(E_n)$ in Pu^{239}.

EXPERIMENTAL METHODS AND RESULTS

Method I. Coincidences between pulses from fission fragment detectors and from detectors of the prompt neutrons accompanying the fission fragments were recorded. Detection of fission events was accomplished with a multilayer ionization chamber, and detection of neutrons by a system of 24 He^3 counters in a cylindrical paraffin block. The counters were arranged coaxially around a central channel inside which a fission chamber with layers of Pu^{239} and Cf^{252} was located. The experimentally determined ratio between the number of true coincidences N_c and the number of fission events N_f in plutonium has the form

$$\rho = N_c/N_f = \bar{\nu}\eta, \tag{1}$$

where η is the detection efficiency for fission neutrons. By measuring a similar ratio for spontaneous fission of Cf^{252}, the average number of prompt neutrons $\bar{\nu}_0$ for which is well known and can be used as a standard, we obtain

$$\rho/\rho_0 = A\,\frac{\bar{\nu}}{\bar{\nu}_0}, \tag{2}$$

where the factor A ($A-1 \ll 1$) appears because of differences between the detection efficiency and a number of other experimental conditions in the detection of fission fragments and fission neutrons from the isotope under study and from the standard. The experimental method and the treatment of the experimental results (determination of the factor A) was described in detail in [1, 2] which were concerned with similar measurements of $\bar{\nu}(E_n)$ for U^{235}.

In this work, we considered the features of this experiment resulting from the nature of the isotope studied. They include the high specific

TABLE 1. Results of Method I

Number of cycles	E_n	$\rho(E_n)/\rho_0$†	$\bar{\nu}(E_n)/\bar{\nu}_0$	$\bar{\nu}(En)$
40	0,00	0,7478±0,0030	0,7679±0,0040	2,884±0,015
20	0,08 *	0,7497±0,0060	0,7689±0,0069	2,888±0,026
34	0,400±0,057	0,7544±0,0031	0,7759±0,0045	2,914±0,017
19	0,550±0,058	0,7643±0,0069	0,7867±0,0077	2,955±0,029
21	0,700±0,058	0,7659±0,0049	0,7884±0,0060	2,961±0,023
35	0,800±0,049	0,7731±0,0054	0,7964±0.0064	2,991±0,024
41	0,900±0,045	0,7694±0,0042	0,7925±0.0053	2,977±0,020
25	1,000±0,043	0,7783±0,0068	0,8026±0,0077	3,015±0,029
41	1,100±0,035	0,7845±0,0037	0,8097±0.0050	3,041±0,019
25	1,150±0,035	0,7787±0,0051	0,8036±0,0061	3,018±0,023
49	1,200±0.035	0,7742±0,0042	0,7989±0,0054	3,001±0,020
30	1,250±0,035	0,8031±0,0041	0,8306±0,0054	3,120±0,020
21	1,300±0,043	0,7974±0,0068	0,8213±0,0077	3,085±0,029
22	1,400±0,042	0,8039±0,0066	0,8297±0,0075	3,116±0,028
22	1,500±0,042	0,8041±0,0061	0,8297±0,0077	3,116±0,029
22	1,600±0,042	0,8046±0,0072	0,8302±0,0088	3,118±0,033

*Proton energy given as 25 keV above the threshold for the T(p, n) reaction.
†Experimental values.

Translated from Atomnaya Énergiya, Vol. 33, No. 5, pp. 901-906, November, 1972. Original article submitted May 15, 1972.

© 1973 Consultants Bureau, a division of Plenum Publishing Corporation, 227 West 17th Street, New York, N. Y. 10011. All rights reserved. This article cannot be reproduced for any purpose whatsoever without permission of the publisher. A copy of this article is available from the publisher for $15.00.

Declassified and Approved For Release 2013/02/27 : CIA-RDP10-02196R000300110005-5

Declassified and Approved For Release 2013/02/27 : CIA-RDP10-02196R000300110005-5

TABLE 2. Results of Method II

E_n, MeV	$\bar{\nu}(E_n)/\bar{\nu}(E_n^0)$ *	$\bar{\nu}(E_n)$
0,08 †	0,9923±0,0068	2,892±0,028
0,200±0,035	0,9932±0,0067	2,912±0,028
0,300±0,033	0,9971±0,0046	2,906±0,024
0,400±0,032	1,000	2,914±0,017 *
0,500±0,031	1,0105±0,0058	2,945±0,026
0,600±0,030	1,0085±0,0050	2,939±0,025
0,700±0,029	1,0199±0,0055	2,972±0,026

*See text.

†Proton energy was given as 20 keV above the threshold for the T(p, n) reaction.

α-activity of Pu^{239} and the presence of an undesirable background of spontaneous fissions associated with contamination by the isotope Pu^{240}. We used well-separated plutonium (Pu^{240} ~0.15%) in this work; thus the background of spontaneous fissions did not exceed 3% of the number of induced Pu^{239} fissions. In the first (generally unsuccessful) attempt to measure $\bar{\nu}$ for Pu^{239} [3], the Pu^{240} content was an order of magnitude greater.

In working with the significant amounts of Pu^{239} in the chamber (of the order of 100 mg) required for this experiment, it is difficult to avoid considerable loss of fission fragments because of the need to discriminate against multiple pile-up of α-particle pulses. This effect should be a limiting factor since, as has been shown [2], ρ exhibits a dependence on the fraction of undetected fission fragments. However, if this fraction does not exceed 30%, the effect of fragment loss is small and can be taken into account by a small correction (of the order of a fraction of a percent).

In order to obtain a sufficiently high efficiency for the detection of fission events, the following measures were taken: a) partitioning of the multilayer fission chamber in which the assembly of 16 layers of PuO_2 (7 mg of Pu^{239} in each layer) was subdivided into eight groups with independent stages of preamplification and discrimination (four groups each to the left and right of the section with the Cf^{252} layer, which was placed in the central plane of the neutron detector); b) consumption of a portion of the energy of the fragments (approximately 1/4-1/10) through a working gas (Ar + 7% CO_2) pressure in the chamber of 200 mm Hg; c) increase in interelectrode spacing to 10 mm in comparison to 3 mm for the U^{235} chamber.

As a result, a fission-fragment detection efficiency of ~ 85% was achieved because of the increase in the length of the assembly of plutonium layers which led to an increase in one of the main factors determining the correction factor A – the difference in detection effeciency for fission neutrons from Pu^{239} and Cf^{252} because of the dependence $\eta(z, r)$ on source position along the detector length z and at a radius r.

To determine the ratio $\eta(0, 0)/\eta(z, r)$, measurements were made of the behavior of $\eta(z, r)$ and of the distribution of the number of fissions in the groups of Pu layers (in experiments with fast and thermal neutrons). For fast neutrons, it was 1.0379 ± 0.002 and in the experiment with U^{235}, 1.0111 ± 0.0015. This factor predominates in the correction factor A (Table 1). In addition, the coefficient A includes corrections for the angular and energy dependence of η, discrimination for the number of fission events, fission contributions from background neutrons, and coincidence losses. We estimate the error in the coefficient A to be 0.4-0.5%.

The results of direct measurements of ρ/ρ_0 and their evaluation $\bar{\nu}/\bar{\nu}_0$ are given in Table 1. The error in ρ/ρ_0 was taken to be the maximum of two errors: the statistical error or the error calculated from the data spread for individual measurement cycles, the number of which is indicated in the second [sic] column. To determine the error in ν/ν_0, the errors in ρ/ρ_0 and A were combined as an rms error. In determining $\bar{\nu}$ for Pu^{239}, the value of $\bar{\nu}_0$ for Cf^{252} was taken to be 3.756 in accordance with the recommendation of [4], the error of which was not taken into account in the error of $\bar{\nu}(E_n)$. The data for $E_n = 0$ was obtained for neutrons with an energy of ~ 300 keV moderated in a paraffin block about 10 cm thick.

Method II. A threshold detector – a multilayer thorium chamber (4 g ThO_2) – which was practically insensitive to source neutrons in the energy range up to $E_n = 0.7$ MeV was used to detect fission neutrons. The low efficiency of the neutron detector was compensated for by the use of a large amount of plutonium subject to irradiation (~ 30 g) in the form of a metal disk 3 mm thick. In the experiment, the total number of fissions F in the disk was not measured but the quantity $n_f = \lambda E$, which is proportional to it and corresponds to the number of fissions in a thin surface layer of the disk. This quantity was measured by a double ionization chamber with a common electrode in the form of a ring in which the disk was placed and having adjacent to its faces layers of PuO_2 about 1 mg/cm^2 thick made of plutonium of the same isotopic composition as that in the disk.

The experimentally measured ratio has the form

$$r(E_n) = \frac{N_{Th}}{n_f} = k\bar{\nu}(E_n), \qquad (3)$$

Declassified and Approved For Release 2013/02/27 : CIA-RDP10-02196R000300110005-5

Declassified and Approved For Release 2013/02/27 : CIA-RDP10-02196R000300110005-5

TABLE 3. Averaged Values of $\bar{\nu}$ for Pu^{239}

E_n, MeV	$\langle\bar{\nu}\rangle$	σ_I	σ_{II}
0,050—0,150	2,899	0,026	0,019
0,150—0,250	2,911	0,007	0,025
0,250—0,350	2,905	0,009	0,013
0,350—0,450	2,925	0,005	0,010
0,450—0,550	2,925	0,009	0,008
0,550—0,650	2,939	0,005	0,007
0,650—0,750	2,953	0,004	0,008
0,750—0,850	2,967	0,011	0,010
0,850—0,950	2,978	0,005	0,010
0,950—1,050	2,998	0,012	0,012
1,050—1,150	3,033	0,007	0,011
1,150—1,250	3,020	0,012	0,014
1,250—1,350	3,089	0,018	0,013
1,350—1,450	3,068	0,019	0,014
1,450—1,650	3,125	0,008	0,017
1,650—1,850	3,133	0,029	0,027
1,850—2,050	3,191	0,010	0,015
2,050—2,250	3,175	0,020	0,027
2,250—2,450	3,213	—	0,048
2,450—2,650	3,226	0,029	0,018

with

$$R(E_n) = \frac{r(E_n)}{r(E_n^0)} = C(E_n, E_n^0)\,\frac{\bar{\nu}(E_n)}{\bar{\nu}(E_n^0)}, \qquad (4)$$

where E_n^0 is a reference neutron energy constant for all measurements and chosen to be 0.4 MeV, and $C(E_n, E_n^0)$ is a coefficient close to one. This coefficient takes into account the dependence on bombarding neutron energy of the following factors which determine the coefficient k in Eq. (3): a) the coefficient λ; b) the angular correlation between fission neutron and primary neutron; c) fission neutron spectrum; d) fission distribution over the radius and thickness of the disk; e) contributions from multiple scattering processes and from neutron multiplication in the disk. This method of measurement of the relative behavior of $\bar{\nu}(E_n)$ has been described in detail in [5], where it was used for the investigation of U^{233} and U^{235}.

The results are shown in Table 2. Note that in method II, a small portion of the delayed neutrons, with energies sufficient to produce fission, may be recorded. It is obvious, however, that because of the smallness of the total fraction of delayed neutrons and the softness of their energy spectrum [6], the data for $\bar{\nu}(E_n)/\bar{\nu}(E_n^0)$, with an error considerably less than the experimental error, can be identified with the sought-for dependence from prompt neutrons. In determining the absolute values $\bar{\nu}(E_n)$ given in the last column, the value $\bar{\nu}(E_n) = 2.914 \pm 0.017$ from Table 1 was used.

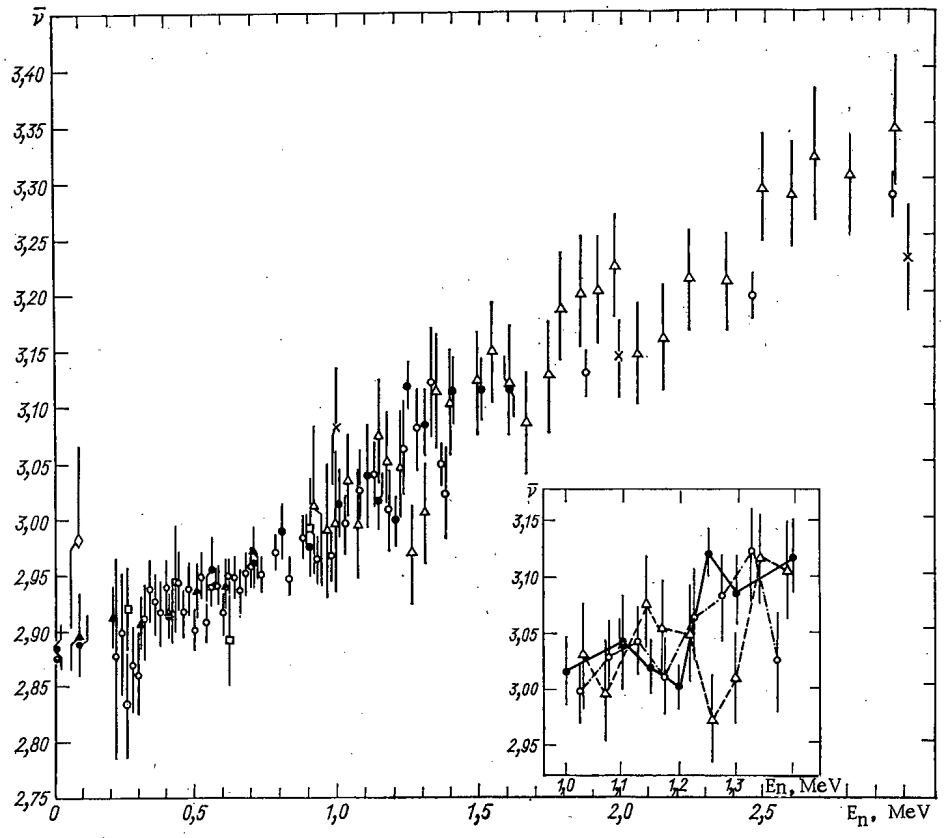

Fig. 1. Average number of prompt fission neutrons, $\bar{\nu}$, for Pu^{239}: □) [7]; ×) [8]; ○) [9,10]; △) [11]; ◇) [20]; ●, ▲) this work, methods I and II respectively. In the insert, lines connect data from – .– .–) [10], – – –) [11], ——) this work.

Declassified and Approved For Release 2013/02/27 : CIA-RDP10-02196R000300110005-5

Declassified and Approved For Release 2013/02/27 : CIA-RDP10-02196R000300110005-5

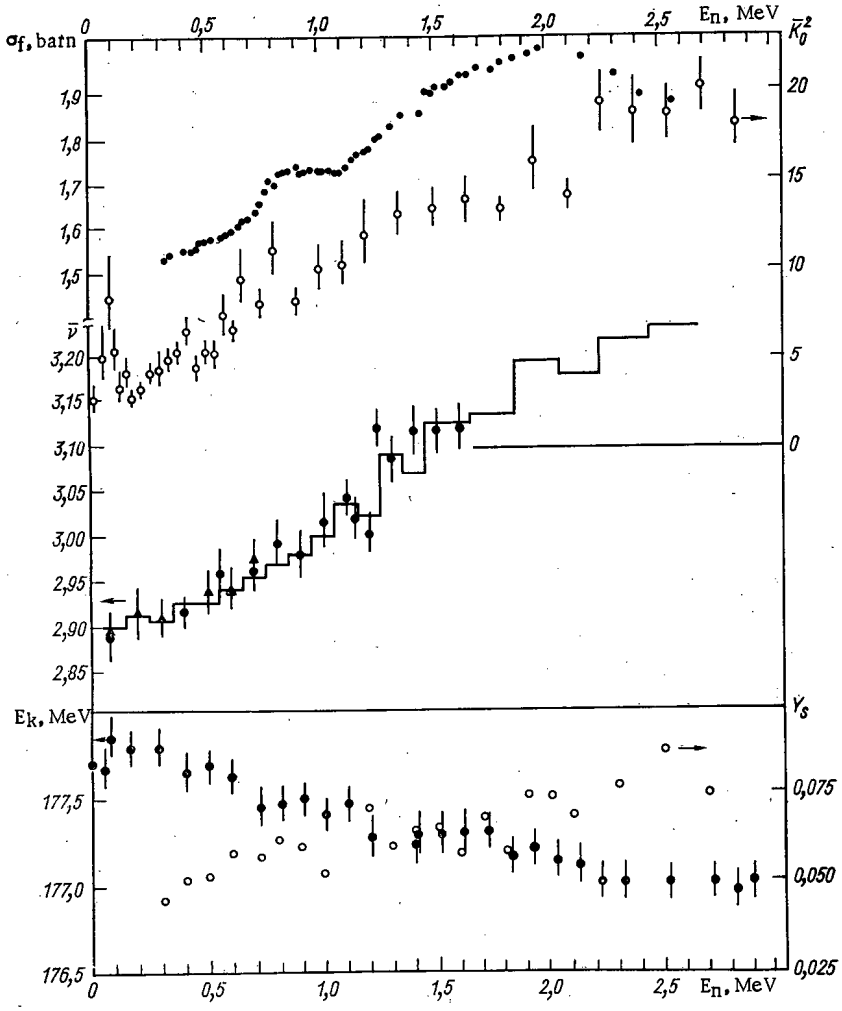

Fig. 2. Energy dependence of σ_f [16], the parameter $\bar{K}_0^2$ [15], $\bar{\nu}$ (●, ▲ are data from this work and the histogram shows the averaged value of $\bar{\nu}$ from Table 3), and the kinetic energy of fission fragments E_n [14] for neutron fission of Pu^{239}.

DISCUSSION OF RESULTS

The compilation of published data for $\bar{\nu}(E_n)$ for Pu^{239}, and also the results of this work in the range $E_n < 3$ MeV, are shown in Fig. 1. The results of measurements by both methods used by us are in agreement with each other and with the data of other authors [7-13], including those for thermal neutrons [7, 8, 12, 13]. This enables us to reject with certainty the results of our preliminary measurements of $\bar{\nu}$, which were carried out under less favorable conditions and which fell sharply in the region $0.4 \leq E_n \leq 1.3$ MeV.

In order to have a clearer representation of the energy dependence of $\bar{\nu}(E_n)$ and to make a quantitative evaluation of the self-consistency of existing experimental data, the data was averaged using weights inversely proportional to the squares of the errors σ_i over intervals $\Delta E_n = 0.1$ MeV for energies 0.05-1.45 MeV and intervals $\Delta E_n = 0.2$ MeV for higher energies. For the E_n ranges shown, Table 3 gives the values of

$$\langle\bar{\nu}\rangle = \frac{\sum \bar{\nu}_i \sigma_i^{-2}}{\sum \sigma_i^{-2}}; \quad \sigma_I = \left[\frac{\sum (\bar{\nu}_i - \langle\bar{\nu}\rangle)^2 \sigma_i^{-2}}{(n-1)\sum \sigma_i^{-2}}\right]^{1/2};$$

$$\sigma_{II} = \left(\sum \sigma_i^{-2}\right)^{-1/2},$$

where σ_I and σ_{II} are errors, the first of which reflects the spread of the data, and the second, the accuracy of the overall average. The closeness of these values is evidence of the absence of significant systematic disagreements in the results of the various papers.

Declassified and Approved For Release 2013/02/27 : CIA-RDP10-02196R000300110005-5

Declassified and Approved For Release 2013/02/27 : CIA-RDP10-02196R000300110005-5

The errors σ_I and σ_{II} are minimal (~ 0.3%) in the region E_n = 0.45-0.65 MeV, where detailed data from a single paper [10] predominates. Therefore they do not reflect the actual accuracy in the measurements of $\bar{\nu}$, which is twice as poor, as follows from the other data in Table 3. The spread in $\bar{\nu}_i$ is most significant in the region E_n = 1.15-1.35 MeV. Evidently, it results to a considerable extent from "fine" structure in the behavior of $\bar{\nu}(E_n)$ and from possible disagreement in the determination of neutron energies in the various papers. In the insert in Fig. 1, the referenced region of $\bar{\nu}(E_n)$ dependence is shown separately. This indicates that in all three sets of the most detailed data, irregularities are observed which have identical form but which are shifted somewhat with respect to one another.

To clarify the nature of the indicated structure, data is given in Fig. 2 for other characteristics of the fission process Pu^{239} (n, f): the average kinetic energy of the fragments [14], the parameter K_0^2, which determines the angular anisotropy of fission [15], and the fission cross section [16]. The last was obtained from measurements of the ratio of the fission cross sections for Pu^{239} and U^{235} using the curve for $\sigma_f(E_n)$ for U^{235} recommended in [17]. The correlation between the irregularities in the behavior of all the quantities shown in Fig. 2 in the range 1.2-1.3 MeV are clearly visible. The correlation of the irregularities in the region 0.5-0.7 MeV is less clearly expressed. In the dependence $\bar{\nu}(E_n)$, a marked variation in the rate of rise occurs there: $d\bar{\nu}/dE_n = 0.088$ MeV^{-1} at $E_n < 0.6$ MeV and 0.160 MeV^{-1} for $0.6 < E_n < 3.0$ MeV. Correlation of data at higher energies is also worthy of note; there is a region of weak variation of $\bar{\nu}$ in the behavior of $\bar{\nu}$ and K^2 in the region 1.3-2.0 MeV.

The existence of correlations between the energy dependence of $\bar{\nu}$ and E_k, the values of which are mainly determined by the configuration of the fragments formed, and the characteristics of the fission probability, which are determined by the properties of the nucleus in the intermediate state, is evidence of a deep-seated relation between these stages of the fission process. The mechanism of the effect on the behavior of $\bar{\nu}(E_n)$ was discussed [18] for nonuniformity in the density of intermediate states in the fissioning nucleus resulting from the discrete nature of quasiparticle excitation [19]. It was shown [15] that a completely satisfactory description of the energy dependence of K_0^2 for Pu^{240} is achieved with its help. To what extent it will prove to be suitable for a description of $\bar{\nu}(E_n)$, future measurements in the region $E_n > 1.6$ MeV will indicate. Existing, but unfortunately presently sparse data on $\bar{\nu}$ and its correlation with the behavior of K_0^2 makes it possible to count on a positive answer. From the practical viewpoint, there is great interest in the insufficiently studied region $E_n < 0.3$ MeV.

The authors are greatful to R. E. Bagdasarov for constructing a multichannel coincidence circuit, to V. V. Glinskii and A. P. Klimov and the entire staff of the accelerator for providing excellent accelerator operation, to V. E. Rudnikov and V. A. Borisenko for helping with the measurements, and to N. E. Fedorova for computer analysis of the data.

LITERATURE CITED

1. L. I. Prokhorova and G. N. Smirenkin, Yad. Fiz., 7, 961 (1968).
2. L. I. Prokhorova et al., At. Énerg., 30, 250 (1971); preprint FÉI-227.
3. V. G. Nesterov et al., Nuclear Data for Reactors, Vol. II, IAEA, Helsinki (1970), p. 167.
4. G. Hanna et al., Atomic Energy Review, VII, No. 3, 4 (1969).
5. V. F. Kuznetsov and G. N. Smirenkin, Nuclear Data for Reactors, Vol. II, IAEA, Paris (1967), p.75.
6. G. R. Keepin, Physical Foundations of Reactor Kinetics [Russian translation], Atomizdat, Moscow (1967).
7. J. Hopkins and B. Diven, Nucl. Phys., 48, 433 (1963).
8. D. Mather et al., Nucl. Phys., 66, 149 (1965).
9. M. Soleilhac et al., Nucl. Energy, 23, 257 (1969).
10. M. Soleilhac et al., Nuclear Data for Reactors, Vol. II, IAEA, Helsinki (1970), p. 145
11. M. V. Savin et al., idem, p. 157.
12. J. Boldeman and A. Dalton, Nucl. News, 10, 27 (1967).
13. D. Colvin and M. Sowerby, Physics and Chemistry of Fission, Vol. II, IAEA, Vienna (1965), p. 25.
14. N. I. Akimov et al., Yad. Fiz., 13, 484 (1971).
15. D. L. Shpak, Yu. B. Ostapenko, and G. N. Smirenkin, Yad. Fiz., 13, 950 (1971).
16. V. G. Nesterov and G. N. Smirenkin, At. Énerg., 24, 185 (1968).
17. W. Hart, ARSB(S)R-169 (1969).
18. L. I. Prokhorova and G. N. Smirenkin, Yad. Fiz., 13, 1170 (1971).

Declassified and Approved For Release 2013/02/27 : CIA-RDP10-02196R000300110005-5

Declassified and Approved For Release 2013/02/27 : CIA-RDP10-02196R000300110005-5

19. V. M. Strutinskii and V. A. Pavlinchuk, Physics and Chemistry of Fission, Vol. I, IAEA, Vienna (1965), p. 127.
20. B. G. Diven et al., Phys. Rev., 101, 1012 (1956).

Declassified and Approved For Release 2013/02/27 : CIA-RDP10-02196R000300110005-5

Declassified and Approved For Release 2013/02/27 : CIA-RDP10-02196R000300110005-5

DESIGN PRINCIPLES AND POSSIBLE APPLICATION OF ACCELERATORS WITH EXPLOSION-PRODUCED ULTRAHIGH MAGNETIC FIELD

V. S. Panasyuk, A. A. Sokolov, and B. M. Stepanov

UDC 621.384.639

The use in accelerator technology of explosively produced ultrahigh magnetic fields of the order of 1 MG and more makes it possible to reduce the dimensions of a cyclic accelerator to a minimum for a given final particle energy [1,2]. Furthermore, two methods of producing megagauss fields in an accelerator configuration are possible: either by compression of the magnetic flux by conducting shells or by excitation of single-turn magnetic systems with magneto-explosive current generators [2].

The technology for creating ultrahigh magnetic fields [3] achieved at this time in the USSR and abroad makes it possible to formulate the problem of its practical use in accelerators. However, the literature lacks detailed discussion of possible designs and possible areas of application for accelerators with an ultrahigh magnetic field. An attempt to fill this gap is made in the following.

In ordinary pulsed cyclic accelerators, the energy capacity of the magnet is the determining factor which decides the type of magnet system and which, in the final analysis, limits the intensity and energy of the accelerator; however, the energy capabilities of magneto-explosive generators make it possible to use magnetic systems like adiabatic traps with even greater energy capacity but structurally simpler. As a result, one can achieve considerable pulse intensity because of the comparatively large phase space of the beam. In the development of designs for such accelerators, it is natural to require that the systems for injection, acceleration, and ejection of particles be as simple as possible and suitable for the magnetic system of an accelerator with respect to size and cost. From the viewpoint of compactness, it is also obvious that the dimensions and weight of the accelerator must be commensurate with the corresponding parameters of magneto-explosive generators.

Particle dynamics in accelerators of this type have been discussed [4]. Experimental verification of the calculations was made with a model accelerator [5].

Induction Acceleration

Ordinarily, acceleration in betatrons is accomplished at a constant orbital radius. Induction acceleration with a variable radius requires an acceleration chamber with too large a radial aperature. Because of this the magnetic field is used inefficiently since the accelerated beam occupies only a small portion of it at the end of acceleration. However, with the production of ultrahigh magnetic fields by means of compressed metal shells, there is the possibility of comparatively efficient acceleration of particles with magnetic field dimensions close to the dimension of the accelerated beam during the entire acceleration cycle.

Let an accelerative configuration of a magnetic field be provided within a shell. Since the ratio of the square of the transverse momentum P to the field H in which a particle revolves is an adiabatic invariant, then*

$$\frac{P_i^2}{H_i} = \frac{P_f^2}{H_f}. \qquad (1)$$

*The subscripts "i" and "f" refer to the initial and final values of the corresponding quantities.

Translated from Atomnaya Énergiya, Vol. 33, No. 5, pp. 907-912, November, 1972. Original article submitted June 4, 1971; revision submitted March 17, 1972.

© 1973 Consultants Bureau, a division of Plenum Publishing Corporation, 227 West 17th Street, New York, N. Y. 10011. All rights reserved. This article cannot be reproduced for any purpose whatsoever without permission of the publisher. A copy of this article is available from the publisher for $15.00.

Declassified and Approved For Release 2013/02/27 : CIA-RDP10-02196R000300110005-5

Declassified and Approved For Release 2013/02/27 : CIA-RDP10-02196R000300110005-5

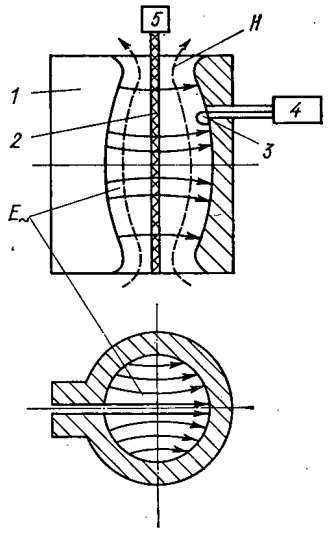

Fig. 1. Diagram of cyclic accelerator with ultrahigh magnetic field and high-frequency acceleration: 1) loop producing the magnetic field; 2) plasma filament; 3) coupling loop; 4) high-frequency oscillator; 5) plasma injector; E~ is high-frequency electric field for H_{111} oscillations.

On the other hand, with the compression of a cylindrical or spherical shell of radius R, there follows from the conservation law for magnetic flux

$$\frac{H_i}{H_f} = \frac{R_f^2}{R_i^2}. \tag{2}$$

Considering that $P \sim Hr$, we have from Eqs. (1) and (2)

$$\frac{P_f}{P_i} = \frac{R_i}{P_f} = \frac{r_i}{r_f}. \tag{3}$$

Thus particle momentum increases in proportion to the compression of the shell. If Δr_i and Δz_i are the initial amplitudes of the radial and vertical betatron oscillations, then [6]

$$\frac{\Delta r_i}{\Delta r_f} = \frac{\Delta z_i}{\Delta z_f} = \frac{H_f^{1/2}}{H_i^{1/2}}, \tag{4}$$

whence from consideration of Eqs. (2) and (3)

$$\frac{r_i}{r_f} = \frac{\Delta r_i}{\Delta r_f} = \frac{\Delta z_i}{\Delta z_f} = \frac{R_i}{R_f} = K,$$

where K is the compression coefficient. Thus within a compressed cylindrical or spherical shell, geometric similarity of the accelerated beam and the radial dimension of the driving magnetic field is fulfilled. Beam density increases in proportion to K^3.

High-Frequency Acceleration

Within a cylindrical loop with shaped internal walls and a particle source located on the loop axis (Fig. 1), let there be excited an ultrahigh pulsed magnetic field by means of a magneto-explosive current generator. If within the internal cavity of the loop used as a cylindrical cavity resonator high-frequency H_{111} waves are excited, the frequency and direction of the high-frequency field for this kind of oscillation is such that acceleration of particles within the cavity to relativistic energies can be ensured.

We consider this process in more detail. As is well known [7], the natural frequency of a cylindrical cavity resonator for H_{111} oscillations is given by the expression

$$f_c = \frac{c\sqrt{1+\left(\frac{2l}{3{,}41R}\right)^2}}{2l} \approx \frac{c}{3.4R} \quad (\text{for } l \gg R), \tag{5}$$

where l and R are the length and radius of the cylinder, and c is the velocity of light. For high-frequency acceleration, the rational frequency of an accelerated particle, $f = v/2\pi r$ (v is the velocity of an equilibrium particle), must coincide with the frequency f_c of the accelerating field (synchronism condition). Using Eq. (5), one can then obtain

Declassified and Approved For Release 2013/02/27 : CIA-RDP10-02196R000300110005-5

Declassified and Approved For Release 2013/02/27 : CIA-RDP10-02196R000300110005-5

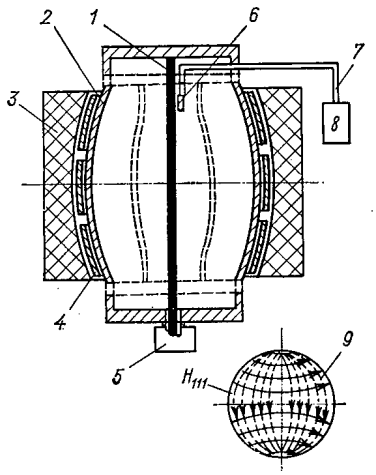

Fig. 2. Explosive betatron with compressed flux and high-frequency preacceleration: 1) plasma filament; 2) compressed shell; 3) explosive material; 4) solenoid for initial magnetic field; 5) plasma injector; 6) coupling loop; 7) high-frequency cable; 8) high-frequency oscillator; 9) distribution of high-frequency field for H_{111} oscillations ———) E; – – – –) H.

$$r = \varkappa\beta R;\ \beta = \frac{v}{c};\ \varkappa = 0{,}54. \tag{6}$$

Thus the orbit of an accelerated equilibrium particle must be an expanding spiral with a radius proportional to β and asymptotically approaching $r = \varkappa R$ for $\beta \to 1$. Such a trajectory can obviously only be provided by an increase in the value of the magnetic field within the cavity in accordance with

$$\beta E = eHr, \tag{7}$$

where E is the total energy of the particle and e is its charge. Strictly speaking, H here is the field at the radius r. For simplicity, however, we shall consider the field H to be uniform within the cavity. We obtain from Eqs. (6) and (7)

$$E = \varkappa eHR. \tag{8}$$

Since $E = Mc^2 + T = E_0 + T$, where M is the particle mass and T is its kinematic energy, it then follows from Eq. (8) that acceleration for a given type of particle is only possible starting at some magnetic field value

$$H_{\text{in}} = \frac{Mc^2}{\varkappa eR}, \tag{9}$$

for which the rational cyclotron frequency of a nonrelativistic particle $\omega_c = eH_{in}/Mc$ equals the rotational frequency of the accelerating field $\omega_{acc} = c/\varkappa R$.

For Eqs. (6), (8), and (9) and the relation $\beta^2 = 1 - (E_0/E)^2$, we find the variation of the radius r of the equilibrium particle as a function of H

$$r(H) = \varkappa R \sqrt{1 - \left(\frac{H_{\text{in}}}{H}\right)^2} \quad \text{for} \quad H \gg H_{\text{in}} \tag{10}$$

The described method of acceleration can be used as the fundamental one in accelerators with a stationary cylindrical magnet and as a preliminary stage of acceleration in accelerators with compressed magnetic flux, making it possible to use small injection energies in those accelerators. In the latter case, by analogy with betatron pre-acceleration in a synchrotron, this method can be called "synchrotron pre-acceleration in a betatron." One of the possible versions of a betatron with compressed magnetic flux and synchrotron pre-acceleration is shown schematically in Fig. 2.

Injection and Ejection of Particles in Explosive Cyclic Accelerators

The absence of an external injector is an ideal alternative for an explosive accelerator. To achieve this, a plasma filament containing particles chosen for acceleration is formed by some means or other along the axis of the acceleration chamber, which is simultaneously the magnet and resonator of the accelerator. With the achievement of a magnetic field value $H = H_{in}$, particles are pulled out of the plasma

Declassified and Approved For Release 2013/02/27 : CIA-RDP10-02196R000300110005-5

Declassified and Approved For Release 2013/02/27 : CIA-RDP10-02196R000300110005-5

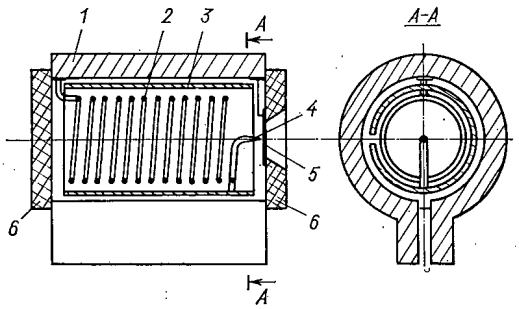

Fig. 3. Explosive direct action accelerator: 1) single-turn coil containing vacuum cavity; 2) secondary coil; 3) metal cylinder split along generatrix; 4) autoemission cathode; 5) foil window; 6) dielectric caps.

filament through the effect of the high-frequency voltage and are captured in phase. Their subsequent acceleration occurs in the manner described above. In some cases, however (for example, in the acceleration of unstable particles and antiparticles), an external injector is the only possibility. In those cases, one can use multiturn injection with filling of the acceleration region along the lines of the force of the magnetic field.

An attempt to estimate beam intensity in an accelerator with a cylindrical single-turn magnet reveals the unsoundness of the traditional approach to accelerators. Indeed, since the rotational radius of the particles is $r \approx 0.5R$ (see Eq. (6)) in our case, and the vertical dimension of the region of acceleration is commensurate with the radius r, resonances here may not lead to unlimited increase in oscillation amplitude and to particle loss because of possible significant nonlinearities in the motion. Because of the very large permissible energy spread, particularly in the betatron mode of acceleration, collective effects and instabilities are also significantly weakened. Calculations in accord with well-known formulas, which evaluate only the space charge of the particles, show that 10^{11}-10^{12} particles can be accelerated in a relativistic orbit for a high-frequency field intensity equal to $5 \cdot 10^5$ V/cm, for example.

Ejection of accelerated particles in a definite direction in an explosive accelerator with stationary magnet walls presents no difficulty. If the internal surface of the magnet has a projection at some azimuth, the high-frequency field is cut off after the achievement of a maximum magnetic field, and the outwardly spiralling particle beam in the decreasing field collides with the edge of the projection. Since the range of heavy particles in metals even at the kinetic energy of 1 GeV is a few centimeters, particles scattered at the edge of the projection, making a few rotations, enter the metal and leave the accelerator unhindered when the projection is sufficiently wide. The magnetic field is absent within the metal because of the skin effect in the walls, and is small outside it.

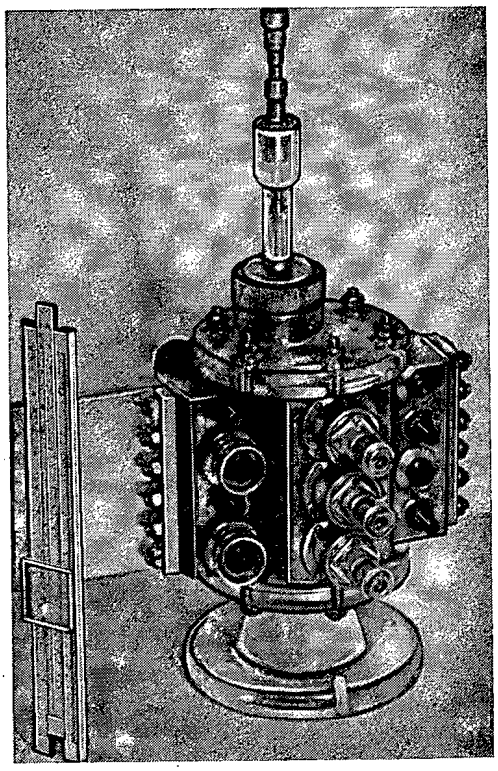

Fig. 4. Accelerator model without power supply circuits and pump.

In an accelerator with compressed magnetic flux, the only possibility for ejection of accelerated particles in a given direction is obviously deformation of the compressed shell at a given azimuth by a specially shaped explosion. If at the end of acceleration, the projection portion of the shell "overtakes" the compressed beam, particles passing through the shell in the region of the projection leave the accelerator.

Direct Action Accelerator

In addition to the possibilities for cyclic acceleration in an ultrahigh magnetic field discussed above, direct acceleration of charged particles is also feasible.

A design for a direct action accelerator of the transformer type is shown in Fig. 3. A single-turn primary coil is fed from a magneto-explosive current generator. A multiturn secondary coil is loaded by a cylinder which together with the primary coil forms a low-impedance coaxial line that provides the production of a large current of accelerated particles in a short pulse. It is obvious that an autoemission cathode can be used in the case of electron acceleration.

Since it is expected that the electrical stability of a vacuum gap for a transverse magnetic field of the order of 10^5 G and above is no less than in a magnetic field of the order

Declassified and Approved For Release 2013/02/27 : CIA-RDP10-02196R000300110005-5

Declassified and Approved For Release 2013/02/27 : CIA-RDP10-02196R000300110005-5

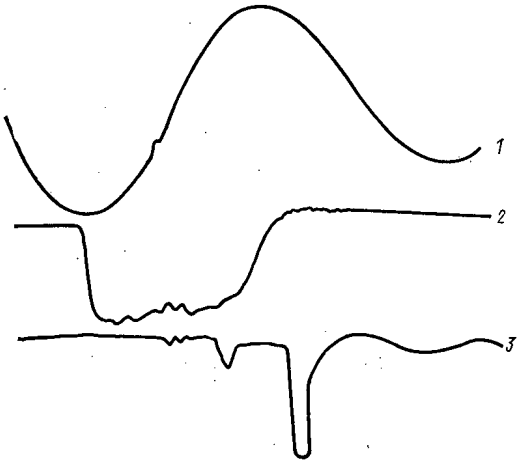

Fig. 5. Oscilloscope traces: 1) magnetic field pulse; 2) envelope of high-frequency voltage pulse; 3) bremsstrahlung pulse.

of 10^4 G [8], it appears possible to design a sufficiently compact accelerator with minimum gap between the transformer windings (low inductance leakage) and between the electrodes of the coaxial line (low wave impedance). The low inductance leakage of the coils makes it possible to produce large currents even without the coaxial line.

It should be noted that with an exponential current rise in magneto-explosive generators, the accelerating voltage and transverse magnetic field increase simultaneously. This ensures the necessary electrical stability of the gaps in the accelerator during the entire cycle of current rise.

Brief Information about the Experiment

Experimental verification of the high-frequency method of acceleration was made on an electron model fed from a condenser bank [5].

The model was constructed in the following manner. A massive copper loop which was the electromagnet and vacuum chamber of the accelerator was shaped internally so that within the cavity inside the loop a magnetic field was formed which was similar in shape to the field in an ordinary adiabatic trap with a mirror ratio approximately equal to two. At the same time, the cavity of the loop was used as a cavity resonator for the production of a high-frequency accelerating field of H_{111} waves. For this purpose, thin metal plates were fastened on the faces of the loop through insulating gaskets; the plates then served as closure for the high-frequency currents at the faces. An electron gun was used as the electron source; it injected a low-voltage electron beam (100 eV) along the loop axis that ionized the residual gas in the paraxial region. A general view of the accelerator without the power supply circuits is shown in Fig. 4.

Basic Model Parameters

Electron kinetic energy at final radius R_f = 1.75 cm	2 MeV
Maximum magnetic field induction at loop center	4.8 kG
Duration of acceleration cycle	2 μsec
Accelerating electric field intensity	500 V/cm
Accelerating field wavelength	11 cm

Figure 5 shows oscilloscope traces of the magnetic field pulse, of the envelope of the high-frequency voltage pulse, and of the bremsstrahlung pulse.

Prospects for the Use of Cyclic Accelerators with Ultrahigh Magnetic Field

The question of producing particles of ultrahigh energies by the methods discussed is quite problematical [2]. The required energy in this case approximates the energy of a thermonuclear explosion.

However, there is a particular area in which the use of explosive accelerators for experiments in the physics of ultrahigh-energy particles is feasible. The point of the discussion is intersecting beams of unstable secondary particles with charges of different signs accelerated by the induction method with compression of a conducting shell. The transverse dimensions of the acceleration region of the designs discussed above are comparable with the relativistic radii of the particles. One can therefore capture in acceleration secondary beams with very large energy and angular spreads. The large acquisition of energy per turn makes it possible to use these accelerators for increasing the energy of muons (lifetime, $2.2 \cdot 10^{-6}$ sec) and even of π mesons (lifetime, $2.5 \cdot 10^{-8}$ sec). The increase in beam density, which is proportional to the cube of the compression coefficient, is extremely important for intersecting beams.

Declassified and Approved For Release 2013/02/27 : CIA-RDP10-02196R000300110005-5

Declassified and Approved For Release 2013/02/27 : CIA-RDP10-02196R000300110005-5

Some quantitative estimates are made. Let the final volume of the magnetic field of a cylindrical conducting shell be, for example, 1 liter (diameter, 10 cm and height, 12 cm), and the final induction be $5 \cdot 10^6$ G. The magnetic field energy is then 100 MJ. In order to obtain such energy it is necessary to explode not less than 300 kg of trinitrotoluol [3]. Based on the initial dimensions of the aperture, one should consider the final orbital radius of the beams which are formed to be equal to half the final radius of the shell. The muon energy in each of the beams is then ~3.75 GeV and the relative energy of the intersecting beams is 300 GeV [6]. We determine the value of the intensity of the accelerating electric field for which particles with a lifetime t_0 in the rest state will live infinitely long in the acceleration mode. As is well known,

$$t = t_0\gamma, \tag{11}$$

where t is the time in the laboratory system and $\gamma = 1/(1-\beta^2)^{1/2} = E/E_0$ [12]. Consequently $t = t_0E/E_0$, and for a relativistic velocity expressed through momentum

$$t \approx t_0 \frac{cP}{E_0}. \tag{12}$$

Differentiating Eq. (12), one obtains

$$\frac{t_0 c}{E_0} \frac{dP}{dt} \approx 1. \tag{13}$$

Since $dP/dt = e\mathscr{E}$ ($\mathscr{E}$ is the electric field intensity) and $E_0 = Mc^2$, we have

$$\mathscr{E} \approx \frac{Mc}{et_0}. \tag{14}$$

Substituting values appropriate for π mesons ($M/e \approx 1.5 \cdot 10^{-9}$ kg/C and $t_0 = 2.5 \cdot 10^{-8}$ sec), we find $\mathscr{E} \approx 1.8 \cdot 10^5$ V/cm. For the induction and orbital radius values given here (respectively, $5 \cdot 10^6$ G and 2.5 cm) and a shell velocity of 20 km/sec [2], we find $\mathscr{E} \approx 10^5$ V/cm. Thus one can obtain an electric field intensity close to that required for the acceleration of π mesons and approximately a factor of 10^2 greater than that needed for the acceleration of muons ($t_0 = 2.2 \cdot 10^{-6}$ sec). Energy loss in synchrotron radiation is ~8 keV per turn for mesons and need not be taken into consideration in comparison with the acquisition of energy.

We further consider the possible areas of application of accelerators with high-frequency acceleration. In selecting the volume and magnitude of the magnetic field for high-frequency acceleration, the range of energy capability and design already developed for magneto-explosive current generators is preferable. The resonance wavelength of the electro-magnet cavity must be chosen in the decimeter range. The latter circumstance is of great importance because there is a large choice of pulsed sources of high-frequency power in that range with power to tens of megawatts.

A small orbital radius for large particle energy makes it reasonable to face the problem of generation in such accelerators of an intense pulse of synchrotron radiation which can be used for the study of the properties of solids and also in metrology [9]. Let the dimensions of the loop be the same as the dimensions of the compressed shell in the previous case. Then the resonance wavelength for H_{111} waves is 11 cm.

According to Eq. (6), the relativistic radius is approximately half the geometric radius and is 2.5 cm. Electron energy for an induction of 10^6 G, for example, is 0.8 GeV and the radiation per turn is 1.3 MeV. In order to keep the electrons in a relativistic orbit with this radiation, an accelerating electric field intensity of ~0.3 MV/cm is required. If, for example, only 10^6 electrons arrive in the relativistic orbit, synchrontron radiation power in a pulse ~3 μsec long (a typical time for the main increase and retention of the magnetic field in a magneto-explosive generator) is 4 MW.

One should turn to a problem which is technically more difficult to resolve but more interesting in principle – acceleration of multiply charged ions. In contrast to the usual cyclotron [10], the open column of plasma must be transparent to the accelerating high-frequency field in the cyclic accelerator designs discussed. This is explained by the fact that the radii of the first turns of heavy particles are of the order of hundredths of a millimeter; consequently, for the normally assumed dimensions of the plasma column, the source of acceleration must occur within it. Further than that, the cyclotron mode is formed under these circumstances long before the escape of an ion from the plasma. Therefore ions with a low charge state (nonresonance e/M) will not escape from the source as in an ordinary cyclotron where particles are extracted by the high-frequency field independently of the value of e/M. Because of this, the number of ions of low charge state, from which multiply charged ions are formed, drops sharply.

Declassified and Approved For Release 2013/02/27 : CIA-RDP10-02196R000300110005-5

Declassified and Approved For Release 2013/02/27 : CIA-RDP10-02196R000300110005-5

We present a few estimates. For a high-frequency field with a wavelength of 11 cm and a ratio e/M $\approx$ 0.2 typical of multiply charged ions, the resonance cyclotron magnetic field must be 5 MG. For example, the energy of octuply charged argon beginning acceleration at the center is ~100 MeV at the boundary of a plasma column 5 mm in diameter, and the energy in a relativistic radius is of the order of 30 GeV.

LITERATURE CITED

1. Ya. P. Terletskii, Zh. Éksp. Teor. Fiz., 32, 1396 (1961).
2. A. D. Sakharov, Usp. Fiz. Nauk, 88, 725 (1966).
3. G. Knopfel' Ultrahigh Pulsed Magnetic Fields [Russian translation], Mir, Moscow (1972).
4. A. V. Gryzlov et al., Zh. Tekh. Fiz., No. 1, 13 (1972).
5. A. V. Gryzlov et al., Report to II All-Union Conference on Charged-Particle Accelerators (Moscow, November 11-18, 1970).
6. A. A. Kolomenskii and A. N. Lebedev, Theory of Cyclic Accelerators [in Russian], Fizmatgiz, Moscow (1962).
7. I. V. Lebedev, UHF Techniques and Instruments [in Russian], Vysshaya Shkola, Moscow (1970).
8. R. B. Baksht and G. A. Mesyats, Izv. Vuzov, Fizika, No. 7, 144 (1970).
9. R. Godvin, Usp. Fiz. Nauk, 101, No. 3, 493 (1970).
10. V. S. Panasyuk, At. Énerg., 3, No. 10, 340 (1957).

Declassified and Approved For Release 2013/02/27 : CIA-RDP10-02196R000300110005-5

Declassified and Approved For Release 2013/02/27 : CIA-RDP10-02196R000300110005-5

ABSTRACTS

THE CONSTRUCTION OF A PROBABILISTIC MODEL OF THE DISTRIBUTION OF NUCLEAR POWER STATION WASTES VENTED TO THE AIR

L. I. Piskunov

UDC 621.039.75:519.21:614.73

Meteorological factors are not consistently given their due share of attention in theoretical calculations of radioactive pollutants vented to the surrounding air from nuclear power stations. This has prompted a new look at the possibility of constructing a probabilistic model which would make it possible to represent the total probability of $G_{i,j}$-events exerting an influence on the distribution of vented discharges Q on the underlying surface.

The probability that some elemental area in the locality will be contaminated is determined by the formula

$$P(A) = 1 - \prod_{i=1}^{l} \nu_i \prod_{j=l+1}^{m} \nu_j,$$

where $\nu_i = 1 - p_i$, $\nu_j = 1 - p_j$, p_i and p_j are the total probabilities due to the set of events Q and $G_{i,j}$ for $Q > 0$. The set of G_i-events includes the wind direction and wind velocity, turbulent exchange, atmospheric stability, dilution and scattering of radioactive impurities, surface roughness factor, temperature inversion, and calms. The G_j-events include washout of impurities by atmospheric precipitation and the factor of secondary contamination due to ash transport of activity over the surface. All of the above factors are considered basic in the problem.

The discrete factors (the height of the ventilation stack, the distance from the stack and the azimuth) and some of the probabilities of the G_i-events are expressed with the aid of results derived from the

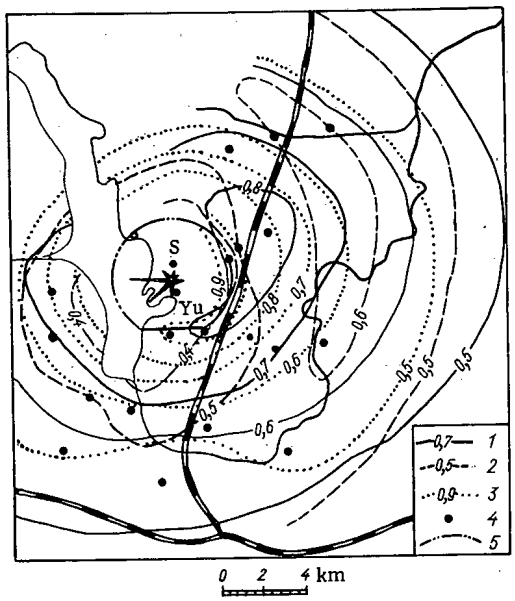

Fig. 1. Probabilistic model of overland distribution of discharges. 1) Isoprobits P(A) over a year's time; 2) same during period from November through March; 3) same over period from May through September; 4) dosimetric monitoring stations; 5) sanitary protection zone.

Translated from Atomnaya Énergiya, Vol. 33, No. 5, p. 913, November, 1972. Original article submitted April 7, 1972; abstract submitted June 26, 1972.

© 1973 Consultants Bureau, a division of Plenum Publishing Corporation, 227 West 17th Street, New York, N. Y. 10011. All rights reserved. This article cannot be reproduced for any purpose whatsoever without permission of the publisher. A copy of this article is available from the publisher for $15.00.

Declassified and Approved For Release 2013/02/27 : CIA-RDP10-02196R000300110005-5

Declassified and Approved For Release 2013/02/27 : CIA-RDP10-02196R000300110005-5

semi-empirical theory advanced by Berlyand [1]. The other probabilities of the $G_{i,j}$-events are treated on the basis of other known data, for example, the surface roughness [2,3], scatter of impurities in the wastes ejection cone [2], and washout of impurities by atmospheric precipitation [4].

The practical application of the model is illustrated by the example of a nuclear power station in the form of isoprobit curves P(A) of the distribution of aerosol waste discharges in the outer zone (see Fig. 1). Clearly, the maximum density of local activity fallout corresponds to the windward side of the nuclear power station, and it is found within the confines of the sanitary protection zone during the summer months (May to September). Over the November-March period, the maximum shifts to a distance of 8-9 km from the nuclear power station, because of the high wind velocities prevailing during the cold period of the year. On the whole, the calculated distribution of wastes discharges is in satisfactory agreement with dosimetric monitoring data.

The described probabilistic model provides a more complete picture than obtainable from calculations based solely on turbulent diffusion formulas. It can be useful in the design and operation of nuclear power stations, and also in forecasting the radiation picture in zones where power stations are cited.

LITERATURE CITED

1. M. E. Berlyand, Trudy GGO, No. 138, Gidrometeoizdat, Leningrad (1963), p. 31.
2. Meteorology and Atomic Energy [Russian translation], IL, Moscow (1959).
3. D. L. Laikhtman et al., Trudy LGMI, No. 15, Izd. Leningrad. Gos. Univ., Leningrad (1963), p. 37.
4. B. I. Styro, Self-Decontamination of Atmosphere Eliminating Radioactive Pollutants [in Russian], Gidrometeoizdat, Leningrad (1968).

MEASUREMENT OF THE MULTIPLICATION FACTOR OF FISSION NEUTRONS IN THE $Be^9(n,2n)$ REACTION IN BERYLLIUM AND BERYLLIUM OXIDE BY THE MANGANESE-TANK METHOD

I. F. Zhezherun and V. A. Taraban'ko

UDC 539.17

The article describes an experiment which is diagrammed in Fig. 1. As the source of fission-spectrum neutrons we used a converter made of $U_3^{235}O_8$ in a thin-walled aluminum container. The converter was placed in a beam of neutrons from the thermal column of a reactor, at the center of a tank filled with a solution of $KMnO_4$ in distilled water.

The measurement procedure was the following. The necessary material was placed in the tank, and the converter was then irradiated with a beam of neutrons. After irradiation, the solution was carefully mixed, and six 5-liter samples were taken from the tank and passed through paper filters. After the filters had been dried, their activity was measured on a number of $\beta-\gamma$ instruments with an accuracy of no worse than 0.5%. The background activity was determined by blocking the neutron beam with cadmium.

The following were successively placed in the cavity around the converter: a) a beryllium sphere, with a thickness of 16.7 g/cm^2 in the spherical layer of beryllium; b) a graphite cube 30 cm on a side, with a thickness of 29 g/cm^2 for an equivalent spherical layer of graphite; c) a cube made of baked beryllium oxide, 20 cm on a side, with a thickness of 30 g/cm^2 for an equivalent spherical layer.

The ratios of the corresponding activities, converted to the values for infinite time of irradiation and averaged over a number of measurements, were found to be:

Translated from Atomnaya Énergiya, Vol. 35, No. 5, p. 914, November, 1972. Original article submitted June 30, 1971; abstract submitted May 31, 1972.

Declassified and Approved For Release 2013/02/27 : CIA-RDP10-02196R000300110005-5

Declassified and Approved For Release 2013/02/27 : CIA-RDP10-02196R000300110005-5

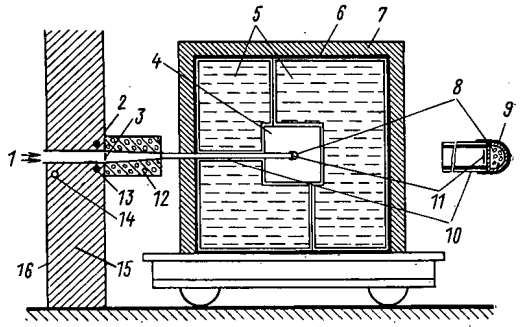

Fig. 1. Geometry of the experiment: 1) beam of neutrons from the thermal column; 2,13,14) neutron monitors (ionization chamber and boron counters); 3,11) copper foil monitors; 4) cavity inside the tank for placement of materials (dimensions of cavity 30 × 30 × 30 cm); 5) demountable aluminum tank (100 × 100 × 100 cm) with manganese solution; 6) cadmium covering of tank; 7) paraffin shielding of tank; 8) neutron converter; 9) cadmium cap of converter; 10) aluminum tube with cylindrical cadmium tube inside; 12) collimator; 15,16) shielding.

$$\frac{\bar{A}_\infty(\mathrm{Be})}{\bar{A}_\infty(\mathrm{C})} = 1.078 \pm 0.010; \quad \frac{\bar{A}_\infty(\mathrm{BeO})}{\bar{A}_\infty(\mathrm{C})} = 1.030 \pm 0.007.$$

To these values we applied corrections (1.0216 ± 0.0100 for beryllium and 1.0101 ± 0.0100 for beryllium oxide) to take account of the difference in the absorption of the neutrons contained in the cavity, and we obtained the multiplication factors for the fission neutrons: $K^{n,2n}_{Be} = 1.101 \pm 0.015$; $K^{n,2n}_{BeO} = 1.040 \pm 0.010$. The corrections were determined experimentally by measuring the activities with the different inserts when we used no converter and when we replaced the converter with a Po + Be neutron source (with or without cadmium in the cavity).

The beryllium layer in the experiment was thick enough to enable us to accept the resulting multiplication factor as the one for an infinite medium. The beryllium oxide layer was not thick enough. However, on the basis of the results found in [1], the measured value of $K^{n,2n}_{BeO}$ was recomputed for the case of an infinite medium and found to be 1.048 ± 0.010.

In this experiment we also conducted a more careful analysis of the results of [1] and found a value of 1.085 ± 0.015 for $K^{n,2n}_{Be}$.

Thus, on the basis of the two experiments, the most probable value of $K^{n,2n}_{Be}$ should be 1.09 ± 0.01.

LITERATURE CITED

1. I. F. Zhezherun et al., At. Énerg., 15, 485 (1963).

PERTURBATION THEORY IN CALCULATIONS OF THERMAL NEUTRON UTILIZATION FACTOR

R. A. Peskov

UDC 621.039.564.5

Perturbation theory based on the multigroup diffusion approximation has been winning increasing favor in calculations of variations in the effective multiplication coefficient and other functionals of the neutron flux levels in homogeneous reactors [1]. That type of method is less suited to calculating variations in the thermal neutron utilization factor θ for thermal neutrons due to the variation in the parameters of multiregion cells, because of the insufficient exactness of the diffusion approximation and because of the large perturbations involved. That means that we cannot rest content with the first approximation in the diffusion theory of perturbations. Integral methods, the albedo method prominent among them [2], are generally used in calculating θ.

Perturbation theory is developed in the present article within the framework of the albedo method for calculating variations of θ in multiregion annular cells. The problem is formulated in the multigroup scheme with thermalization of neutrons taken into account. Numerical examples are cited for the one-group

Translated from Atomnaya Énergiya, Vol. 33, No. 5, pp. 914-915, November, 1972. Original article submitted October 20, 1971.

Declassified and Approved For Release 2013/02/27 : CIA-RDP10-02196R000300110005-5

Declassified and Approved For Release 2013/02/27 : CIA-RDP10-02196R000300110005-5

case, illustrating the high accuracy of the method proposed in the face of appreciable variations in absorption cross sections in the different zones of the cell.

The increment in θ is calculated in the first approximation of perturbation theory for the albedo method ($\Delta\theta_{alb}$) in terms of increments in the probabilities describing neutron diffusion through "perturbed zones" of the cell, and also in terms of unilateral currents impinging on those zones of neutrons and "unilateral worths" (probabilities of capture in the fuel) for neutrons escaping from those zones.

The neutron currents and neutron worths are calculated only for the principal variant. Variations in $\Delta\theta_{alb}$, in contrast to the first approximation of diffusion theory, contain a correction not only of the first order in the perturbed parameters (cross sections and dimensions of zones or regions) but also higher-order corrections since the probabilities are nonlinear functions of those parameters. The second-order correction is taken into account in an approximate manner, but its exactness is in inverse proportion to the perturbation of the unilateral currents impinging on the zones of neutrons in question or the worths of the escaping neutrons. That is more or less the case, for instance, for a central absorbing rod in a cell, since the neutron currents and worths are in that case due primarily to neutrons that do not enter the rod immediately.

It is anticipated that the use of the method proposed here will drastically shorten computational time in many-group multiregion problems. The method of perturbation theory is indispensable in calculating subtle effects when perturbations are small and when the effects we are interested in are comparable to the error in "direct calculations."

LITERATURE CITED

1. G. I. Marchuk, Nuclear Reactor Design Computational Techniques [in Russian], Gosatomizdat, Moscow (1961).
2. V. P. Slizov, Inzh.-Fiz.Zh., No. 1, 80 (1964).

AN EFFECTIVE METHOD FOR CALCULATING THE NEUTRON FIELD IN GEOMETRICALLY COMPLEX LATTICES OF HETEROGENEOUS REACTORS

V. V. Smelov

UDC 539.125.52

The microstructure of the neutron field in the lattice of a heterogeneous reactor must be known in order to calculate the major parameters of the heterogeneous reactor (thermal neutron utilization factor, disadvantage factor, etc.). Calculations of such a field come to constitute a rather complicated problem whenever blocks or slugs of different types are located in the medium. The present article, which puts forth an approximate method for solving the single-velocity transport equation in cylindrical lattices of complex configuration,* is devoted to precisely that problem.

The first element in the method proposed is that a network of curves L separating slugs of different types from one another and obeying the same doubly periodic law as the lattice itself is overlaid on the transverse cross section plane of the lattice. Further, in each of the regions formed by the network L

*It is assumed that slugs of each type are arranged in the medium in some periodically recurrent pattern, and that they are multilayered circular-base cylinders.

Translated from Atomnaya Énergiya, Vol. 33, No. 5, pp. 915-916, November, 1972. Original article submitted October 20, 1971; revision submitted June 17, 1972.

Declassified and Approved For Release 2013/02/27 : CIA-RDP10-02196R000300110005-5

Declassified and Approved For Release 2013/02/27 : CIA-RDP10-02196R000300110005-5

(with an isolated slug of some particular form) we construct a polar system of coordinates with the pole in the center of the slug. In each of those regions D_i ($i = 1, 2, \ldots$), the neutron flux φ_i will be a function of the variables r_i, ω_i, μ, ψ_i, where r_i, ω_i are the polar coordinates of the space lattice, and $\mu = \cos\theta$ and ψ_i are angular coordinates of the neutron velocity vector in the spherical system of coordinates fixed in the point (r_i, ω_i) in the usually accepted manner.

The second element in the method is to undertake a search for a neutron flux function with respect to φ_i (r_i, ω_i, μ, ψ_i) in the form of the following series:

$$\varphi_i(r_i, \omega_i, \mu, \psi_i) = \frac{1}{4\pi} \sum_{n=0}^{\infty} \sum_{m=-n}^{n} \sum_{\nu=-\infty}^{\infty} (2n+1)(n+m)!(n-m)! C_{nm}^{(\nu)}(r_i) S_{nm}^{(\nu)}(\mu, \psi_i, \omega_i) \quad (1)$$

in terms of a complete orthogonal system of functions $S_{nm}^{(\nu)}(\mu, \psi, \omega)$ of the three independent variables

$$S_{nm}^{(\nu)}(\mu, \psi, \omega) = \frac{(-1)^m}{(n+m)!} P_n^{(m)}(\mu) e^{i\left(m\psi + \frac{\pi\nu}{l}\omega\right)}$$

$$(n = 0, 1, 2, \ldots; \; m = 0, \pm 1, \pm 2, \ldots \pm n;$$

$$\nu = 0, \pm 1, \pm 2, \ldots),$$

where l is the minimum period of the function $\varphi(r, \omega, \mu, \psi)$ in ω. We end up with an infinite system of ordinary differential equations with respect to the functions $C_{mn}^{(\nu)}(r)$.

The proposed approximate algorithm for solving the problem is based on retention of a finite number of terms in the expansion (1), so that the system of differential equations becomes converted into a finite system. It is fortunate that the system of differential equations, as well as the conditions prevailing at the pole and on the boundaries of the annular zones, "split" with respect to the variable ν. That enables us (while ignoring, for the time being, the "matching" or "joining" conditions along the network L, where the split with respect to ν no longer occurs) to derive, for each value of ν, a general solution of the corresponding finite system of differential equations which will satisfy the conditions prevailing at the pole and on the boundaries of the annular zones. That general solution can be found numerically, and contains four (three) arbitrary constants when $\nu \neq 0$ (when $\nu = 0$).

The concluding step in the method is to determine all of the arbitrary constants on the basis of the fully determined joining conditions along the network L.

A fairly general-purpose working program in ALGOL language worked out at the Computing Center of the Siberian Division of the Academy of Sciences of the USSR demonstrated how effective the method actually is: complete calculations for a complicated lattice requiring the P_3-approximation were carried out within 5-7 sec on a BÉSM-6 digital computer.

ESTIMATION OF PRODUCTION COSTS OF CHEMICALS PRODUCED IN NUCLEAR REACTORS

E. A. Borisov and V. D. Timofeev

UDC 621.039.5

Chemical processes utilizing the radiation from nuclear fuel will be possible in principle within the not-too-distant future. This radiation constitutes a cheap form of energy. If the cost of power derived from isotope sources of radiation is 1 dollar per kWh, then the use of mixed radiations from a nuclear reactor can cut that cost down to 0.1 dollar per kWh, and the cost can be lowered still further to 0.001 dollar

Translated from Atomnaya Énergiya, Vol. 33, No. 5, p. 916, November, 1972. Original article submitted December 7, 1971; revision submitted May 22, 1972.

Declassified and Approved For Release 2013/02/27 : CIA-RDP10-02196R000300110005-5

Declassified and Approved For Release 2013/02/27 : CIA-RDP10-02196R000300110005-5

per kWh, by using the fission fragments of fissionable material [1]. From that standpoint, prospects for engineering chemical processes involving the practical use of nuclear reactors appear highly promising.

But net production cost estimates for streams based on such reactions as synthesis of nitrogen oxides, monoxide, etc., have led to the conclusion that those processes are still not economically competitive with conventional chemical technology. That has brought about a need to expand searches for new reactions and ways of estimating prospects of various processes at a sufficiently early stage in research and development.

A procedure for making cost estimates of the outlook for radiation-chemical synthesis processes involving the use of a nuclear reactor as the source of radiations has been worked out on the basis of tentative laboratory data. The following structure of costs governing net production costs when a nuclear reactor is used has been accepted: raw materials and processed materials (including auxiliary materials), nuclear fuel costs (fuel component), power costs, amortization writeoff, department costs (including building erection and upkeep costs, costs of structures and equipment, personnel wages, etc.), total-plant costs, income from side products (including power generated by the nuclear reactor).

Possibilities of calculating each of the cost items are discussed. A procedure is worked out to handle estimates of net production costs of chemical items when a nuclear reactor is used as the radiation source, on the basis of limited information on the process. The calculations call for knowledge of the radiation-chemical yield of the product at a specified content by weight of material in the feed mixture under conditions realizable in the given reactor, as well as costs of raw materials and yield of side products.

No less importance is given in the article to the reverse method of calculations, when the productivity that has to be attained in order for the net production costs of a given production item to satisfy practical needs is determined. That procedure can be used, consequently, in the selection of research trends and in posing the problem to be tackled by investigators.

LITERATURE CITED

1. M. Steinberg, Chem. Engng. Progress, 62, No. 9, 105 (1966).

THE INTERACTION BETWEEN URANIUM MONOCARBIDE AND NITROGEN

A. R. Beketov, V. G. Vlasov, V. A. Bezdenezhnykh, and V. A. Talinin

UDC 541.661.879.1

This article discusses the kinetics and the mechanism of nitration of uranium monocarbide in 923-1223°K temperature range at a gas pressure of $(6.67 \cdot 10^{-3})$-$(80.0 \cdot 10^4)$ N/m^2. As the starting materials we used: a) powdered uranium carbide ($UC_{0.99}$) containing 95.25% uranium and 4.75% carbon; b) gaseous nitrogen containing no more than 10^{-3} vol. % impurities. The process was monitored by directly measuring the weight of the materials used, with constant circulation of the gaseous reagent. The reaction products were analyzed for free and bound carbon, nitrogen, and uranium content, and, in addition, their phase composition was measured by an x-ray method.

During the initial stage the process is described by the following kinetic equation:

$$g^2 = k_1\tau, \quad (1)$$

which is valid for conversions up to 13% at 923 and 1023°K, and for conversions up to 20% at temperatures of 1123-1223°K (we took 100% conversion to be the complete conversion of uranium monocarbide to the

Translated from Atomnaya Énergiya, Vol. 33, No. 5, pp. 916-917, November, 1972. Original article submitted December 3, 1971.

Declassified and Approved For Release 2013/02/27 : CIA-RDP10-02196R000300110005-5

Declassified and Approved For Release 2013/02/27 : CIA-RDP10-02196R000300110005-5

TABLE 1. Values of the Constants in Eqs. (1) and (2).

T, °K	Eq. (1)	Eq. (2)		
	k_1	τ_0, min	g_0, %	k_2
923	3,2	50	20	0,12
1023	6,2	30	20	0,14
1123	13,3	30	30	0,36
1223	20,1	20	30	0,67

sesquinitride). During the second stage the weighed portion increases in weight in accordance with the equation

$$(g-g_0)=k_2(\tau-\tau_0). \quad (2)$$

The nature of the subsequent stages of the nitration depends on the experimental temperature. The values of the constants in Eqs. (1) and (2) are shown in Table 1.

The constant k_1 varies with temperature according to the equation

$$k_1=10^{6.2}\exp\left(-\frac{12900}{T}\right),$$

and with gas pressure according to the equation

$$k_1=1.18\cdot10^{-4}(P)^{1.15},$$

where P is expressed in N/m^2. The composition of the reaction products $UC_{1-x}N_x$ and U_2N_{3+x}, as well as the relationship between the phases, depends on the temperature, the nitrogen pressure, and the duration of the experiment. The nitration of uranium oxycarbide takes place at faster rates than that of uranium carbide. It is assumed that the process is determined by the amount of nitrogen reaching the reaction zone through the covering layer of uranium nitrides.

DISTRIBUTION OF CHARGED AND NEUTRAL PARTICLE CONCENTRATIONS IN A QUASISTATIONARY HIGH TEMPERATURE TURBULENT PLASMA

A. G. Kitainer and G. V. Sholin

UDC 533.9.17

In recent years, experimental data has been published which, upon analysis, indicates the role of diffusion processes in the determination of the degree of ionization of a laboratory plasma [1], while the degree of ionization is not determined by the volumetric balance of the ionization and recombination processes, but by the ionization in the volume and by the diffusion of the plasma at the wall.

In the present paper, this problem is solved for the case of a high temperature, turbulent, confined plasma. Quasistationary conditions are considered, in which the mean free path of the atoms, as compared with the ionization, charge transfer, and elastic scattering length l_0, exceeds the dimensions of the system. The diffusion coefficient D and the ionization rate coefficient for atoms due to electron collisions S are assumed to be constants. With these assumptions, the density, averaged over the cross section, of neutral atoms N_0 depends on the transverse diffusion of the plasma D and the coefficient of ionization S. For cylindrical geometry this relationship has the form

$$N_0=\frac{\beta_1^2 D}{R_0^2 S}, \quad (1)$$

where β_1 is the first root of the Bessel function $I_0(x)$; R_0 is the radius of the system.

The distribution of the electrons with respect to the radius is found:

$$N_e(r)=N_e(0)\,I_0\left(r\sqrt{\frac{N_0 S}{D}}\right) \quad (2)$$

Translated from Atomnaya Énergiya, Vol. 33, No. 5, p. 917, November 1972. Original article submitted December 3, 1971.

Declassified and Approved For Release 2013/02/27 : CIA-RDP10-02196R000300110005-5

Declassified and Approved For Release 2013/02/27 : CIA-RDP10-02196R000300110005-5

and for the neutral atoms:

$$N_0(r)=\frac{4I}{u}\left\{1-\frac{2}{3}N_e(0)\frac{R_0}{u}\left[S+\langle\sigma v\rangle_{\text{slow}}\left(1-\frac{u}{u_i}\right)\right]\left[\frac{2}{3}\left(2-\frac{r^2}{R_0^2}\right)E\left(\frac{r}{R_0}\right)-\frac{1}{3}\left(1-\frac{r^2}{R_0^2}\right)K\left(\frac{r}{R_0}\right)\right]\right\}. \quad (3)$$

Here, K(x) and E(x) are the complete elliptic integrals of first and second order; $\langle\sigma v\rangle_{\text{slow}}$ is the charge transfer coefficient; u and u_i are the velocities of the neutral atoms and the ions, respectively.

The results of the investigation carried out can also be applied to the case of a system containing two types of neutral atoms: 1) slow, originating at the wall and having a mean free path with respect to charge transfer and ionization $l_{\text{slow}} \ll R_0$; 2) fast, generated as a result of the charge transfer of hot ions and having $l_{\text{fast}} > R_0$. In addition, the density of the fast atoms, averaged over the cross section, is virtually constant and obeys Eq. (1), while the density of the slow atoms is vanishingly small at the center of the chamber and increases exponentially at the limits of the region, attaining the value

$$N_{\text{slow}}=N_{\text{fast}}\ \frac{u_i}{u}\cdot\frac{\langle\sigma v\rangle_{\text{slow}}+S}{\langle\sigma v\rangle_{\text{slow}}}.$$

The results obtained are necessary for a correct analysis of spectroscopic measurements, in particular, for the determination of the excited containment time for particles in confined systems from the absolute intensities of spectral lines [2].

LITERATURE CITED

1. K. Bergstedt, Z. Naturforsch, 24a, 299 (1969).
2. G. A. Bobrovskii et al., Pis'ma ZhÉTF, 9, 269 (1969).

THE EFFECT OF NEUTRON RADIATION ON THE SPECTROMETRIC CHARACTERISTICS OF Si(Li) DETECTORS

S. M. Solov'ev, L. I. Tybin, and V. P. Éismont

UDC 539.1.074.88

It is known that the spectrometric properties of all silicon semiconductor detectors are impaired by the action of neutrons. Diffusion-drift detectors are especially sensitive, since they operate at relatively low electric field intensities. The literature does not give any quantitative data on the effect of irradiation with fast neutrons on the spectrometric characteristics of modern Si(Li) detectors.

In our investigations we used detectors which had an energy resolution of 1.3-1.6 keV for x-rays and gamma quanta with energies of 6-60 keV at T = −140°C. The measurements were conducted with a spectrometer described in an earlier report [1]. We used the isotope Cf^{252} as our source of neutrons (with an average energy of 2.3 MeV).

We tested three detectors. The first and second detectors were irradiated in a flux with a density of $\psi = 2.6 \cdot 10^5$ neutrons/cm^2·sec at T = −140°C. The third detector was irradiated in a flux with a density of $\psi = 1.1 \cdot 10^4$ neutrons/cm^2·sec and refrigerated only while the measurements were being made. All the detectors were made of the same material (silicon with a resistivity of ρ = 2000-3000 Ω·cm and a lifetime of τ = 1500 μsec) and by the same manufacturing process.

The data on the variation of energy resolution for the three detectors are shown in Fig. 1. For a quantitative representation of the degree of damage in the detectors, it is convenient to represent the half-width ΔE for a spectral as the geometric sum of the initial resolution ΔE_0 and the increment due to the irradiation, $\Delta E_n(\Phi)$, which depends on the integral neutron flux $\Phi = \psi_t$, $\Delta E^2(\Phi) = \Delta E_0^2 + \Delta E_n^2(\Phi)$. According

Translated from Atomnaya Énergiya, Vol. 33, No. 5, pp. 918-919, November, 1972. Original article submitted January 24, 1972; revision submitted May 15, 1972.

Declassified and Approved For Release 2013/02/27 : CIA-RDP10-02196R000300110005-5

Declassified and Approved For Release 2013/02/27 : CIA-RDP10-02196R000300110005-5

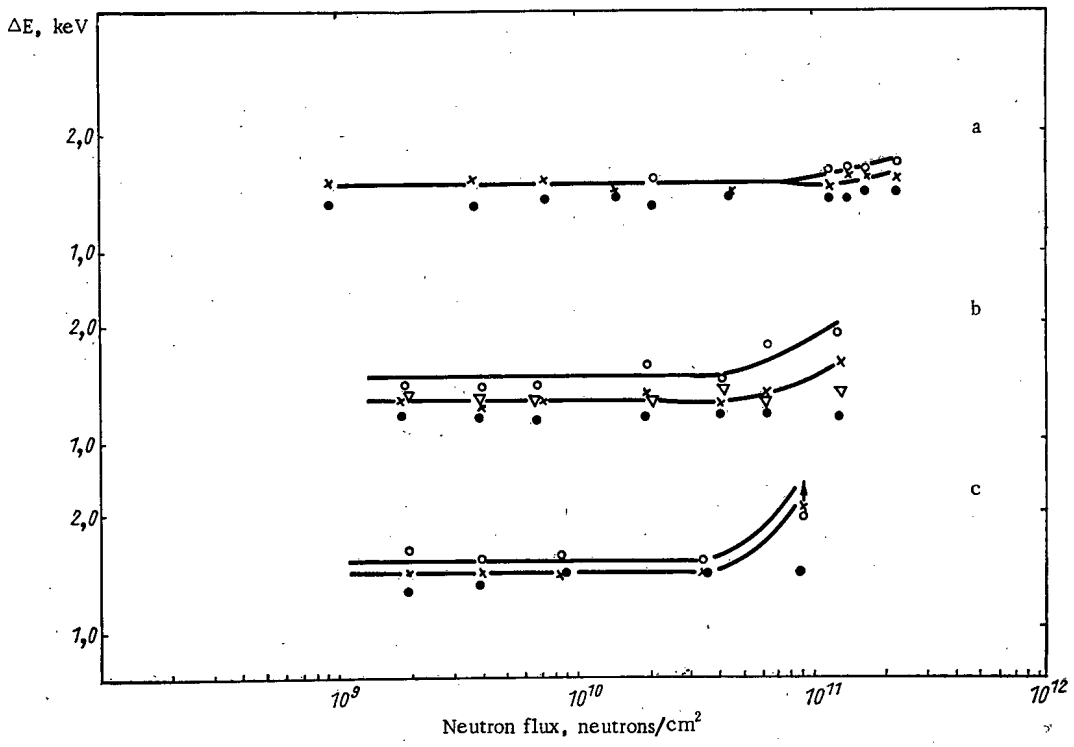

Fig. 1. Variation of energy resolution of first detector (a), second detector (b), and third detector (c) with the integral neutron flux. ▽) 6 keV line; ×) 14-keV line; ○) 60-keV line. The curves are drawn only for the 14 keV and 60 keV lines, since no appreciable variation was found in the other cases; ●) line for stable-amplitude pulse generator.

to the data in Fig. 1, the limiting integral flux value at the 1 keV level, i.e., the value giving rise to an increment $\Delta E_n = 1$ keV, is $(0.5\text{-}1.0) \cdot 10^{11}$ neutrons/cm^2. Lines with lower energies are found to be more resistant to radiation effects. This is due to the different depths of absorption of quanta with different energies:

$$\bar{X}(E) = \frac{1+[1+\mu(E)\,d]\exp[-\mu(E)\,d]}{\mu(E)\{1-\exp[-\mu(E)\,d]\}},$$

where μ(E) is the linear coefficient of absorption and d is the thickness of the detector.

We also investigated the most probable amplitude, shape, and area of the spectral line. All of these parameters may vary as a result of irradiation because there is increased recombination or variation of the thicknesses of the dead and sensitive zones of the detector. The measurement results indicate that for integral flux values of $(0.5\text{-}1.0) \cdot 10^{11}$ neutrons/cm^2 the shapes of the lines do not change appreciably, the values of the most probable amplitude remain the same to within 1%, and the thickness of each zone changes by no more than 5% from the original value.

LITERATURE CITED

1. S. M. Solov'ev, L. I. Tybin, and V. P. Éismont, Pribony i Tekh. Éksperim., No. 1, 52 (1972).

Declassified and Approved For Release 2013/02/27 : CIA-RDP10-02196R000300110005-5

Declassified and Approved For Release 2013/02/27 : CIA-RDP10-02196R000300110005-5

A METHOD OF INVESTIGATING THE α-ACTIVITY OF A SUBSTANCE RELATIVE TO SOURCE DEPTH *

A. L. Kononovich, N. V. Bogolapov, V. N. Klochkov, and I. E. Konstantinov

UDC 539.128.4.03

A spectrometric method is considered for the determination of the distribution law for the α-activity of a substance relative to source depth. The method is based on the application of matrices to the spectra obtained. During measurement, the samples of material were not subjected to any special treatment and did not disintegrate during the measuring process. A method was specially developed for studying sorption and diffusion in polymeric materials. Therefore, special consideration is given to the choice of geometric conditions for the measurement. Serial spectrometric equipment, incorporated into a 9063-02 Amur assembly, was utilized in the experiments.

The control experiments indicated that the measurement technique is not sensitive over wide limits to mechanical changes in the shape of the samples.

The matrices, enabling one to convert the α-radiation spectrogram for Pu^{239} to the distribution function for the specimen inside the source, are cited. A control experiment was performed in which the distribution of plutonium nitrate in aqueous acid solution was measured. The results obtained are presented in Fig. 1. The solid and the dotted curves correspond to two different thicknesses of the inactive absorber, which was located above the solution to prevent it from vaporizing in vacuum.

The error in the determination of the form of the distribution function (correct to an error in the normalization factor) did not exceed 5% on the average.

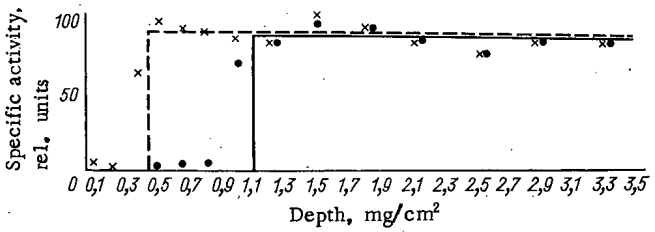

Fig. 1. Model distribution functions: ●, × are the experimentally determined values, pertaining to the solid and the dotted curves, respectively.

CALCULATION OF THE CHARACTERISTICS OF BACKWARD GAMMA RADIATION FROM TARGETS BOMBARDED WITH ELECTRONS†

V. A. Él'tekov, É. I. Dubovoi, T. S. Lim, and V. G. Nadtochii

UDC 539.12.122:539.12.175

The Monte Carlo method has been used to simulate the production of gamma radiation by bombarding aluminum, iron, tin, and lead targets with a monoenergetic beam of electrons with energies of 10, 30, and

*Translated from Atomnaya Énergiya, Vol. 33, No. 5, p. 919, November, 1972. Original article submitted December 9, 1971.

†Translated from Atomnaya Énergiya, Vol. 33, No. 5, pp. 919-920, November, 1972. Original article submitted January 24, 1972; abstract submitted May 24, 1972.

Declassified and Approved For Release 2013/02/27 : CIA-RDP10-02196R000300110005-5

Declassified and Approved For Release 2013/02/27 : CIA-RDP10-02196R000300110005-5

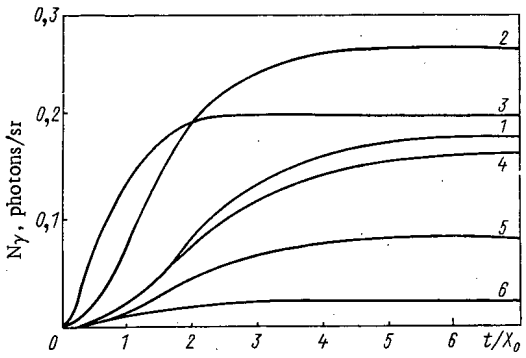

Fig. 1. Yield of backwardly directed photons with energies greater than E as a function of the target thickness in radiation units X_0 for E_0 = 100 MeV. 1-3) Pb, Fe, Al respectively for E = 0.1 MeV; 4-6) Pb, Fe, Al respectively for E = 0.4 MeV.

100 MeV. The spectral characteristics of the gamma radiation escaping from a semiinfinite target into the rear hemisphere, together with the yield of backwardly directed photons as a function of the target thickness have been obtained. The maximum in the photon spectra occurs at an energy E_{max} which increases with the atomic number Z of the target material. Thus the values of E_{max} for iron and lead are 0.2 ± 0.1 and 0.6 ± 0.1 MeV respectively. The contribution of the high-energy part of the spectrum increases with increasing Z. This is a consequence of the increase in annihilation radiation and the photoelectric absorption of the low-energy portion of the spectrum. For high Z target material the fraction of photons with energies above 0.5 MeV due to bremsstrahlung from multiply scattered electrons amounts to tenths of a percent.

For E_0 = 100 MeV we studied the photon spectrum and the angular distribution of backward gamma radiation as functions of the thickness of an iron target. The low-energy ($E_\gamma < 0.5$ MeV) and high-energy ($E_\gamma \geq 0.5$ MeV) portion of the spectrum become saturated at target thicknesses of 4 and 10 cm respectively. From iron 1 cm thick the angular distribution has its maximum at 90° with the direction of the electron beam, but the distribution becomes isotropic for 4 cm of iron.

Figure 1 shows the yield of backwardly directed photons as a function of the target thickness for E_0 = 100 MeV. It is clear that the yield of photons with $E_\gamma \geq 0.4$ MeV increases with Z whereas the yield of radiation with $E_\gamma \geq 0.1$ MeV reaches a maximum for intermediate Z (iron). This difference in the Z dependences of the soft and hard photon yields is accounted for by the significant increase in the photoelectric absorption of soft photons with increasing Z. At high energies and high Z, where pair production and the annihilation of positrons are important, saturation is reached for target thicknesses comparable with the pair production mean free path. This is confirmed qualitatively by the behavior of the curves showing the photon yield as a function of the target thickness.

Declassified and Approved For Release 2013/02/27 : CIA-RDP10-02196R000300110005-5

Declassified and Approved For Release 2013/02/27 : CIA-RDP10-02196R000300110005-5

LETTERS TO THE EDITOR

DENSITY AND THERMAL EXPANSION OF CERTAIN URANIUM ALLOYS

V. A. Makhova and L. I. Gomozov

UDC 669.017

For physical computations of fuel elements it is necessary to know the uranium content per unit volume of the core at different temperatures. Besides, the change of the density of the fuel due to phase transitions can noticeably affect the power coefficient of the reactor.

In [1] the effect of phase change and thermal expansion of an alloy in different phase states on the power coefficient of a reactor was investigated for an alloy of uranium with 5 wt. % of fissium used in the EBR-II reactor. The coefficients of thermal expansion for different alloys of uranium with Zr, Nb, Mo, and Fs are presented in [1-3].

Below we present some results of determination of transition temperatures of moderately alloyed melts of uranium with 15 at. % addition of Zr, Nb, Mo, and Ti in single-phase γ-state, the coefficients of thermal expansion of these alloys, and also the density of uranium alloys containing Zr, Nb, Mo, and Ti up to 40 at. %. The alloys were prepared by the method of argon-arc fusion from industrial uranium (99.8%; main impurities: 0.02% C and 0.02% Fe), iodides of Ti and Zr, and also Nb and Mo of about 99.7% purity. Molten samples were homogenized at 0.8-0.9 T_m for 48 h and chilled in water.

The roentgen density d of the alloys was computed from the determination of the parameters of bcc lattice of γ-phase fixed by chilling:

$$d = \frac{n(A_1N_1 + \ldots + A_iN_i)\,1.66 \cdot 10^{-24}}{V}, \quad (1)$$

where n = 2 is the number of atoms in an elementary cell of γ-phase, A_i is the atomic weight of the component, N_i is its atomic fraction, $V = a^3$ is the volume of the elementary cell (here a is a parameter of bcc lattice of γ-phase).

The lattice parameters at 20°C were determined for the U–Zr–Nb [4], U–Zr–Ti [5], U–Nb–Mo [6-9], and U–Nb–Ti [10] systems. The value of the γ-phase parameter for unalloyed uranium at 20°C was obtained by extrapolation of the parameter-composition curves and comprises 3.473 Å. The parameters of the γ-phase in the regions where it is not fixed by chilling were assumed to lie on the additive straight lines.

The change of the density of the alloys of four (a-d) ternary systems of uranium, which the alloys would have at 20°C if the γ-phase were fixed for all compositions, is shown in Fig. 1. These data can be used for the determination of the density of alloys at temperatures of equilibrium existence of the γ-phase. In such cases it is necessary to extend the value of the coefficient of thermal expansion in the γ-region (see Fig. 2, curve d) to the entire temperature range from 20°C to the operating temperature.

After chilling, oversaturated solid α' solution is formed from the γ-phase in the region of small admixtures and then a number of intermediate deformed structures appear. The increase of density in $\gamma \rightarrow \alpha$ conversion can be taken into consideration if it is assumed that the density jump decreases linearly from 1.8% for unalloyed uranium to zero for alloys with γ-phase fixed by chilling. This was confirmed experimentally by the data obtained by hydrostatic floating of molten homogenized alloys in CCl_4. The profitable part of the casting (with increased porosity) was sheared off.

Translated from Atomnaya Énergiya, Vol. 33, No. 5, pp. 921-924, November, 1972. Original article submitted June 30, 1971.

© 1973 Consultants Bureau, a division of Plenum Publishing Corporation, 227 West 17th Street, New York, N. Y. 10011. All rights reserved. This article cannot be reproduced for any purpose whatsoever without permission of the publisher. A copy of this article is available from the publisher for $15.00.

Declassified and Approved For Release 2013/02/27 : CIA-RDP10-02196R000300110005-5

Declassified and Approved For Release 2013/02/27 : CIA-RDP10-02196R000300110005-5

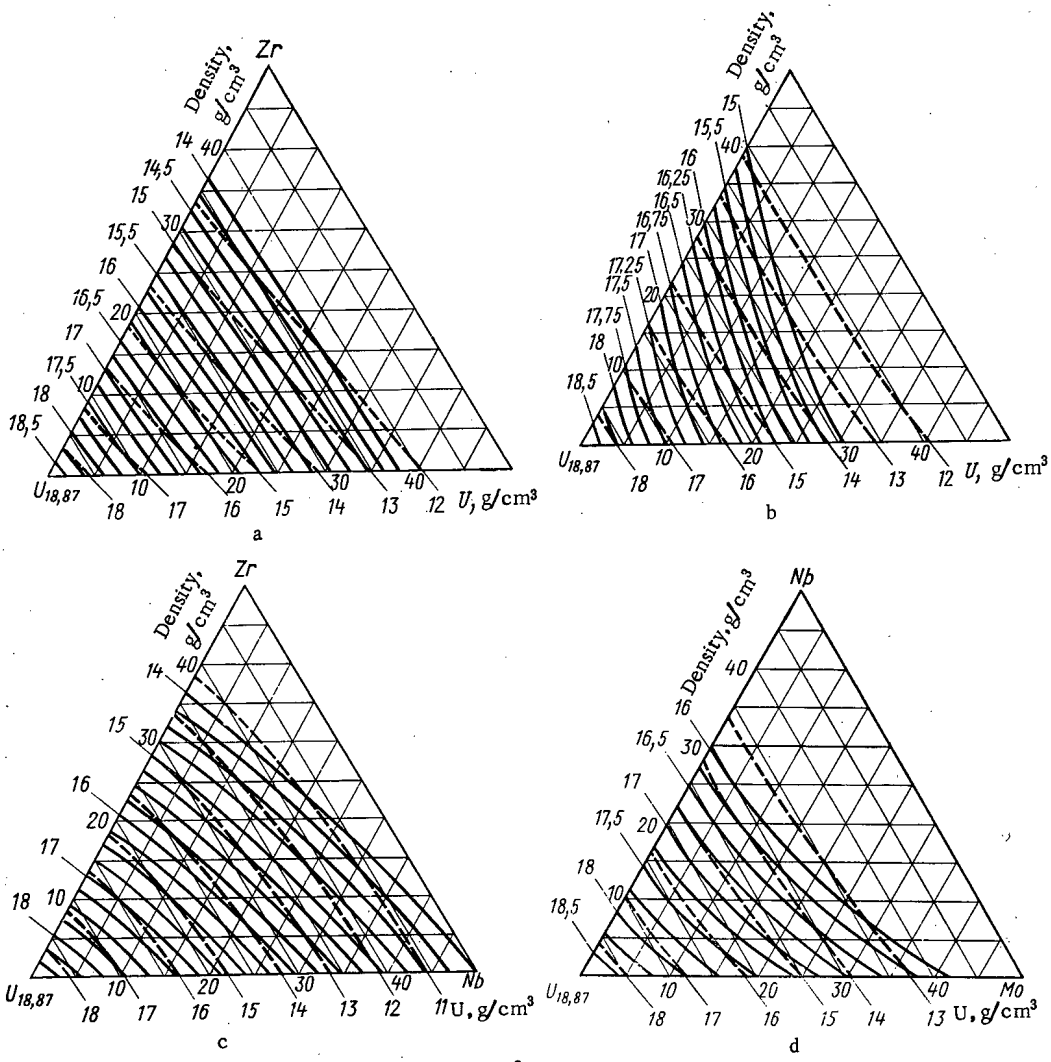

Fig. 1. Density of alloys in γ-state at 20°C (continuous lines) and uranium content in 1 cm³ of the alloy (dashed lines) as function of content of Ti, Zr, Nb, Mo (at. %).

The band of scatter of the values of the density 14-18.6 g/cm³ is described by the relation

$$d_h = (d_c - 0.22) \pm 0.12, \quad (2)$$

where d_h is the density obtained from the data of hydrostatic floating and d_c is the computed value. The decrease of the density is caused by the porosity of the molten samples and carbon impurities. According to [11] for a carbon content of 0.6 at.%, which is typical for molten samples, the decrease of the density must be 0.12 g/cm³.

The curves for equal volume content of uranium (product of density and the weight fraction) in the alloys are also shown in Fig. 1. For sufficient alloying the dimension of the atoms of the alloying element has a significant effect on the volume content of uranium in alloys with identical atomic concentration of admixture. Thus in alloys with 60 at.% of uranium alloyed with Zr, Nb, Ti, and Mo the volume content of uranium is 10.76, 11.84, 12.1, and 12.7 g/cm³ respectively.

The transition temperatures of these alloys in γ-state are given in Fig. 2; these are obtained from published data and dilatometric and metallographic investigations.

The thermal expansion coefficient of alloys was determined on a dilatometer with quartz transmitting system [12] for a heating rate of 10 deg/min. For obtaining equilibrium values in $\alpha + \gamma(\delta)$ region the samples were annealed beforehand at 550°C for 200 h. A typical temperature–expansion curve is shown in Fig. 3. In the heterophase $\alpha + \gamma(\delta)$ region the thermal expansion coefficient at temperatures above ~300°C becomes practically consant (see Fig. 2, curve e). The values of αt for the investigated alloys at temperatures below 300°C are smaller by ~40-60%.

Declassified and Approved For Release 2013/02/27 : CIA-RDP10-02196R000300110005-5

Declassified and Approved For Release 2013/02/27 : CIA-RDP10-02196R000300110005-5

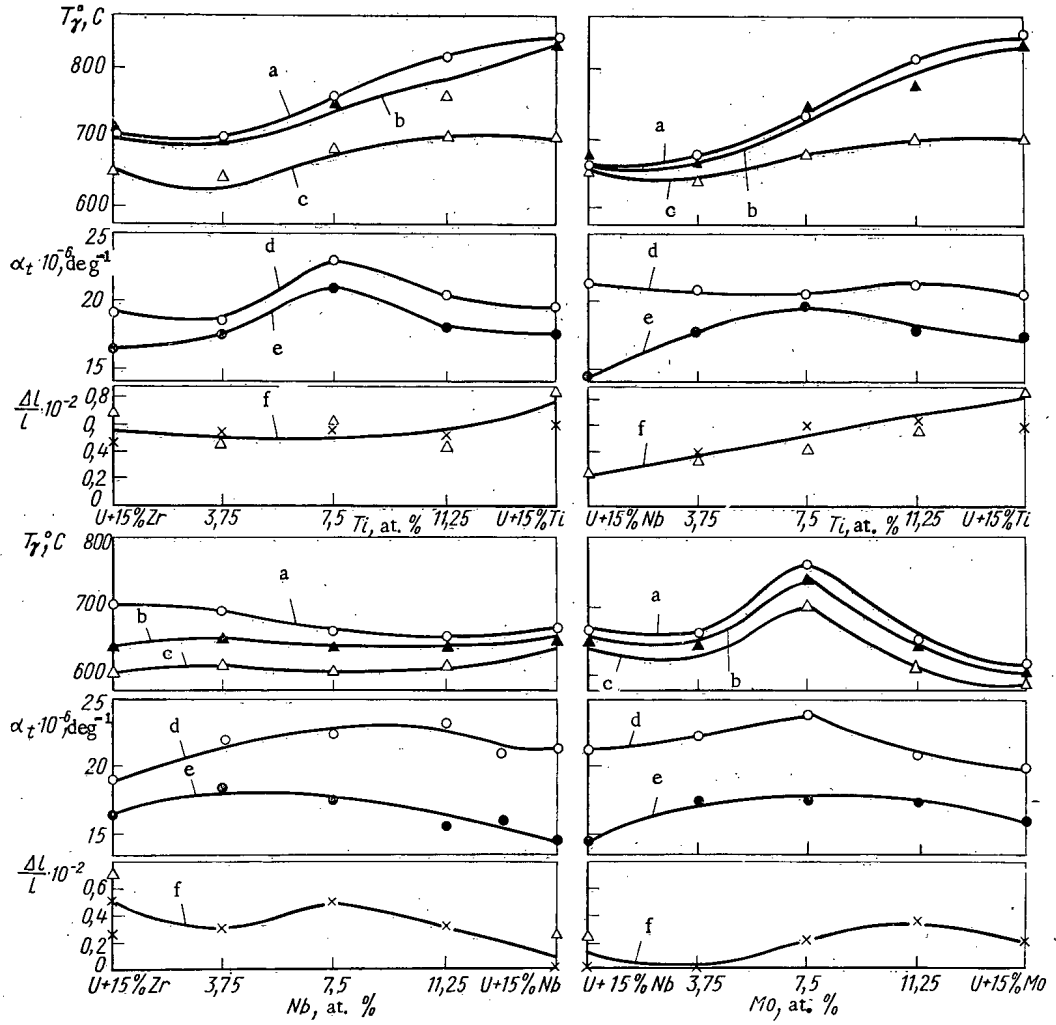

Fig. 2. Characteristics of thermal expansion of alloys of uranium with 15 at. % of alloyed alements of the U–Zr–Nb, U–Nb–Mo, U–Zr–Ti, and U–Nb–Ti systems.

A sharp increase of the length of the sample is observed during the transition to γ-state due to the large atomic volume of the bcc lattice of uranium. The temperatures at the beginning and the end of the intensive $\alpha + \gamma(\delta) \rightarrow \gamma$ conversion of annealed (heterogeneous) samples, obtained from dilatometric data, are plotted in Fig. 2 (curves b and c). Curve b lies somewhat below the equilibrium temperature of transition to the single-phase γ-region (curve a) obtained from microstructure data. This is explained by the fact that the dissolution of the last portions of the excess phases in γ-phase is not recorded by dilatometer. On cooling the rate of decay depends substantially on the rate of cooling; overcooling reached 100°C.

The length increment $\Delta l/l$ (see Fig. 2, curve e) in the phase transition is arbitrarily referred to the equilibrium transition temperature of the alloy to γ-state for the sake of convenience (see Fig. 2, curve a).

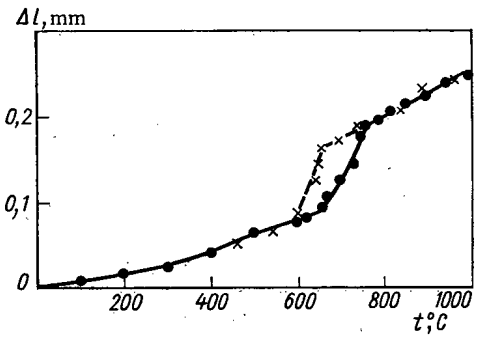

Fig. 3. Change of length of a sample of alloy of uranium with 15 at.% of zirconium in heating (●) and cooling (×).

Declassified and Approved For Release 2013/02/27 : CIA-RDP10-02196R000300110005-5

Declassified and Approved For Release 2013/02/27 : CIA-RDP10-02196R000300110005-5

For U–Nb alloys and alloys of the ternary system adjoining the niobium side the increase of length in the region of conversion is atomically small. This is due to the fact that for alloys rich in niobium the high-melting phase γ_{Nb} (or γ_{Nb-Mo} and γ_{Nb-Zr}) is in a highly dispersed state at the preannealing temperature and smooths out the effect of corrosion by gradually dissolving α-uranium.

The total length of the samples on heating from t_1 to t_2 can be determined from the values given in Fig. 2 according to the formula

$$l_2 = l_1\left[1+\alpha_{\alpha+\gamma}(T_\gamma - t_1)+\frac{\Delta l}{l}+\alpha_\gamma(t_2-T_\gamma)\right], \quad (3)$$

where l_1 and l_2 are the lengths at t_1 and t_2, T_γ is the equilibrium temperature of $(\alpha+\gamma) \rightarrow \gamma$ conversion, $\Delta l/l$ is the linear expansion in this conversion, and $\alpha_{\alpha+\gamma}$ and α_γ are the mean values of the thermal expansion coefficient in $(\alpha+\gamma)$ and γ regions.

LITERATURE CITED

1. J. Long, Nucl. Appl. Technol., 10 (1971).
2. G. A. Mochalov et al., in: Physicochemistry of Alloys and High-Melting Compounds with Thorium and Uranium [in Russian], Nauka, Moscow (1968), p. 53.
3. D. M. Skorov et al., Reactor Material Science [in Russian], Atomizdat, Moscow (1968).
4. L. I. Gomozov and O. S. Ivanov, in: Construction of Alloys of Certain Systems with Uranium and Thorium [in Russian], Gosatomizdat, Moscow (1961), p. 128.
5. A. T. Semenchenkov and O. S. Ivanov, in: Construction of Alloys of Certain Systems with Uranium and Thorium [in Russian], Gosatomizdat, Moscow (1961), p. 312.
6. O. S. Ivanov and G. I. Terekhov, in: Construction of Alloys of Certain Systems with Uranium and Thorium [in Russian], Gosatomizdat, Moscow (1961), p. 199.
7. S. Maxwell et al., J. Nucl. Mater., 11, 119 (1964).
8. W. Justusson, J. Nucl. Mater., 4, 37 (1961).
9. G. Bannister and J. Murray, J. Less Common Metals, 2, 372 (1960).
10. L. I. Gomozov et al., in: Construction and Properties of Alloys of Uranium, Thorium, and Zirconium [in Russian], Gosatomizdat, Moscow (1963), p. 92.
11. R. Wakelin, AWRE 063/70.
12. L. I. Gomozov et al., Zavod. Lab., No. 7, 874 (1968).

Declassified and Approved For Release 2013/02/27 : CIA-RDP10-02196R000300110005-5

Declassified and Approved For Release 2013/02/27 : CIA-RDP10-02196R000300110005-5

ONE POSSIBILITY FOR SIMULATING DIFFUSION OF THERMAL NEUTRONS

V. N. Starikov

UDC 621.039.512.4

The application of the Monte Carlo method to one-velocity thermal neutron diffusion problems involves the multiple selection of range and scattering to simulate the trajectory of a thermal neutron until it is absorbed [1]. In stationary problems when it is necessary to obtain the distribution of radiative capture gamma sources such a scheme is not efficient because of the large number of scatterings ($\Sigma_s/\Sigma_a \gg 1$), but the neutron is never far removed from the thermal neutron source; in rocks the diffusion length L varies from 2.5 to 20 cm. Another algorithm is possible using the fact that when $\Sigma_s \gg \Sigma_a$ the steady-state diffusion of thermal neutrons is adequately described by the simple equation

$$D\nabla^2\Phi(\rho) - \Sigma_a\Phi(\rho) = -q, \tag{1}$$

where D is the thermal neutron diffusion coefficient, Σ_a is the macroscopic absorption cross section, $\Phi(\rho)$ is the thermal neutron flux at point ρ, and q is the source density.

For a point isotropic source of strength Q at the origin ($q = Q\delta(\rho)$) Eq. (1) has the solution [2]

$$\Phi(\rho) = \frac{Q}{4\pi L^2\rho\Sigma_a}\, e^{-\rho/L}.$$

The thermal neutron absorption density in 1 cm^3 (radiative capture gamma source density) is

$$\nu(\rho) = \Sigma_a\Phi(\rho). \tag{2}$$

Equation (2) shows that the probability density for the random variable ρ, the distance from the source $\mathbf{r}_1$ to the point of absorption $\mathbf{r}_n$, will be

$$f(x) = Ax\, e^{-x}. \tag{3}$$

It is known that the quantity $\xi = -\ln\alpha_1\alpha_2$ has a probability density described by (3) [3]. Hence forth α_1 and α_2 are pseudorandom numbers equidistributed on the interval (0, 1).

In a homogeneous medium the point $\mathbf{r}_n$ where the neutron is absorbed can be obtained at once without simulating the trajectory of the thermal neutron until it is absorbed. The algorithm for this is the following: 1) choose the direction cosines of Ω at random; 2) compute $\rho = -L\ln\alpha_1\alpha_2$ and $\mathbf{r}_n = \mathbf{r}_1 + \rho\Omega$.

The concept of using a solution of the diffusion equation instead of choosing the trajectories of a thermal neutron can be extended to heterogeneous media.

We consider a domain D with boundary G. In D there is a region D_2 with boundary G_2 which may partially or completely coincide with G. We assume that for region D_2 placed in a black absorber there is a solution of the diffusion equation with the absorption density $\nu_{D_2}(\mathbf{r})$. Then the absorption density in domain D can be written as

$$\nu_D(\mathbf{r}) = \begin{cases} \nu_{D_2}(\mathbf{r}) + \nu'_{D_2}(\mathbf{r}), & \text{if} \quad \mathbf{r} \in D_2; \\ \nu'_{D_2}(\mathbf{r}), & \text{if} \quad \mathbf{r} \bar{\in} D_2, \end{cases} \tag{4}$$

where $\nu'_{D_2}(\mathbf{r})$ is the absorption density due to neutrons which have diffused across G_2.

Thus $\nu_{D_2}(\mathbf{r})$ is known, and $\nu'_{D_2}(\mathbf{r})$ can be found by the Monte Carlo method, simulating the trajectories of thermal neutrons. It is simplest to choose D_2 as a sphere.

Translated from Atomnaya Énergiya, Vol. 33, No. 5, pp. 924-925, November, 1972. Original article submitted December 27, 1971; revision submitted May 11, 1972.

© 1973 Consultants Bureau, a division of Plenum Publishing Corporation, 227 West 17th Street, New York, N. Y. 10011. All rights reserved. This article cannot be reproduced for any purpose whatsoever without permission of the publisher. A copy of this article is available from the publisher for $15.00.

Declassified and Approved For Release 2013/02/27 : CIA-RDP10-02196R000300110005-5

Declassified and Approved For Release 2013/02/27 : CIA-RDP10-02196R000300110005-5

The solution of the diffusion equation for a sphere of radius R_c placed in a vacuum with an isotropic thermal neutron source of unit strength (Q = 1 neutron/sec) at the center has the form [2]

$$\Phi(\rho) = \frac{1}{4\pi\Sigma_a L^2 \operatorname{sh}(R/L)} \frac{\operatorname{sh}\left(\frac{R-\rho}{L}\right)}{r},$$

where $R = R_c + 0.71/\Sigma_{tr}$.

The probability that a neutron is absorbed in the sphere is

$$p = P(\rho < R) = \int_0^{2\pi} \int_{-1}^{+1} \int_0^R \Sigma_a \Phi(x)\, x^2\, dx\, d\cos\theta\, d\varphi = 1 - \frac{R/L}{\operatorname{sh}(R/L)}. \tag{5}$$

The probability that a neutron escapes from the sphere is

$$q = 1 - p = P(\rho > R) = \frac{R/L}{\operatorname{sh}(R/L)}. \tag{6}$$

The probability density for ρ is

$$f(x) = Ax \operatorname{sh}\left(\frac{R-x}{L}\right). \tag{7}$$

ρ can be chosen by the following algorithm: 1) choose a pair of α's, α_1 and α_2, and compute $\rho_1 = -L \ln \alpha_1\alpha_2$; if $\rho_1 > R_c$ discard α_1 and α_2 and choose a new pair of α's; 2) if $(1-e^{-2(R-\rho_1)/L}] \geq \alpha_3 (1-e^{-2R/L})$ $\rho = \rho_1$; otherwise repeat the procedure from the point with new α's. The algorithm described can be used to simulate the coordinates of the point in a multilayered medium where the thermal neutron is absorbed.

Let S be the minimum distance from the source $\mathbf{r}$ to the boundary of the medium. Assuming that $R_c = S$ with probability p(5), we choose at random the point of absorption on a sphere of radius ρ which was selected by the algorithm described above.

With probability q (6) we simulate the trajectory of a thermal neutron until it is absorbed. The trajectory begins at the surface of the sphere of radius R_c with the initial direction of Ω_0 outside the sphere being chosen at random.

The initial coordinates $\mathbf{r}_0$ and the direction Ω_0 can be chosen as follows: 1) choose Ω_n, the direction cosines of the normal to the sphere, at random and compute $\mathbf{r}_0 = \mathbf{r}_1 + R_c\Omega_n$; 2) choose Ω_0' at random, and if $\Omega_n \cdot \Omega_0' > 0$, $\Omega_0 = \Omega_0'$; otherwise $\Omega_0 = -\Omega_0'$.

When the source is far enough away from the boundary ($S \gg L$), the probability (5) is close to unity, the term $\nu_{D_2}^{\dagger}(\mathbf{r})$ in (4) is small, and the distribution $\nu_D(\mathbf{r})$ is close to the distribution in a homogenous medium. Therefore the point of absorption can be found by an approximate algorithm using the probability density for a homogeneous medium (3).

The probability that a neutron is absorbed in a sphere of radius S of an infinite homogeneous medium is

$$p_1 = P(\rho < S) = \int_0^S \nu(x)\, dx = \int_0^S ax\, e^{-x/L}\, dx = 1 - e^{-S/L}(1 + S/L).$$

The following algorithm can be used: 1) with probability p_1 we choose ρ as in a homogeneous medium but under the condition $\rho < S$; if $\rho > S$ we take another pair α_1, α_2; in this case the particle is assigned the weight p_1; 2) with probability $q_1 = 1 - p_1$ we simulate the trajectory; the point where the neutron is absorbed is given the weight

$$W = \begin{cases} 1/q \text{ if the particle is absorbed outside the sphere;} \\ 1 \text{ if the particle is absorbed in the sphere.} \end{cases}$$

It should be noted that when S is very large the latter algorithm is more suitable although it is also approximate. It involves significantly fewer calculations than the algorithm using the solution of the diffusion equation for a sphere in a vacuum.

By using the algorithms described the point of absorption of a neutron in a homogeneous medium can be found almost Σ_s/Σ_a times as quickly as by the usual simulation of trajectories. In multilayered media where the dimensions of the region are larger than the diffusion length, the gain in simulation time also approaches Σ_s/Σ_a.

Declassified and Approved For Release 2013/02/27 : CIA-RDP10-02196R000300110005-5

Declassified and Approved For Release 2013/02/27 : CIA-RDP10-02196R000300110005-5

LITERATURE CITED

1. S. A. Denisik, R. A. Rezvanov, and B. E. Lukhminskii, in: Nuclear Geophysics [in Russian], Gostoptekhizdat, Moscow (1965), p. 22.
2. K. Beckurts and K. Wirtz, Neutron Physics, Springer, New York (1964).
3. G. A. Mikhailov, The Theory of Probability and Applications [in Russian], Vol. X (1965), p. 749.

Declassified and Approved For Release 2013/02/27 : CIA-RDP10-02196R000300110005-5

Declassified and Approved For Release 2013/02/27 : CIA-RDP10-02196R000300110005-5

SELECTIVE MONITORING OF IMPURITY CONTENT IN SODIUM–POTASSIUM COOLANT BY PLUG INDICATOR

M. N. Arnol'dov, M. N. Ivanovskii,
S. S. Pletenets, and A. D. Pleshivtsev

UDC 621.039.564.5

The plug indicator is the most widely used device for monitoring impurity content in liquid-metal coolants. Repeated references have been made in the literature to the impossibility of determining a specific impurity responsible for fouling the indicator. For that reason, the indicator has been regarded to date as only a gage of the overall "clogging potential of the entire system" [1].

It is clear, however, that the pattern of flow obstruction and the rate of clogging must be functions of the properties of the impurity fouling the indicator: its specific gravity, rate of crystallization, and so on. That lends interest to investigations of the relationship between the rate of fouling of the indicator and the type of impurity involved, leading to estimates of the possibility of selective monitoring of the content of impurities by the indicator on that basis.

Our investigation was performed on sodium–potassium coolant and hydrogen and oxygen were the impurities under investigation. An indicator of design similar to the one described earlier [1] was employed. There were 60 grooves, sized 0.32 × 0.32 mm, in the indicator. The rate of cooling of the alloy was in the range 8-12 deg/min. The initial rate of flow of the alloy through the indicator was 500 kg/h. During the investigation, all the performance parameters of the test stand and indicator were kept constant except for the content of the impurities (hydrogen and oxygen). The results of the investigation are plotted in Fig. 1 as a dependence of the rate of clogging of the indicator on the clogging temperature, i.e., on the impurity content. It is clear from the diagram that the points cluster in explicit layers representing the respective hydrogen and oxygen impurities. If the rate of clogging of the indicator is measured as well as the clogging temperature, we can determine the type of impurity settling in the sludge collected in the indicator. Once the dependence of the impurity concentration on the saturation temperature is known, we can determine the content of the impurity.

Consider this possibility and example. Oxygen and hydrogen impurities interact to form the hydroxyl group OH [2]. In our experiment, hydrogen was introduced in batches into sodium–potassium coolant containing about $1.5 \cdot 10^{-2}$ wt.% oxygen. The resulting OH group seemed to be sufficiently soluble, so that introduction of hydrogen did not lead at first to a rise in the clogging temperature, but on the contrary, brought the temperature downward. The rate of clogging of the indicator by hydrogen remained equal to the rate of clogging by oxygen, attesting to a drop in the content of unbound oxygen in the coolant.

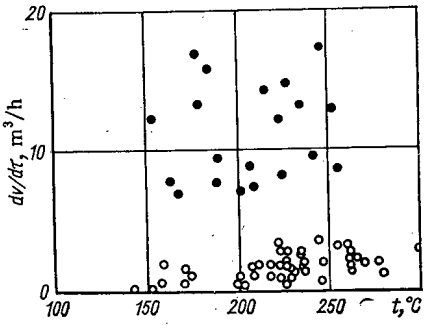

Fig. 1. Effect of type of impurity on rate of clogging of indicator: ●) hydrogen; ○) oxygen.

Translated from Atomnaya Énergiya, Vol. 33, No. 5, pp. 925-926, November, 1972. Original article submitted January 24, 1972.

© 1973 Consultants Bureau, a division of Plenum Publishing Corporation, 227 West 17th Street, New York, N. Y. 10011. All rights reserved. This article cannot be reproduced for any purpose whatsoever without permission of the publisher. A copy of this article is available from the publisher for $15.00.

Declassified and Approved For Release 2013/02/27 : CIA-RDP10-02196R000300110005-5

Declassified and Approved For Release 2013/02/27 : CIA-RDP10-02196R000300110005-5

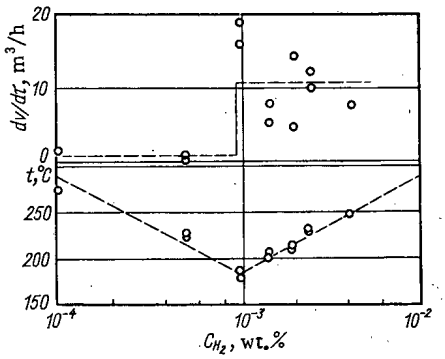

Fig. 2. Variation in rate of clogging and clogging temperature when hydrogen impurity is introduced into coolant stream containing oxygen impurity.

After all of the oxygen available under those conditions had been bound by the hydrogen, further additions of hydrogen brought about a rise in the clogging temperature. The way the indicator became clogged after that varied from the oxygen mode to the hydrogen mode, as is clearly evident from the rate of clogging (Fig. 2). We infer from the redistribution of the available oxygen between the free and bound forms that measurements of the clogging rate can be used to monitor and analyze reasonably involved processes occurring in the coolant stream.

LITERATURE CITED

1. A. E. Sheindlin (editor), Liquid–Metal Coolants [Russian translation], IL, Moscow (1958).
2. M. N. Arnol'dov et al., Teplofiz. Vys. Temp., 8, No. 1, 88 (1970).

Declassified and Approved For Release 2013/02/27 : CIA-RDP10-02196R000300110005-5

Declassified and Approved For Release 2013/02/27 : CIA-RDP10-02196R000300110005-5

MEASUREMENT OF ENERGY RELEASE IN COMPENSATING ROD OF A REACTOR

V. A. Kuznetsov, A. I. Mogil'ner,
V. P. Koroleva, Yu. A. Prokhorov,
V. S. Samovarov, S. N. Fokin,
and L. A. Chernov

UDC 621.039.51

Up to the present, the energy release in rods containing boron have been estimated mainly by computational methods. Therefore it is of interest to have a direct measurement of this quantity. Experimental investigations carried out earlier [1] were not methodologically perfect, since activation detectors with an energy dependence of the cross section different from the capture cross section of B^{10} were used. The total energy release in the compensating rod is caused by $B^{10}(n, \alpha)Li^7$ reaction and the absorption of γ- and β-radiations of the reactor; for boron carbide rods the last part is small and comprises 8-10% of the total energy release.

The object of the present work is to measure the specific energy release in a boron rod as a result of (n, α) reaction on B^{10} with the use of modern semiconductor and track detectors together with indicator layers of B^{10} and U^{235}.

Fundamentals of the Method

Let a thin layer of B^{10} with weight Δm (in g) be placed at a fixed point (ρ_0, φ_0, z_0) of a homogeneous reactor. Then the specific energy release in this layer is

$$Q_B^0 = \frac{q_B r_0}{\Delta m W} \text{ MeV/sec} \cdot \text{g} \cdot \text{W}, \quad (1)$$

where q_B (MeV) is the energy of the reaction released per absorbed neutron, r_0 is the number of (n, α) reactions in the boron layer per unit time, and W (W) is the reactor power.

If N_B^0 is the intensity of α-particle count in (n, α) reaction from the boron layer and ξ_B is the recording efficiency, then

$$r^0 = N_B^0 / \xi_B. \quad (2)$$

We express the reactor power in terms of fission intensity f_0 of a thin layer of U^{235} with weight ΔM (g) placed at the same point of the reactor as the boron layer:

$$W = \frac{f_0 G}{\Delta M K_0 \, 3.26 \cdot 10^{10}} \text{ W}. \quad (3)$$

Here G is the total charge of U^{235} in the reactor, $K_0 = q(\rho_0, \varphi_0, z_0)$ is the density of energy release at the point (ρ_0, φ_0, z_0), and $\bar{q}$ is the density of energy release averaged over the volume of the active zone of the reactor. If N_f^0 is the intensity of counts of the fission events of the U^{235} layer and ξ_f is the efficiency of their recording, then

$$f_0 = N_f^0 / \xi_f. \quad (4)$$

TABLE 1. Ratios of Count Intensities Measured by Different Detectors

N_f^T/N_f^0	N_B^0/N_B^T	N_B^B/N_B^0	Correction	Q_B^B, W/g · B_{nat} · W	Detector used
0,634 ±0,001	0,829 ±0,003	0,466 ±0,005	0,841	(1,323 ±0,028)·10⁻⁶	Semiconductor counter
0,729 ±0,010	0,700 ±0,036	0,440 ±0,011	0,973	(1,403 ±0,083)·10⁻⁶	Track detector

$$Q_B^B = (1{,}365 \pm 0{,}50) \cdot 10^{-6}$$

Translated from Atomnaya Énergiya, Vol. 33, No. 5, pp. 926-928, November, 1972. Original article submitted January 31, 1972.

© 1973 Consultants Bureau, a division of Plenum Publishing Corporation, 227 West 17th Street, New York, N. Y. 10011. All rights reserved. This article cannot be reproduced for any purpose whatsoever without permission of the publisher. A copy of this article is available from the publisher for $15.00.

Declassified and Approved For Release 2013/02/27 : CIA-RDP10-02196R000300110005-5

Declassified and Approved For Release 2013/02/27 : CIA-RDP10-02196R000300110005-5

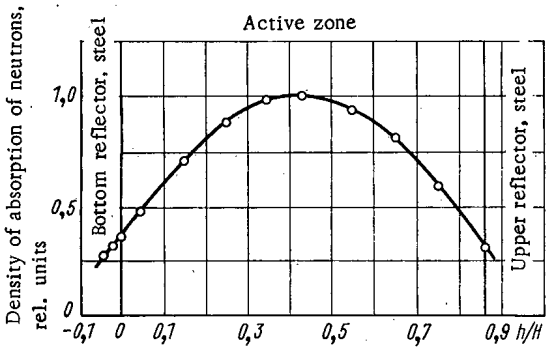

Fig. 1. Distribution of density of absorption of neutrons along the height of boron carbide rod, measured by semiconductor counter.

Substituting expressions (2)-(4) into formula (1) and considering that $\Delta m = n_B A_B/6.02\cdot10^{23}$ and $\Delta M = n_f A_f/6.02\cdot10^{23}$ (n_B and n_f are the numbers of B^{10} of U^{235} nuclei in the layer, A_B and A_f are the atomic weights of boron and uranium), we obtain

$$Q_B^0 = q_B \frac{N_B^0}{N_f^0}\frac{A_f}{A_B}\frac{K_0 3.26\cdot10^{10}}{G}\frac{n_f\xi_f}{n_B\xi_B}. \qquad (5)$$

The calibration of the boron and uranium layers in the same flux of thermal neutrons offers the possibility of eliminating the expression from formula (5). The count intensity of α-particles of boron layer N_B^T and of fission fragments of uranium N_f^T in the thermal flux are given by

$$N_B^T = n_B\xi_B\sigma_B^T\Phi_T, \quad N_f^T = n_f\xi_f\sigma_f^T\Phi_T, \qquad (6)$$

from which we get

$$n_f\xi_f/n_B\xi_B = N_f^T\sigma_B^T/N_B^T\sigma_f^T, \qquad (7)$$

where σ_f^T is the fission cross section of U^{235} and σ_B^T is the cross section of (n, α) reaction on B^{10} for thermal neutrons.

If σ_f^T and σ_B^T are taken for the velocity of neutrons equal to 2200 m/sec, then in the fission cross section of uranium it is necessary to introduce a correction $K_{1/v}$ for the departure from the 1/v law. Considering that the energy release Q_B^B in the boron layer, placed in the transverse section of a boron rod and screened by it, is connected with the energy release in the same layer Q_B^0 at a fixed point of the reactor by the relation

$$Q_B^B = Q_B^0\frac{N_B^B}{N_B^0} \qquad (8)$$

(N_B^B is the count intensity of α-particles of a boron layer placed on the rod), and substituting (5) and (7) into (8), we obtain the final formula for the specific energy release:

$$Q_B^B = \left(\frac{N_B^B}{N_B^0}\frac{N_f^T}{N_f^0}\frac{N_B^0}{N_B^T}K_0\right)\left(\frac{A_f}{A_B}\frac{\sigma_B^T}{\sigma_f^T K_{1/v}}\frac{q_B 3.26\cdot10^{10}}{G}\right)\text{MeV/sec}\cdot\text{g}\cdot\text{W}. \qquad (9)$$

Unlike the experimental boron layer the corresponding conversion is done from the enrichment of B^{10} isotopes from the compensating rod. Thus the problem of measurement of energy release in the boron rod reduces to the measurement of the ratios for the indicators of intensity of absorptions and fissions and to the investigations of the fields of energy release in the reactor for obtaining the value of K_0.

Measurements

The experiments on the measurement of energy release in a rod containing boron were carried out on the critical assembly PF-4F8 [2], at the center of which a rod of B_4C with 19.2 mm diameter was placed. In order to obtain K_0 the fields of energy release in the reactor were measured by the activation method. The ratio of the γ-activity of the fuel elements placed at the corresponding points of the reactor to the activity of a monitor fuel element placed at the point (ρ_0, φ_0, z_0) was measured. The γ-quantas were recorded by a scintillation spectrometer with NaI(Tl) crystal 100 × 100 mm in size. The distribution of the energy release was integrated over the height of each fuel element and over the area of the active zone. As a result the value $K_0 = 1.451 \pm 0.008$ was obtained for the given assembly.

The ratios N_B^0/N_B^T, N_B^B/N_B^0, and N_f^T/N_f^0 occurring in formula (9) were measured by two types of detectors for obtaining a large reliability: by semiconductor gold–silicon counter and by solid track detectors (nitrocellulose and mica) together with indicator layers of B^{10} (thickness 0.05 mg/cm^2) and U^{235} (thickness 0.1 mg/cm^2). As a result of the measurements experimental corrections were introduced for the background from the backing of the indicator layer, for the gap in the transverse section of the boron rod in putting the counter or the nitrocellulose in it, and also for the edge effect in the counter due to the leakage of charged particles from the edge of the layer. The last two corrections were measured experimentally by the method of extrapolation to the zero value of the gaps in the rod and the counter.

Declassified and Approved For Release 2013/02/27 : CIA-RDP10-02196R000300110005-5

Declassified and Approved For Release 2013/02/27 : CIA-RDP10-02196R000300110005-5

The results obtained with the use of different detectors are shown in Table 1. The fission cross section of U^{235} and the capture cross section of boron $\sigma_B^T = 721.5(18.8\%.B^{10})$ for thermal neutrons for $q_B = 2.34$ MeV were used in the computation. As seen from the table, the values of the specific energy release obtained by the two types of detectors coincide within the limits of experimental error.

The distribution of the density of absorption of neutrons along the height of a boron carbide rod, measured by a semiconductor counter, is shown in Fig. 1. It can be useful in the computation of the total energy release in the rod.

The method of measurement of specific energy release in rods containing boron, developed by us, is quite reliable and simple. For these measurements it is convenient to use a semiconductor counter as well as solid track detectors.

LITERATURE CITED

1. A. Leipunskiy et al., Physics of Fast and Intermediate Reactors, SM-18/80, Vienna, IAEA, 1962.
2. A. I. Mogil'ner, V. A. Osipov, and G. N. Fokin, Atomnaya Énergiya, 24, 42 (1968).
3. I. V. Gordeev et al., Nuclear-Physical Constants, Gosatomizdat, Moscow (1963).
4. J. Stehn et al., Neutron Cross Section, BNL-325. Suppl. No. 2, Vol. III, z = 88 to 98 (1965).

Declassified and Approved For Release 2013/02/27 : CIA-RDP10-02196R000300110005-5

Declassified and Approved For Release 2013/02/27 : CIA-RDP10-02196R000300110005-5

A RADIATION-RESONANCE NEUTRON DETECTOR FOR GEOPHYSICAL INVESTIGATIONS

B. S. Bakhtin, V. S. Ivanov,
A. V. Novoselov, and E. M. Filippov

UDC 539.1.074.88.004.1

The two reactions principally used for detecting neutrons are the elastic scattering of neutrons by protons and the capture of neutrons by nuclei of boron, helium, or lithium. In addition, neutrons can be detected by recording the induced beta and gamma activity of foils made of certain metals (the resonance-indicator method) [1] or by recording gamma quanta from radiative capture [2]. This principle was used by the authors in a radiation-resonance detector, which they used for the investigation of boreholes drilled through layers containing high concentrations of boron.

It is known [3] that neutron–neutron coring (NNC) and neutron–gamma coring (NGC) are used for determining the presence of boron. In NNC work, phosphors based on T-1 and T-2 and having low efficiency, or else LDNM-type scintillators, are used as neutron detectors. These neutron detectors make it possible to determine the boron content up to concentrations not exceeding 3-5% B_2O_3.

The gamma-ray detectors most used in NGC work are scintillation counters. NGC, like NNC, is used only for low boron concentration, since its readings also depend on the degree of absorption of thermal neutrons in the rocks.

The radiation-resonance detector consists of a foil and a radiation counter. The foil used may be made of silver, rhodium, indium, thulium, or other elements which exhibit resonance absorption of neutrons and emit gamma quanta when resonance capture takes place.

Using such detectors, we can record neutrons in the resonance region of these elements, where the cross section of absorption of neutrons by boron is not more than 755 barns, as for thermal neutrons, and

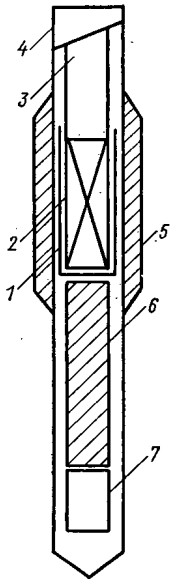

Fig. 1. Arrangement of radiation-resonance neutron detector: 1) foil; 2) scintillator; 3) photoelectron multiplier; 4) casing; 5, 6) lead; 7) neutron source.

Translated from Atomnaya Énergiya, Vol 33, No. 5, pp. 928-929, November, 1972. Original article submitted January 10, 1972.

© 1973 Consultants Bureau, a division of Plenum Publishing Corporation, 227 West 17th Street, New York, N. Y. 10011. All rights reserved. This article cannot be reproduced for any purpose whatsoever without permission of the publisher. A copy of this article is available from the publisher for $15.00.

Declassified and Approved For Release 2013/02/27 : CIA-RDP10-02196R000300110005-5

Declassified and Approved For Release 2013/02/27 : CIA-RDP10-02196R000300110005-5

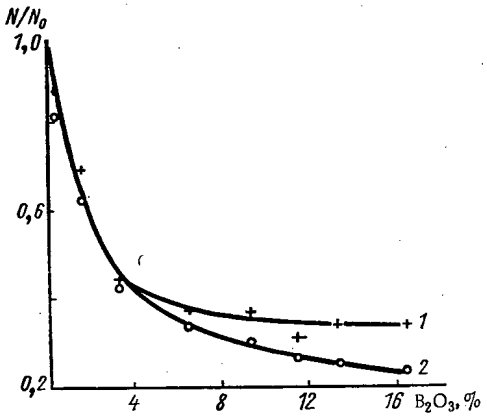

Fig. 2. Calibration curves based on borehole data: 1) NGC; 2) NNC-r.

100 barns in the resonance region of rhodium and indium, 52 barns in the resonance region of silver, etc. [4]. Thus, the range of boron concentrations identifiable in rocks can be extended.

The detector, shown in Fig. 1, consists of a foil and a scintillation counter, which are enclosed in a casing. Attached to the shell of the casing is a lead shield which attenuates the gamma radiation coming from the borehole. Another lead shield is used for shielding the detector from the gamma rays emitted by the neutron source. The foil has the shape of a cup slipped over the scintillator.

Laboratory investigations were carried out in order to determine the optimal parameters for this detector. The choice of the foil for a given detector was based, first of all, on the existence of resonances in this element in the 0.025-10 eV energy range. Among the foils investigated, the ones that satisfied such conditions were cadmium (resonance energy E_r = 0.18 eV), rhodium (E_r = 1.26 eV), indium (E_r = 1.45 eV), thulium (E_r = 3.9 eV), tantalum (E_r = 4.28 eV), gold (E_r = 4.94 eV), and silver (E_r = 5.23 eV). A second criterion was the existence of sufficiently intense lines in the gamma-ray spectrum in the 0.1-0.2-2-3 MeV energy range. As the measurement results show, the most clearly defined spectra are observed in cadmium, silver, rhodium, and thulium in the 0.5-1.0 MeV energy range.

The results of measurements made with and without foils in models containing 0%, 12%, and 25% B_2O_3 were compared for groups of five channels corresponding to gamma-quantum energies of 0.5-1.0 MeV. The curves showing counting rate as a function of boron content that were plotted from the data of measurements using no foil become more flattened in the 12-25% B_2O_3 region than the curves obtained from measurements made with foils. The largest differences in counting rate for the models with 12% and 25% B_2O_2 content are observed for silver, rhodium, and thulium foils, i.e., these foils can be used in the radiation-resonance detectors for determining high concentrations of boron. The cadmium foil is most sensitive to a change in boron concentration in the range from 0 to 12% B_2O_3. Consequently, in such a detector a cadmium foil can be used for determining low concentrations of boron.

For investigations in boreholes we selected a probe with a detector consisting of six foils (cadmium, rhodium, indium, thulium, tantalum, and silver) covering a range of approximately 0.1 to 6 eV. The distance from the center of the detector to the center of the neutron source (the length of the probe) was chosen to be 25 cm. A plutonium–beryllium source with a yield of $1.1 \cdot 10^6$ neutrons/sec was used.

Figure 2 shows the calibration curves plotted from the data of measurements made in a borehole with known composition from a chemical assay of the core. Curve 1 is plotted from the NGC results, and curve 2 is plotted from the results of NNC using a radiation-resonance detector (NNC-r). It can be seen that the NGC curve drops steeply in the range of low boron concentrations (up to 4% B_2O_3) and then flattens out, beginning at 8-10% B_2O_3. Curves of similar appearance are obtained from NNC based on thermal neutrons (NNC-t) [3]. The NNC-r curve is identical with the NGC curve in the concentration range from 0% to 4% B_2O_3. In the region of high boron concentrations this curve is almost linear. Consequently, the use of radiation-resonance neutron detectors makes it possible to extend the range of boron content identification.

The sensitivity threshold of the method is 0.2-0.3% B_2O_3.

Radiation-resonance detectors may also be used for determining the concentration of some rare-earth and other elements in rocks.

LITERATURE CITED

1. V. I. Golubev et al., At. Énerg., 23, No. 2, 130 (1967).
2. W. G. Allen, Neutron Recording [Russian translation], Gosatomizdat, Moscow (1962).
3. V. I. Boranov et al., Neutron Methods of Prospecting for and Analysis of Boron Ore [in Russian], Nauka, Moscow (1964).
4. Atlas of Neutron Cross Sections [in Russian], Atomizdat, Moscow (1952).

Declassified and Approved For Release 2013/02/27 : CIA-RDP10-02196R000300110005-5

Declassified and Approved For Release 2013/02/27 : CIA-RDP10-02196R000300110005-5

INVESTIGATION OF EUROPIUM-ACTIVATED KCl SINGLE CRYSTALS FOR RADIOTHERMOLUMINESCENCE DOSIMETRY

V. P. Avdonin, O. Yu. Begak,
I. A. Vasil'ev, V. P. Glinin,
G. A. Mikhal'chenko, and B. T. Plachenov

UDC 539.12.08

In the investigation of the radioluminescence of a number of alkali-halide crystals activated by lanthanides, it has been shown that some of them may be used as thermoluminescence dosimeters for ionizing radiation. The present report is devoted to a study of the properties of such a dosimeter made with KCl–Eu crystals and having uniquely high sensitivity in comparison with the systems generally used.

The KCl–Eu thermoluminescence spectrum, irrespective of the nature of the exciting radiation (α, β, or γ), consists of a single band with a maximum at about 420 nm. The thermoluminescence curve of crystals irradiated under normal conditions has two peaks: at ~100°C and 190°C (Fig. 1). The low-temperature peak, as was shown in [1], is caused by the liberation of electrons from the activator centers, and its value increases linearly with the concentration of the activator. The high-temperature peak is evidently related to the destruction of the F-centers [2], and its value is practically independent of the activator concentration.

The values and relationships of these thermal peaks depend on the ionizing-radiation dose and dose rate. For low doses of beta and gamma radiation, the amplitude of the low-temperature maximum is about 1.5 times the amplitude of the high-temperature maximum. Both of the thermal peaks increase as the dose increases, but the high-temperature peak increases faster. Even at doses of about 10 rads, the value of the high-temperature peak becomes greater than that of the low-temperature thermal peak. When the crystals are irradiated with alpha particles, the high-temperature maximum is predominant even at low doses.

It was found that the amplitude of the low-temperature peak is independent of the dose rate only at low values of the absorbed dose (up to about 0.5 rad). For doses of more than 0.5 rad, beginning at dose rates of 10^{-3} rad/sec, the value of this thermal peak drops somewhat as the dose rate increases. The amplitude of the high-temperature peak is independent of the dose rate.

By using the low-temperature thermoluminescence peak, the dosimeter sensitivity can be considerably increased, but at the same time, the length of time the information is retained (several days) will be

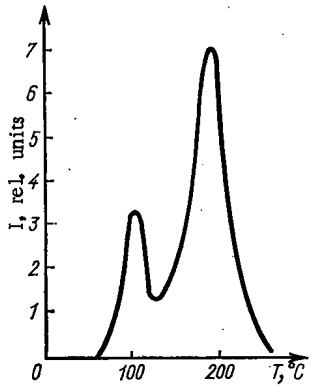

Fig. 1. Thermoluminescence curve for KCl–Eu crystals irradiated at 20°C with beta particles from an $Sr^{90} + Y^{90}$ source.

Translated from Atomnaya Énergiya, Vol. 33, No. 5, pp. 929-930, November, 1972. Original article submitted December 20, 1971; revision submitted March 1, 1972.

© 1973 Consultants Bureau, a division of Plenum Publishing Corporation, 227 West 17th Street, New York, N. Y. 10011. All rights reserved. This article cannot be reproduced for any purpose whatsoever without permission of the publisher. A copy of this article is available from the publisher for $15.00.

Declassified and Approved For Release 2013/02/27 : CIA-RDP10-02196R000300110005-5

Declassified and Approved For Release 2013/02/27 : CIA-RDP10-02196R000300110005-5

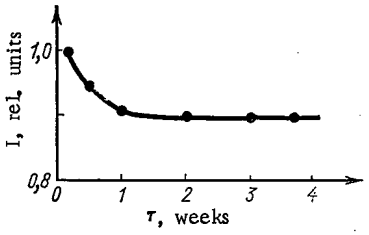

Fig. 2

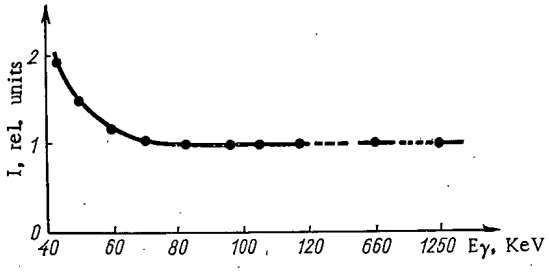

Fig. 3

Fig. 2. Amplitude of the high-temperature thermal peak of KCl – Eu crystals irradiated with beta particles from a $Sr^{90} + Y^{90}$ source, as a function of retention time after irradiation ("seeding" of the crystals).

Fig. 3. Sensitivity of KCl–Eu crystals placed in plastic cassettes 1 mm thick, plotted as a function of energy.

reduced. Recording the dose on the basis of the high-temperature maximum not only prolongs the time the information is retained (Fig. 2) but also makes it possible to use the crystal for radiation dosimetry at high temperatures (up to 150°C).

The sensitivity of thermoluminescence dosimeters using KCl–Eu crystals may be as good as 0.8 erg/cm^2 for alpha particles and 5 μrad for gamma rays when the absorbed dose is determined on the basis of the amplitude of the low-temperature thermoluminescence maximum. The absolute radiothermoluminescence yield of KCl – Eu crystals is $4.2 \cdot 10^{11}$ quanta/rad. The light sum stored by the crystal varies linearly with the dose in the range from $5 \cdot 10^{-6}$ rad to 10^5 rads. A crystal can be used many times without any appreciable change in its dosimetric properties.

KCl–Eu crystals measuring 10 × 10 × 1.5 mm were placed in plastic cassettes 1 mm thick, and the change in their sensitivity was studied for the gamma-ray energy range of 40 keV to 1.25 MeV (Fig. 3). It can be seen from Fig. 3 that for gamma-quantum energies higher than 70 keV the dosimeter readings are practically independent of the energy of the ionizing radiation.

From our investigations, we can conclude that the KCl–Eu system is entirely suitable for use in dosimetric instruments, since dosimeters using this crystal have very high sensitivity and can be used to measure doses over a wide range (11 orders of magnitude). Furthermore, in view of the fact that in this system, at low doses, the ratio between the values of the high-temperature and low-temperature thermoluminescence peaks resulting from irradiation with alpha particles differs from the ratio for irradiation with beta particles or gamma quanta, it is possible in some cases to distinguish between the contributions of alpha particles and those of beta particles, or between the contributions of alpha particles and those of gamma quanta, to the absorbed dose.

LITERATURE CITED

1. G. A. Mikhal'chenko, Izv. Akad. Nauk SSSR, Ser. Fiz., 30, 1409 (1966).
2. V. P. Glinin, Dissertation [in Russian], Leningrad (1970).

Declassified and Approved For Release 2013/02/27 : CIA-RDP10-02196R000300110005-5

Declassified and Approved For Release 2013/02/27 : CIA-RDP10-02196R000300110005-5

MINIMIZATION OF DEGRADATION OF LEATHER AND HIDE MATERIALS BY RADIATION STERILIZATION

A. B. Kipnis, P. I. Levenko, I. P. Strakhov, and I. G. Shifrin

UDC 539.12:620.179.15

In the search for the most efficacious ways of sterilizing hides to be made into leather, the conclusion was reached that ionizing radiations are most suitable for the purpose. However, irradiation of raw hides with sterilizing doses (2 to 3 Mrad) leads, under ordinary conditions, to an appreciable deterioration of the physicomechanical qualities of the leather subsequently made from the sterilized hides [1]. In our efforts to find methods for retaining the properties of the raw hides through radiation sterilization, we made a study of the nature and influence of irradiation conditions on the processes occurring in the hides when irradiated.

It had been demonstrated earlier [2] that processes of structuration (three-dimensional crosslinking) and degradation occur simultaneously in the basic protein of the hide (collagen) under γ-irradiation.

We used clean raw sheepskin hide, carefully washed and dehydrated by acetone, as our object of investigation. The experimental specimens and the control specimens were cut from symmetrical portions of the hide. The experimental specimens were irradiated by doses of 0.1, 0.5, 1.0, 2.5, and 5.0 Mrad in vacuum (10^{-2} mm Hg), in oxygen, in air, and in water at 293°K. The control specimens were exposed to the same media. The number of covalent crosslinkages in the collagen was determined by the Florey–Rainer equation in conformity with the procedure worked out by Cater [3]. The results we obtained, characterizing the effect of the irradiation conditions on the number of covalent crosslinkages in the irradiated collagen, are plotted in Fig. 1. For comparison, Fig. 2 shows the variation in the temperature at which collagen specimens fused together, as a function of the dose and the irradiation conditions.

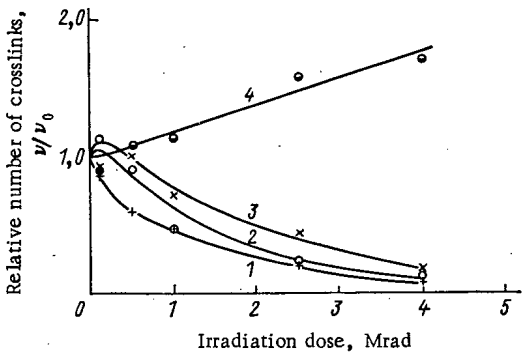

Fig. 1

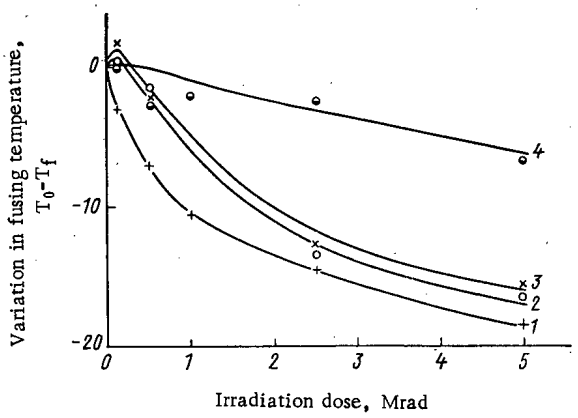

Fig. 2

Fig. 1. Dependence of number of crosslinkages in clean raw sheepskin hide as a function of irradiation dose and irradiation conditions: 1) in vacuum; 2) in oxygen; 3) in air; 4) in water.

Fig. 2. Dependence of the temperature at which clean raw sheepskin hide specimens fuse as a function of the irradiation dose and the irradiation conditions: 1) in vacuum; 2) in oxygen 3) in air; 4) in water.

Translated from Atomnaya Énergiya, Vol. 33, No. 5, pp. 931-932, November, 1972. Original article submitted September 13, 1971; revision submitted April 26, 1972.

© 1973 Consultants Bureau, a division of Plenum Publishing Corporation, 227 West 17th Street, New York, N. Y. 10011. All rights reserved. This article cannot be reproduced for any purpose whatsoever without permission of the publisher. A copy of this article is available from the publisher for $15.00.

Declassified and Approved For Release 2013/02/27 : CIA-RDP10-02196R000300110005-5

Declassified and Approved For Release 2013/02/27 : CIA-RDP10-02196R000300110005-5

TABLE 1. Comparative Quality Indices of Leather Made from Irradiated and Unirradiated Raw Hides

Raw hide	Fusing temperature, °C	Tensile strength, kg/mm²
Unirradiated	101	2,19
Irradiated in air*	95	1,17
Irradiated in water*	103	1,74

*Exposure dose 2.5 Mrad.

It is clear from the preceding data that the most intensive decrease in the number of covalent crosslinkages and the greatest reduction in the temperature at which the hides fuse occurs in irradiation in vacuum. When air-dried specimens are irradiated in oxygen, this process slows down slightly, but the slowdown is even more conspicuous in irradiation in air. In the range of small doses a relatively slow drop in the number of crosslinkages is observed with increasing exposure dose, but the number actually increases in irradiation in air. That fully confirms, and seems to offer an explanation for, the results reported in [1], where it was shown that crosslinking processes predominate at small exposure doses (0.1 to 0.3 Mrad) in collagen under certain conditions.

The number of covalent crosslinkages increases with increasing exposure dose in irradiation in water, and it exceeds the number of linkages in the unirradiated specimens by a factor of 1.7 when the dose is 5.0 Mrad. At the same time, the temperature at which specimens irradiated in water fuse drops with increasing exposure dose, despite the increase in the number of covalent crosslinkages.

The drop in the temperature at which the irradiated specimens fuse, which characterizes the overall stability of the collagen structure, is due to the ruptures of the links stabilizing that structure. In particular, breaks in the polypeptide chain have been brought to light by the methods of ultracentrifugation and electron spin resonance, in collagen specimens irradiated in vacuum [5-7], and the decrease in the number of covalent crosslinkages has been detected by us and by others [4]. In addition to the covalent linkages, other crosslinkages apparently also suffer rupture (e.g., hydrogen bonds stabilizing the collagen structure). Consequently, the total number of crosslinkages decreases when collagen specimens are irradiated in water, despite the increasing number of covalent crosslinkages, and that is responsible for the slight fall-off in the temperature at which the irradiated specimens fuse together.

It can be assumed that crosslinking of the collagen is due to the aldehydes whose formation was reported [2] in γ-irradiation and ultraviolet irradiation of various amino acids, and which are known [3, 8] to exhibit tanning properties.

The formation of aldehydes in response to irradiation occurs only in the presence of water, and obviously because of an intermediary imine product that can be hydrolyzed by water [2]. The formation of CHO-type free radicals in specimens in collagen irradiated by ultraviolet light in vacuum and exposed to air [9] has been ascertained by the ESR method. The aldehyde tanning effect is enhanced by irradiation [10]; that is accounted for in terms of the interaction between the aldehyde and the active collagen centers formed during irradiation.

On the basis of these investigations, we can infer that the degree of degradation of the collagen can be decreased substantially when raw hides are irradiated in water. A preliminary check test was run on the possible practical utilization of the method by irradiating wet salted goatskin with a dose of 2.5 Mrad in air and in water, after which leather was prepared from the skins so treated and so irradiated. The tabular data provide comparative quality indices of the leather made from the unirradiated hides and leather made from the hides irradiated in air and water.

It is clear from the tabular data that irradiation of wet salted raw hides in water at doses on the order of 2.5 Mrad makes it possible to seriously curtail radiation-induced degradation of raw hides to be processed into leather, and to produce leather of satisfactory quality from those hides.

LITERATURE CITED

1. I. P. Strakhov et al., At. Énerg., 29, 26 (1970).
2. I. P. Strakhov and I. G. Shifrin, Radiation Chemistry of Polymers [in Russian], Nauka, Moscow (1966).
3. C. Cater, J. Soc. Leather Trade Chem., 47, 259 (1963).
4. A. Bailey et al., Radiation Research, 22, 606 (1964).

Declassified and Approved For Release 2013/02/27 : CIA-RDP10-02196R000300110005-5

Declassified and Approved For Release 2013/02/27 : CIA-RDP10-02196R000300110005-5

5. R. Davidson and D. Copper, Biochem. J., 107, 29 (1968).
6. I. P. Strakhov et al., Izv. Vuzov. Tekhnologiya Legkoi Prom., No. 3, 54 (1971).
7. A. B. Kipnis et al., Biofizika (1972).
8. I. P. Strakhov (editor), Technology of Leather and Fur [in Russian], Legkaya Industriya, Moscow (1970).
9. W. Forbes and P. Sullivan, Biochim. Biophys. Acta, 120, 222 (1966).
10. I. G. Shifrin et al., in: Reports of the Science and Industry Conference on Uses of Ionizing Radiations in the National Economy, No. 4 [in Russian], Triokskoe Knizhnoe Izd-vo, No. 4, Tula (1972).

Declassified and Approved For Release 2013/02/27 : CIA-RDP10-02196R000300110005-5

Declassified and Approved For Release 2013/02/27 : CIA-RDP10-02196R000300110005-5

ANGULAR DISTRIBUTIONS OF ELECTRONS WITH INITIAL ENERGIES OF 12-25 MeV BEHIND TUNGSTEN, CADMIUM, AND COPPER BARRIERS

V. P. Kovalev, V. P. Kharin,
V. V. Gordeev, and V. I. Isaev

UDC 539.171.2

We measured the angular distributions of electrons with initial energies of 12-25 MeV after passing through scattering foils of various thicknesses. The measurements were performed with a beam from a linear electron accelerator in "slab" geometry. The scattering foils were of tungsten, cadmium, and copper. The foils were 40 mm in diameter and were located in air close to the exit window of the accelerator. The electron beam was 6 mm in diameter at the foil position. The detector was a thimble chamber with a sensitive volume of 0.25 cm^3 placed 13 cm from the foil and could be moved by remote control along the arc of a circle with its center at the middle of the foil. The aluminum chamber wall was 0.5 cm thick and the chamber had angular dimensions of 4.6°. The current of incident electrons was monitored during the measurements.

The ionization chamber recorded both electrons which had passed through the foil and bremsstrahlung from the scattering foil. We measured the yields and angular distributions of bremsstrahlung as functions of target thickness previously [1]. In processing the experimental data the current due to bremsstrahlung was subtracted from the total ionization chamber current. The "joining" was performed by means of the angular distribution of bremsstrahlung from a target of thickness 2.5 R which was measured under experimental conditions. The maximum contribution of bremsstrahlung was 36% for a tungsten target of thickness 5.35 g/cm^2. The angular distributions obtained in this way for electrons which passed through the foil are shown in Fig. 1. The open curves represent the distribution $W(\theta) \sim \cos^2\theta$. It is clear that the angular distribution approaches the $\cos^2\theta$ law as the foil thickness is increased.

The diffusion depth does not have a sharp boundary. To determine the "diffusion thickness" the family of functions

$$\eta(E_0, t) = \frac{3}{W_t(0)} \int_0^{\pi/2} W_t(\theta) \sin\theta \, d\theta, \quad (1)$$

was constructed, where $W_t(0)$ is the value of the measured distribution $W_t(\theta)$ at $\theta = 0$. For the diffusion thickness, t_d, $\eta(E_0, t_d) = 1$. The value of t_d is determined by the point of intersection of the function $\eta(E_0, t)$ with the horizontal line $\eta(E_0, t_d) = 1$. The "diffusion thicknesses" determined in this way are shown in Table 1.

TABLE 1. Diffusion Thickness and Extrapolated Electron Ranges

Electron energy E_0, MeV	R, g/cm^2			t_d in units of R		
	W	Cd	Cu	W	Cd	Cu
12,8	4,8	6,5	7	0,45	0,54	0,67
18	6,2	8,2	10	0,63	0,75	0,85
25	8,7	—	12	0,84	—	0,98

Note: For electron energies of 18 and 25 MeV the values of t_d were obtained by extrapolating by the $\cos^2\theta$ law.

The transmission coefficients and the extrapolated electron ranges were also determined from the experimental data. The transmission coefficients $K(E_0, t)$ for electrons of energy E_0 passing through a foil of thickness t were calculated by the formula

Translated from Atomnaya Énergiya, Vol. 33, No. 5, pp. 932-934, November, 1972. Original article submitted February 28, 1972.

© 1973 Consultants Bureau, a division of Plenum Publishing Corporation, 227 West 17th Street, New York, N. Y. 10011. All rights reserved. This article cannot be reproduced for any purpose whatsoever without permission of the publisher. A copy of this article is available from the publisher for $15.00.

Declassified and Approved For Release 2013/02/27 : CIA-RDP10-02196R000300110005-5

Declassified and Approved For Release 2013/02/27 : CIA-RDP10-02196R000300110005-5

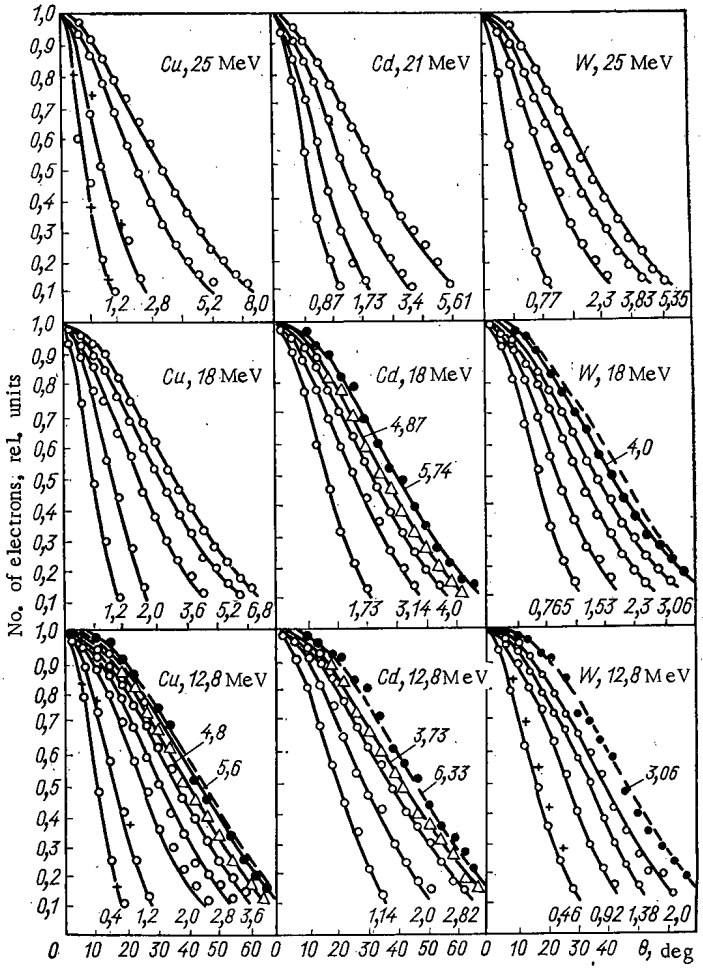

Fig. 1. Angular distributions of transmitted electrons. The numbers on the curves are the foil thicknesses in g/cm^2.

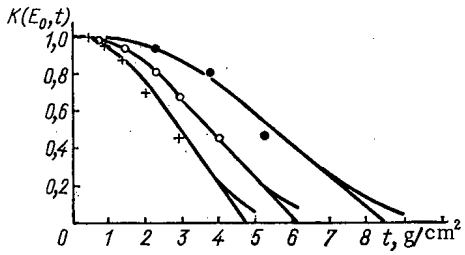

Fig. 2. Transmission curves for tungsten: +) 12.8 MeV; ○) 18 MeV; ●) 25 MeV.

$$K(E_0, t) = \frac{\int_0^{\pi/2} W_t(\theta) \sin\theta \, d\theta}{\int_0^{\pi/2} W_{t=0}(\theta) \sin\theta \, d\theta}, \qquad (2)$$

where $W_{t=0}(\theta)$ is the distribution of electron density along the radius of the beam measured by the chamber without the scattering foil, and $W_t(\theta)$ is the angular distribution of electrons which have passed through a foil of thickness t (g/cm^2). The functions $W_{t=0}(\theta)$ and $W_t(\theta)$ were normalized to unit current of incident electrons. In calculating the transmission coefficients a correction was introduced for the backscattering of electrons. The value of the backscattering cross section $\varepsilon(E_0, \infty)$ for semiinfinite geometry was taken from [2]. Following [2] the dependence of ε on the thickness of the scattering foil was taken into account by the formula

Declassified and Approved For Release 2013/02/27 : CIA-RDP10-02196R000300110005-5

Declassified and Approved For Release 2013/02/27 : CIA-RDP10-02196R000300110005-5

$$\varepsilon(E_0, t) = \varepsilon(E_0, \infty)\{1 - \exp[-\alpha(2t/R)^n]\}, \quad (3)$$

where $\alpha = 3.5$, $n = 1.65$, and R is the electron range.

The transmission curves for tungsten are shown in Fig. 2. The extrapolated ranges are shown in Table 1.

The crosses in Fig. 1 show angular distributions of electrons calculated by the Moliere formula. The effect of a layer of air on the width of the angular distribution was estimated by the Moliere formula for $\theta_{1/e}$ using the "equivalent addition" to the foil thickness. This procedure estimates the increase in the width $\theta_{1/e}$ due to the layer of air as no more than 1.5%. A comparison with experiment confirms the conclusion of Tabata et al. [3] that the Moliere theory gives a satisfactory description of the angular distributions of transmitted electrons for thickness ≤ 0.1 R.

LITERATURE CITED

1. V. P. Kovalev et al., At. Énerg., 31, 289 (1971); 32, 77 (1972).
2. T. Tabata, Phys. Rev., 162, 336 (1967).
3. T. Tabata et al., Ann. Rep. Rad. Center, Osaka Pref., 8, 60 (1967).

Declassified and Approved For Release 2013/02/27 : CIA-RDP10-02196R000300110005-5

Declassified and Approved For Release 2013/02/27 : CIA-RDP10-02196R000300110005-5

SPECTRA AND ABSOLUTE YIELDS OF NEUTRONS FROM THICK TARGETS BOMBARDED WITH 23.2 MeV DEUTERONS

V. K. Daruga, E. S. Matusevich, and Kh. Narziev

UDC 539.125.5.7

Studies have been made of the energy distributions and absolute yields of neutrons from thick targets of Be, Al, Ni, Nb, Ag, Ta, and Pb of natural isotopic composition bombarded with deuterons from the 1.5 m FÉI cyclotron. The mean energy of the bombarding deuterons was 23.2 ± 0.2 MeV; this was determined by their ranges in calibrated aluminum foils and by direct measurements with a silicon solid state detector.

The energy spectra of neutrons above 0.5 MeV were measured with a single-crystal stilbene spectrometer at angles θ of 0, 45, 90, and 135° with respect to the direction of the primary deuteron beam. Discrimination against the gamma-ray background was by decay time [1]. The amplitude distributions of recoil protons were converted into neutron energy spectra by the program described in [2]. The experimental errors and the errors in processing the spectra were determined by the method described in [3].

The results are shown in Fig. 1. The shape of the neutron spectrum from the Be target at $\theta = 0$ is similar to that obtained in [4] for 22 MeV deuterons. Table 1 shows the neutron yield $Y(\theta)$ from various targets obtained by integrating the $N(E_n)$ distribution curves over E_n from 1 to 13 MeV.

The total neutron yields ($E_n > 0$) from targets of Al, Ni, Nb, Ta, and Pb in the direction $\theta = 0$ were measured with a long counter of standard construction [3]. Figure 2 shows the neutron yields at $\theta = 0$ measured with this counter and those obtained by integrating the $N(E_n)$ curves (Table 1), plotted as functions of the atomic number Z of the target nucleus. For comparison the figure also shows the results obtained with the long counter of [4]. The lowered neutron yield from the Ni target should be noted; a similar result was found in [5] for 10 MeV deuterons.

To estimate the total integrated neutron yields the measured energy distributions (Fig. 1) were extrapolated to lower and higher neutron energies. The data in [6] were used in extrapolating into the range $E_n > 13$ MeV. Then the angular distributions of the total neutron yields were constructed. In Table 2 the values of $Y_{4\pi}$ obtained by integrating the angular distribution curves are compared with the results for 24 MeV deuterons obtained in [7] by using a $MnSO_4$ tank.

TABLE 1. Neutron Yields at Various Angles θ

Target	$Y(\theta) = \int_1^{13} N(E_n)\, dE_n$, $sr^{-1} \cdot \mu C^{-1}$			
	0°	45°	90°	135°
Be	$7{,}3 \cdot 10^{10}$ (±16,5)*	$1{,}8 \cdot 10^{10}$ (±17)	$7{,}6 \cdot 10^{9}$ (±13)	$4{,}0 \cdot 10^{9}$ (±15,5)
Al	$2{,}5 \cdot 10^{10}$ (±12)	$6{,}0 \cdot 10^{9}$ (±12)	$3{,}7 \cdot 10^{9}$ (±11,5)	$2{,}6 \cdot 10^{9}$ (±12)
Ni	$1{,}0 \cdot 10^{10}$ (±12)	$4{,}5 \cdot 10^{9}$ (±11)	$2{,}1 \cdot 10^{9}$ (±12)	$1{,}65 \cdot 10^{9}$ (±12)
Nb	$1{,}1 \cdot 10^{10}$ (±18)	—	$3{,}6 \cdot 10^{9}$ (±11)	—
Ag	$1{,}2 \cdot 10^{10}$ (±17)	—	$3{,}3 \cdot 10^{9}$ (±15)	—
Ta	$9{,}0 \cdot 10^{9}$ (±11,5)	$2{,}5 \cdot 10^{9}$ (±16)	$2{,}1 \cdot 10^{9}$ (±10,5)	$1{,}67 \cdot 10^{9}$ (±17)
Pb	$8{,}0 \cdot 10^{9}$ (±15)	—	$2{,}1 \cdot 10^{9}$ (±14,5)	—

*Percentage errors are shown in parentheses.

Translated from Atomnaya Énergiya, Vol. 33, No. 5, pp. 934-936, November, 1972. Original article submitted June 6, 1972.

© 1973 Consultants Bureau, a division of Plenum Publishing Corporation, 227 West 17th Street, New York, N. Y. 10011. All rights reserved. This article cannot be reproduced for any purpose whatsoever without permission of the publisher. A copy of this article is available from the publisher for $15.00.

Declassified and Approved For Release 2013/02/27 : CIA-RDP10-02196R000300110005-5

Declassified and Approved For Release 2013/02/27 : CIA-RDP10-02196R000300110005-5

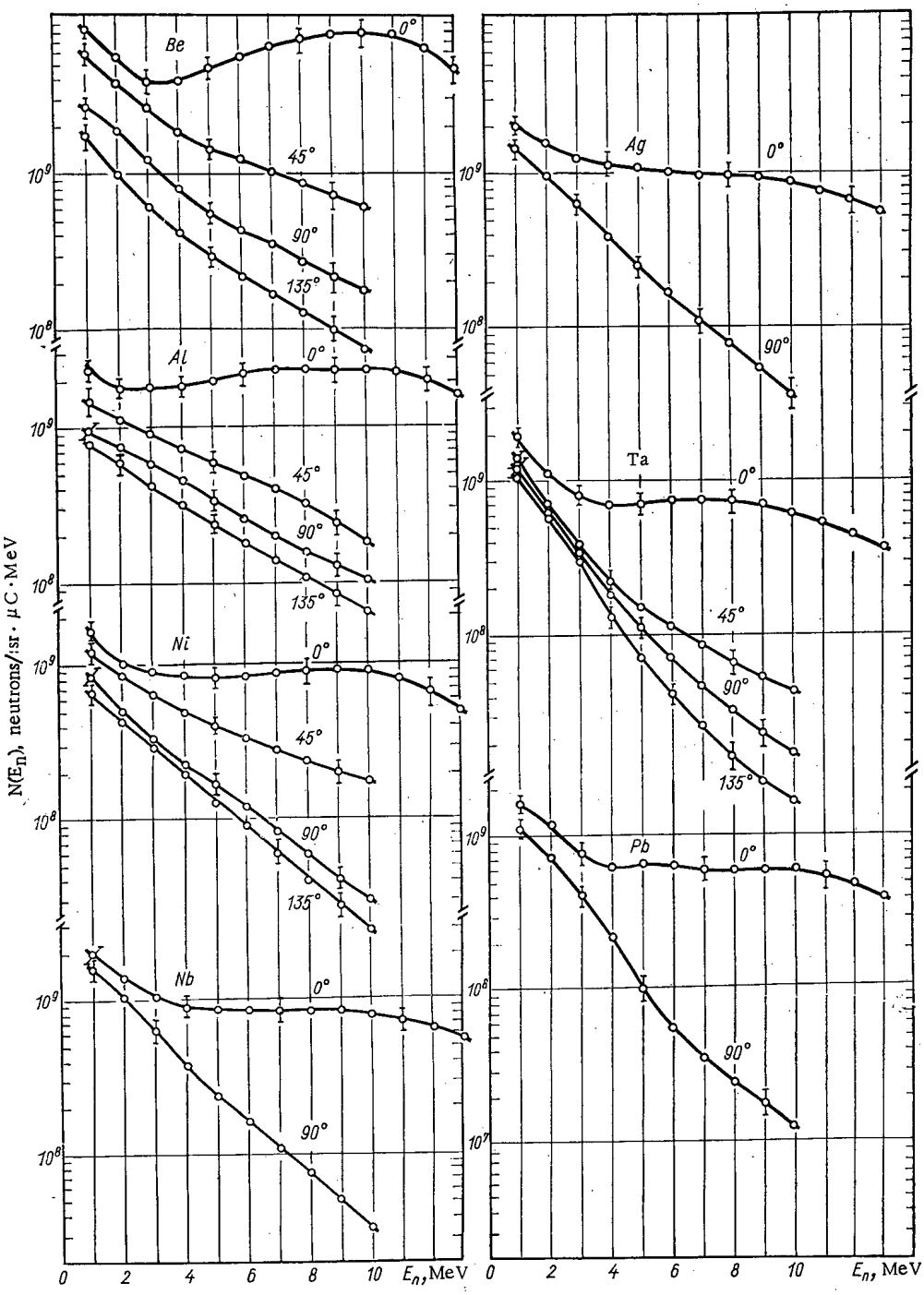

Fig. 1. Differential energy distributions of neutrons from targets bombarded with 23.2 MeV deuterons.

Declassified and Approved For Release 2013/02/27 : CIA-RDP10-02196R000300110005-5

Declassified and Approved For Release 2013/02/27 : CIA-RDP10-02196R000300110005-5

TABLE 2. Integrated Neutron Yields

Target	$Y_{4\pi} \cdot 10^{10}$, neutrons/μC		Target	$Y_{4\pi} \cdot 10^{10}$, neutrons/μC	
	our data.	[7]		our data.	[7]
Be	20±3,5	18,5±1	Cu	—	5,5±0,3
Al	7,7±1,3	—	Ta	4,7±0,8	5,2±0,3
Ni	4,6±0,7	—	U	—	7,3±0,6

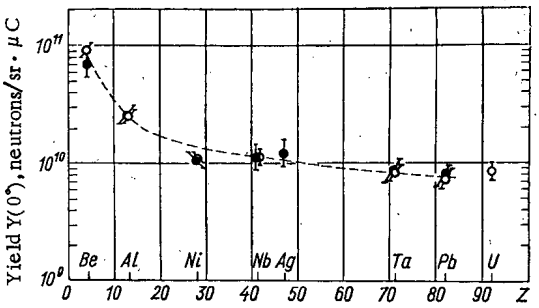

Fig. 2. Absolute neutron yields in the direction $\theta = 0$ from targets bombarded with 23.2 MeV deuterons. ○) $E_n > 0$; ●) $1 \leq E_n \geq 13$ MeV.

In conclusion the authors thank N. N. Krasnov for making it possible to work at the cyclotron, A. A. Ognev for measuring the deuteron energy, N. N. Pal'chikov, S. S. Prokhorov, and V. I. Regushevskii for help with the measurements and in processing the results.

LITERATURE CITED

1. F. Brooks, Nucl. Instrum. and Methods, 4, 151 (1959).
2. Yu. A. Kazanskii et al., At. Énerg., 10, 143 (1966).
3. V. K. Daruga, Dissertation [in Russian], OIYaI, Dubna (1971).
4. V. I. Daruga and N. N. Krasnov, At. Énerg., 30, 399 (1971).
5. L. Smith and P. Kruger, Phys. Rev., 83, 1137 (1951).
6. I. Heertje and A. Aten Jr., Physica, 30, 978 (1964).
7. W. Crandall and G. Millburn, J. Appl. Phys., 28, 273 (1957).

Declassified and Approved For Release 2013/02/27 : CIA-RDP10-02196R000300110005-5

Declassified and Approved For Release 2013/02/27 : CIA-RDP10-02196R000300110005-5

COMECON SYMPOSIUM ON WATER MANAGEMENT AT WATER REACTOR FACILITIES, RADIATION MONITORING, AND MEANS OF MINIMIZING RADIATION HAZARD IN COOLANTS

B. A. Alekseev

Delegations from Bulgaria, Hungaria, the German Democratic Republic, Poland, Rumania, the USSR, and Czechoslovakia were in attendance at a symposium held May 9-12, 1972, at Strahlsund (German Democratic Republic), as well as specialists from various organizations of the German Democratic Republic.

Results achieved in the time elapsed since the last symposium held in November, 1968 (Gera, German Democratic Republic) in the principal fields covered in the plan of collaboration between COMECON member-nations were detailed in the 37 reports presented. Those results pertained to:

1) water management of reactor loops and corrosion behavior of structural materials;

2) water cleanup and water treatment at nuclear power stations;

3) formation and migration of deposits (both ordinary and radioactive in reactor loops);

4) chemical and radiochemical analysis of coolant;

5) leaktesting of fuel element cladding.

Four review reports discussed the present state of the art in these areas. Papers on the first two topics were prepared by specialists of the Soviet Union, papers on the third topic were prepared by GDR specialists, and papers of the fourth topic were prepared by Hungarian specialists.

New information on the kinetics of ammonia radiolysis under operating conditions of the Rheinsberg (GDR) nuclear power station, and on equilibrium in that reaction, which would be useful for estimating water conditions for new high-level power-generating units incorporating VVÉR-1000 reactors, were communicated by K. Ortel. Some of the papers dealt with corrosion of structural materials in the reactor loop. A paper by E. S. Chernorotov (USSR) contained concrete data on the behavior of austenitic and pearlitic steels (Kh18N10T, 48TS, steel-20) in boron control situations, and in work with a mixed ammonia – potassium water management system adopted in the USSR for VVÉR-440 power-generating units. The adequate stability of 48TS steel to corrosive attack makes it possible to do without stainless steel protective hardfacing in reactor pressure vessels. Long-term corrosion tests on several steels in the loops of the MR reactor of the I. V. Kurchatov Institute of Atomic Energy (V. V. Gerasimov, A. I. Gromova, et al.) demonstrated the effect of radiation on corrosion, and made it possible to assess dangerous (for corrosion cracking of Kh18N10T austenitic steel) concentrations of chloride ions and dissolved oxygen. These estimates are somewhat more pessimistic than those made by K. Langecker (GDR) on the basis of short-term corrosion tests. G. Mandru et al. (Rumania) gave an account of an investigation into the effect of the state of the surface of 1Kh18N10T steel on the corrosion rate in high-temperature water; the slowest corrosion rate was found on electrolytically ground specimens. W. Bergeman and D. Legler (GDR) found that metals with a rough (as-cast) surface respond less well to deactivation than do machined surfaces.

J. Beran (Czechoslovakia) reported on an interesting electrochemical method for remote monitoring of corrosion in pressurized-water loops. The method still lacks some finishing touches, and will make it possible to estimate only the development of local corrosion, but it might be improved into a valuable method for monitoring the state of metal on stream at nuclear power stations.

Translated from Atomnaya Énergiya, Vol. 33, No. 5, pp. 937-938, November, 1972.

© 1973 Consultants Bureau, a division of Plenum Publishing Corporation, 227 West 17th Street, New York, N. Y. 10011. All rights reserved. This article cannot be reproduced for any purpose whatsoever without permission of the publisher. A copy of this article is available from the publisher for $15.00.

Declassified and Approved For Release 2013/02/27 : CIA-RDP10-02196R000300110005-5

Declassified and Approved For Release 2013/02/27 : CIA-RDP10-02196R000300110005-5

Many of the reports discussed various aspects of the problem of cleaning up reactor loop coolant. A large number of papers on the results of laboratory studies and experiments at the Rheinsberg nuclear power station were presented by GDR specialists. Soviet specialists shed further light on those problems in a review paper. But the concepts entertained by the GDR specialists and USSR specialists diverged strongly, and that called for a special and thorough discussion. The results of reactor loop tests and the operating experience of the first and third power-generating units at the Novaya Voronezh' nuclear power station have demonstrated the feasibility of continuous coolant cleanup procedures (without degassing the coolant) on ion exchange resin filters in the pressurized loop. The cleanup step is efficient in getting rid of chloride ions and corrosion products. The GDR representatives, on the basis of extremely pessimistic assessments of the effectiveness of ion exchange resin filters under boron control conditions, held that cleanup must be performed episodically when the coolant becomes excessively contaminated. They recommend low-pressure facilities with partial or complete degassing of the coolant (most particularly for power-generating units incorporating VVÉR-1000 reactors). Several aspects of the problem were aired in the discussion, which covered process and performance topics and also topics pertaining to pollution of the environment by radioactive gases and by iodine. A need for broader coordinated research was highlighted, particularly in order to clarify the reasons for the differences in the effectiveness of ion exchange filtration under different conditions, the effect of water treatment regimes on the relationship between rates of deposition and contamination of the loop water by corrosion products, which determine the rate at which the water is to be withdrawn from the loop via bypass cleanup steps, etc.

In some of the reports, representatives of Hungary and of the USSR discussed an approach to selection of ion exchange resins for cleanup of coolant, with the radiation stability and thermal stability of the resins taken into cognizance, as well as the physicomechanical properties of the resins and their response to radiation. Practical recommendations were put forth. The investigations in progress in those two countries supplement each other quite well both from the standpoint of techniques and in terms of the lists of ion exchange resins tested.

Reports on the formation and composition of radioactive deposits in the reactor loop were made by specialists from the GDR, Rumania, and the USSR. One of the GDR papers reported on an improved method for deactivating the primary loop of the nuclear power station at Rheinsberg, so that the volume of waste effluents could be reduced somewhat.

A large number of papers dealt with chemical and radiochemical monitoring of coolant purity and possible automation and computerization of coolant monitoring work. An automated method for determining the concentration of boric acid in the coolant by potentiometric titration in the presence of chromotropic acid (W. Panowski, K. Ortel, H. Felsberg, GDR). Equipment manufactured in batch lots in the GDR was used with that method. Some automated systems for γ-ray spectrometric analysis, both with and without preseparation of the specimen into fractions, were described in reports by Hungarian and Soviet specialists.

Unfortunately, there were only three reports on systems for leaktesting fuel element cladding, even through that problem is one of front-ranking importance, and despite the many unsolved problems in that area, particularly where large nuclear power stations are concerned. Such problems include arriving at a well validated criterion for acceptance or scrapping of fuel elements.

The symposium took place in an excellent businesslike and friendly atmosphere, and showed that the nations participating in the COMECON PKIAÉ coordination plan have achieved remarkable results over the past four years. One factor contributing to this has been the systematic holding of discussions on the results, another updating of current plans and long-term plans to conferences of specialists. It has been found that some problems are still not being solved fast enough or thoroughly enough. The development of nuclear power in the COMECON member nations calls for further concentration of efforts geared to the solution of the major problems in this arena, and accordingly greater and more clearly defined coordination of efforts. In the opinion of the participants of this symposium, that can be done successfully through the auspices of the Coordination Scientific-Technical Council to be organized (in line with COMECON PKIAÉ decisions) by the German Democratic Republic as the coordinator-nation in this area.

Declassified and Approved For Release 2013/02/27 : CIA-RDP10-02196R000300110005-5

Declassified and Approved For Release 2013/02/27 : CIA-RDP10-02196R000300110005-5

COLLABORATION DAYBOOK

The first session of KNTS [Coordination Scientific-Technical Council] and a conference of specialists on fuel element reprocessing were held March 27 through April 1, 1972, at Orlik (Czechoslovakia).

The work done in this area during 1967-1970 was summarized. The increasing significance of reprocessing of spent nuclear fuel for nuclear power development in the COMECON member-nations, and the need for cooperation on an international level in scientific and industrial research for the solution of the problems confronting the industry, were pointed out. Progress in line with the collaboration program during 1971 was discussed, as well as some proposals advanced by the delegations of Hungary, East Germany, and Rumania on revisions of the program.

Special importance is attached to the transportation of spent fuel, since that affects all of the COMECON member-nations engaged in building nuclear power stations, and necessitates coordination of the work in all aspects.

Participating in the work of the KNTS session were delegations from Bulgaria, Hungary, the GDR, Poland, Rumania, the USSR, and Czechoslovakia.

* * *

A conference of specialists from East Germany, Poland, the USSR, and Czechoslovakia on safe disposal techniques for radioactive wastes in geological formations was held April 24-28, 1972, in Moscow, in line with the COMECON PKIAÉ work plan.

The general characteristics of the method of underground disposal of liquid radioactive wastes were discussed, requirements applicable to geological and hydrogeological materials, geological formations, and reservoir strata, as well as to designs of prospecting and exploration wells and boreholes, needed in order to achieve radiation safety in the planning and building of underground burial sites, were formulated. The sequence to be followed in conducting hydrogeological and physicochemical investigations involved in the prospecting phase of the operations, detailed exploration, and special research in fluid dynamics, was discussed; determinations of the parameters of aquifer horizons, including filtration inhomogeneity of a stratum, were discussed, and recommendations were advanced on the best ways of conducting laboratory research and field research on sorption and migration of radioisotopes.

The conference materials dealing with techniques and procedures are recommended for use in prospecting and exploration of geological structures in the COMECON member-nations suitable for safe disposal of radioactive wastes. Topics pertaining to research on safe disposal of high-level wastes in salt formations, from the standpoints of radiation safety, public health, and hydrogeological considerations, and assessments of possible consequences of radioactivity gaining access to surface deposits, were also discussed.

Completion of a comprehensive research program in this area by the COMECON member-nations will be of significant practical interest in contributing to the building of safe underground burial sites not only for radioactive wastes, but also for highly toxic wastes and effluents of many chemical processes.

Translated from Atomnaya Énergiya, Vol. 33, No. 5, pp. 938, November, 1972.

© 1973 Consultants Bureau, a division of Plenum Publishing Corporation, 227 West 17th Street, New York, N. Y. 10011. All rights reserved. This article cannot be reproduced for any purpose whatsoever without permission of the publisher. A copy of this article is available from the publisher for $15.00.

Declassified and Approved For Release 2013/02/27 : CIA-RDP10-02196R000300110005-5

Declassified and Approved For Release 2013/02/27 : CIA-RDP10-02196R000300110005-5

INFORMATION

MULTIPURPOSE USE OF LINEAR PROTON ACCELERATOR I-2

V. A. Batalin, V. I. Bobylev,
E. N. Danil'tsev, I. M. Kapchinskii,
A. M. Kozodaev, R. P. Kuibida,
N. V. Lazarev, and V. I. Édemskii

At the Institute of Theoretical and Experimental Physics (ITEP) a system has been developed which makes it possible to use the linear accelerator–injector I-2 [1] of the 7 GeV proton synchrotron not only for its direct intended use but also as an intense source of protons with energies of 6 and 25 MeV for experiments in the field of nuclear physics. As an injector the linear accelerator operates with alternate pauses of 0.8 and 3.2 sec, specified by the periodicity of operation of the synchrotron. However, the accelerator I-2 itself can operate with a repetition frequency of 1 Hz for 3-50 μsec pulse length. This makes it possible to use it simultaneously as an injector and as an independent proton source.

The beam of the accelerator I-2 is deflected into the transportation channel to the proton synchrotron [2] by a rotating dc magnet (see Fig. 1). The second channel is placed at the axis of the linear accelerator beyond the rotating magnet and is equipped with electromagnetic lenses, correctors, and observation chambers. For leading out the beam into the second channel the constant field of the rotating magnet is compensated for by the pulsed field of a stationary six-turn winding placed together with charged pole pieces in the vacuum chamber. The brass walls of the chamber serve as a screen for the pulsed field and restrict it within its volume. The position of the winding and the replacement of the solid pole pieces in the gap of the rotating magnet by charged pole pieces did not distort the configuration of the constant field.

The analyzing magnet and special instruments placed in the observation chambers enable one to measure the beam parameters. When the analyzing magnet is disconnected, the beam passes into the next segment of the channel equipped with pulsed quadrupole lenses and correctors. The pulsed lenses have poles

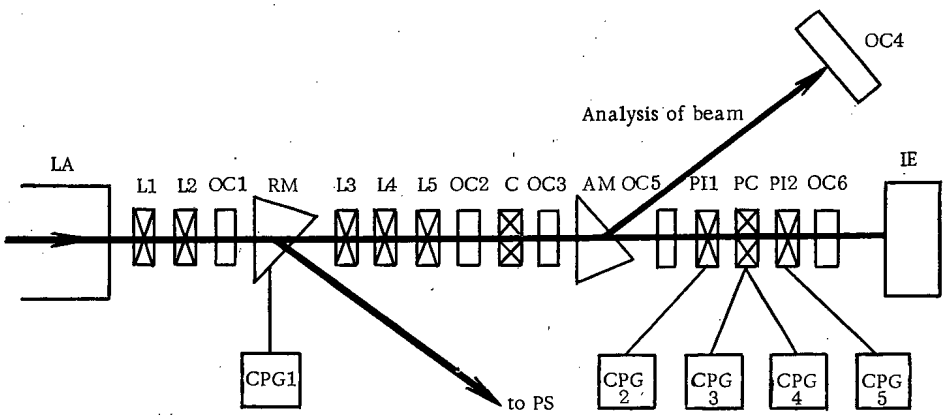

Fig. 1. Scheme for the separation of beams. LA) linear accelerator; L1-L5) dc quadrupole lenses; OC1-OC6) observation chambers; RM) rotating magnet; C) dc correctors; AM) analyzing magnet; PI1-PI2) pulsed quadratic lenses; CP) pulsed correctors; CPG1-CPG5) current pulse generators; PS) proton synchrotron; IE) instrumentation for experiments.

Translated from Atomnaya Énergiya, Vol. 33, No. 5, pp. 939-940, November, 1972.

© 1973 Consultants Bureau, a division of Plenum Publishing Corporation, 227 West 17th Street, New York, N. Y. 10011. All rights reserved. This article cannot be reproduced for any purpose whatsoever without permission of the publisher. A copy of this article is available from the publisher for $15.00.

Declassified and Approved For Release 2013/02/27 : CIA-RDP10-02196R000300110005-5

Declassified and Approved For Release 2013/02/27 : CIA-RDP10-02196R000300110005-5

that are not clearly defined; their magnetic circuits are made up of ferrite rings. The core of the correctors is made of transformer iron. The beam is led out into the atmosphere through a 0.3 mm thick aluminum foil.

The pulsed electromagnetic devices of the ion duct are fed from the corresponding current pulse generators; a half-period of the resonance discharge of a condensor is used for the formation of these current pulses. The half-period is chosen equal to 1 μsec from the requirement of stability of the field during the transit time of the beam. Thyristors T-150 in series–parallel connection operate as current commutators in the generator circuits. The amplitude of the current in the windings of the lenses and the correctors reaches 1 kA. The constant field of the rotating magnet is compensated for when the current amplitude in the loop is 17 kA. The stability of the residual field in the gap of the magnet (with reference to that of the constant field) is determined by the circuit parameters of the constant and the pulsed supply and comprises 0.07%.

In the regime of simultaneous operation of the accelerator I-2 with the proton synchrotron and the second lead-out channel it is necessary to regulate the instants of switching on the pulsed devices of the linear accelerator and the ion duct, which is accomplished by a specially developed synchronization block.

The operation of the accelerator I-2 in the regime described above started in October, 1971. With the use of the pulsed loop particle losses beyond the rotating magnet do not exceed 10%; the current amplitude in the atmosphere is more than 100 mA. Experiments are conducted regularly on the beam of the second lead-out channel.

LITERATURE CITED

1. V. A. Batalin et al., Pribory i Tekhnika Éksperimenta,, No. 5, 9 (1967).
2. L. Z. Barbash et al., Pribory i Tekhnika Éksperimenta, No. 6, 14 (1969).

Declassified and Approved For Release 2013/02/27 : CIA-RDP10-02196R000300110005-5

Declassified and Approved For Release 2013/02/27 : CIA-RDP10-02196R000300110005-5

INTERNATIONAL SYMPOSIUM ON PHYSICS OF ELEMENTARY PARTICLES

V. M. Dubovik and R. M. Muradyan

An international symposium on the theory of elementary particles was held in Reinhardsbrunn (GDR) from April 12 to 23, 1972. It was organized by the Joint Institute of Nuclear Research (Dubna) and the Institute of High Energy Physics of the Academy of Sciences of the GDR. About 60 persons from the participating countries of the Joint Institute and eight representatives of East European countries took part in the symposium. Thirty papers were presented and considerable time was allotted for discussions.

The papers covered three main directions of research: deep inelastic scattering of electrons on protons; regularities of strong inclusive processes; dual models.

The paper by A. N. Tavkhelidze (USSR) was devoted to the first problem. He discussed the rigorous investigation, carried out jointly with N. N. Bogolyubov and V. S. Vladimir, on the asymptotic behavior of current commutator in the configuration space based on the axiomatic approach of the quantum field theory. The authors determined the conditions for Iost–Leman–Laison spectral function ensuring a generalized self-similar behavior of the form factors in the region of deep inelastic scattering.

D. Robashik and E. Vitsorek (JINR) presented a paper entitled "Behavior of dual models on the light cone." In particular, the models of Nambu and Venetsiano were discussed from the point of view of the configuration space. J. Polkinghorn (England) gave a covariant formulation of the parton model leading to scale invariance of self-similarity in the deep inelastic region. The consequences of identification of partons and quarks were discussed. Using duality arguments structure functions were computed, which qualitatively agree with the experimental results. The equivalence of the parton model and the algebra of the currents on the light cone was demonstrated.

On the second problem of the self-similar behavior in the presence of strong interactions, R. M. Muradyan (JINR) presented a paper based on the work carried out jointly with V. A. Matveev and A. N. Tavkhelidze. It was shown that using the generalized analysis of dimensionalities with two scales of length (along the axis of impact and in the transverse plane) in conjunction with the requirements of similarity in the scale transformation of the pulses with $q_z \to \lambda q_z$ and $\mathbf{q}_\perp \to \mathbf{q}_\perp$, one can obtain the results of many contemporary models of strong interactions. In particular, the connection of the proposed approach with the multi-Regge analysis of Muller was discussed.

The construction of phenomenological form factors for the description of highly energetic spectra was discussed in the paper by G. Zats (FRG). The pattern of two fireballs was taken as the basis. The connection between the thermodynamic and the dual approaches was investigated.

J. Ranft (GDR) discussed the consequences of using strong buttstrap solution for inclusive spectra. The behavior of the spectra for asymptotically large energies is predicted. G. Ranft (GDR) spoke of the possibility of describing inclusive spectra with the use of exchange of Regge poles. She stressed that so far the region of pionization for high energies has not been investigated in detail. Her computations are useful for the description of inclusive spectra obtained at CERN with the use of intersecting counter beams.

K. Kayanti (Finland) discussed a simple statistical model which enables one to compute inclusive spectra and correlation functions explicitly.

The paper by G. M. Zinov'ev (USSR), based on the work done jointly with V. P. Shelest and coworkers, was devoted to the dual models. It was concerned with the statistical interpretation of the dual

Translated from Atonmaya Énergiya, Vol. 33, No. 5, pp. 940-941, November, 1972.

© 1973 Consultants Bureau, a division of Plenum Publishing Corporation, 227 West 17th Street, New York, N. Y. 10011. All rights reserved. This article cannot be reproduced for any purpose whatsoever without permission of the publisher. A copy of this article is available from the publisher for $15.00.

Declassified and Approved For Release 2013/02/27 : CIA-RDP10-02196R000300110005-5

Declassified and Approved For Release 2013/02/27 : CIA-RDP10-02196R000300110005-5

models. Interesting results were obtained on the distribution of the resonance spins. It was shown that the nature of the "effective" Regge trajectories is significantly nonlinear. The average characteristics of a number of dual resonances were computed.

F. Kashlun (GDR) communicated on the construction of dual amplitude with Mandel'stam analyticity. Regge limit for the physical values of Mandel'stam variables was investigated. The results were generalized to n-point functions.

New experimental data on s-wave pion–pion interaction near the threshold of kaon–antikaon generation were theoretically interpreted in the paper by M. Fraussar (France).

The papers devoted to other problems were: by I. Todorov (Bulgaria), which discussed how to construct a skeleton theory of perturbations without ultraviolet divergences making use of the requirement of invariance in conjunction with the idea of anomalous dimensionalities; by V. M. Dubovik (JINR) discussing the problem of determination of multipole radiation sources in classical and quantum field theories. M. K. Polivanov and V. Ya. Fainberg (USSR) elucidated the essential problems of the asymptotic approach to the quantum field theory.

A. Ulmann (GDR) presented an original work making use of the powerful topological method of the group theory. This paper discussed the relation between the conformal group and Poincaré group.

The diversity of the themes and the high scientific level of the work of the theoreticians was noteworthy.

The results of the symposium were summed up in the concluding remarks of M. K. Polivanov (USSR) noting the special significance of small conferences permitting the synthesis of views of scientists of many countries the most important fundamental problems of the contemporary physics of elementary particles. He stressed the significance of extensive theoretical and experimental investigation of multiparticle processes providing the necessary additional information on the structure of elementary particles. The construction of a theory of strong interactions is not possible without these informations.

It is proposed to publish in GDR the abstracts of the papers presented at the symposium. Some of the papers will be published in the journal Fortschritte der Physik.

Declassified and Approved For Release 2013/02/27 : CIA-RDP10-02196R000300110005-5

Declassified and Approved For Release 2013/02/27 : CIA-RDP10-02196R000300110005-5

GORDON CONFERENCE ON NUCLEAR CHEMISTRY

V. A. Druin

The XII Gordon annual national conference on nuclear chemistry in the USA was held this year from June 26-30 in a small town, New London (New Hampshire). It was devoted to the study of the properties of fissionable nuclei and nuclear reactions caused by very heavy ions (Kr, Xe) of moderate energies (~7 MeV/nucleon) and high energy particles (p, α, N^{14}, O^{16}).

About 130 persons, mainly from the USA, participated in the conference. The European countries were represented by a relatively large number of physicists from FRG (14 persons) and also representa- from France, Italy, Poland, GDR, Yugoslavia, and the international nuclear centers CERN and JINR (two persons). Physicits from Israel, Japan, and India were also present.

The task of the Gordon conference is to discuss the contemporary state of the problems of nuclear chemistry and the recent original works on the subject. Accordingly the program included review papers (as a rule, by leading specialists in their fields) and communications on the results of new investigations in some direction. Unfortunately the proceedings of Gordon conferences are not published.

This year (chairman M. Blann, Rochester university) was exceptionally packed and diverse. Along with the papers devoted to purely nuclear-physical theoretical and experimental problems of stability of heavy and extra-heavy particles, the fission of nuclei mainly in isomer and excited states, and the mechanism of nuclear reactions in the range of moderate and high energies, there was a paper by H. Mazursky (Astrogeological Center, Arizona) on the geological evolution of Mars (based on the data obtained by Mariner-9).

In all 19 papers and communications were presented. Three papers were directly related to the study of the possible mechanism of synthesis and prediction of the fission properties of heavy and extra-heavy elements. These were reports on the experiments on the acceleration and the investigation of the mechanism of interaction of krypton (I. Le Beiek, Orse, France) and xenon (V. A. Druin, JINR, USSR) ions with different nuclei, and the report of U. Mosel (Washington University) about the estimates of the kinetic energy, the energy of excitation of the fission fragments, and the average energy of neutrons released in spontaneous fission of the nuclei. A large part of the material contained in Mosel's paper has already been published (Nucl. Phys., A186, 1 (1972)).

The principal results of the investigations of the French physicists from Orse were summarized by Beiek as follows.

1. The results on the observation of α-particles with energies 13-15 MeV, published by them earlier and related to the decay of a hypothetical extra-heavy particle, were found to be erroneous. Actually, two successive decays with a very small interval between them were recorded.

2. From the experiments on the irradiation of cadmium by krypton ions with the formation of a composite polonium nucleus, and also from the experiments on elastic scattering of accelerated krypton by nuclei, it is concluded that r_0 is equal to 1.32 and not 1.45 fermi as obtained from numerous experiments with multiply charged ions from boron to argon. This means that the effective Coulomb barrier in the interaction of heavy krypton and xenon ions with uranium nucleus must be larger than the classical electrostatic barrier by several tens of megaelectron volts.

3. In the irradion of thorium by krypton ions the cross section of formation of fragments in the fission of a composite nucleus with Z = 126 into two fragments of comparable mass is smaller than a few millibarns. Hence it is concluded that a composite nucleus with Z = 126 is not formed.

Translated from Atomnaya Énergiya, Vol. 33, No. 5, pp. 940-941, November, 1972.

© 1973 Consultants Bureau, a division of Plenum Publishing Corporation, 227 West 17th Street, New York, N. Y. 10011. All rights reserved. This article cannot be reproduced for any purpose whatsoever without permission of the publisher. A copy of this article is available from the publisher for $15.00.

Declassified and Approved For Release 2013/02/27 : CIA-RDP10-02196R000300110005-5

Declassified and Approved For Release 2013/02/27 : CIA-RDP10-02196R000300110005-5

This contradicts the conclusion of G. N. Flerov's group (JINR), who observed the reaction products of complete fission of an accelerated xenon ion with tantalum nucleus with the formation of a composite nucleus having Z = 127. Estimates show that in this case the cross section of formation of the composite nucleus reaches 100 mb. In the paper by the author of the present note the preliminary results on the synthesis of extra-heavy elements (Z = 110-114) during the irradiation of uranium by xenon ions accelerated in tandem-cyclotron were also communicated. Using an original technique the scientists of the JINR observed the effect of spontaneous fission in the products of interaction of uranium and xenon. This effect requires a careful and detailed investigation.

The experimental and theoretical studies of the mechanism of interaction of high energy protons and relativistic nuclei with nuclei took an important place in the program of the conference.

American physicists have at their disposal beams of accelerated ions N^{14} (29 GeV) and (from June of this year) O^{16} (35 GeV) with intensity of 10^4-10^5 ions/pulse. The papers by V. Katkoff (Brookhaven) and I. Price (Berkeley) presented the experimental results of the measurement of the cross sections of double and triple fission of uranium, bismuth, gold, and silver nuclei under the action of accelerated nitrogen ions, and also the data on angular and energy distributions of the fragments (from carbon to iron) formed during the interaction of N^{14} ions (29 GeV) with uranium and gold nucleii.

The production of beams of relativistic ions was stimulated by the development of the models of interaction of nuclei with nuclei. Two papers (H. Bertini, Oak Ridge and V. D. Toneev, JINR, USSR) were devoted to this. The theoretical bases of both models are similar, but their concrete realization is most developed in the investigations of the staff of JINR. The class of characteristics of nuclear reactions, which can be computed by the JINR model, is considerably wider.

Among the theoretical papers mention should be made of the paper by V. Grainer (FRG) devoted to atomic phenomena in the collision of heavy ions. I. Ya. Pomeranchuk, A. I. Akhiezer, and V. B. Berestetskii were among the first who paid attention to such processes. J. Heising (Rochester University) discussed in the framework of statistical mechanics a general approach to the computation of the density of the levels of an excited nucleus $\rho(E)$. Taking many nuclear models he demonstrated the effect of the structure of single-particle spectrum on $\rho(E)$.

A lively interest was aroused by the review papers by G. Temmer (USA) on the measurement of short life times of excited states (10^{-12}-10^{-18} sec) by different methods and by H. Britt (Los Alamos) on the parameters of fission barrier from the analysis of data on the isomers of form and the results of fission in direct reactions. The phenomenon of isomers of form of nuclei was discovered at JINR in 1962 and its theoretical interpretation in the framework of a double-humped barrier was given in the works of V. M. Strutinskii (USSR).

The main part of the results presented on the fission theory is already published and well known to Soviet specialists. Theoretical investigations in this direction are being carried out extensively in the Soviet Union. The achievements of V. M. Strutinskii, V. V. Pashkevich, and Yu. A. Muzychka were acknowledged in the papers and during their discussions.

Declassified and Approved For Release 2013/02/27 : CIA-RDP10-02196R000300110005-5

Declassified and Approved For Release 2013/02/27 : CIA-RDP10-02196R000300110005-5

INTERNATIONAL SYMPOSIUM ON NUCLEAR STATES WITH HIGH SPIN

N. I. Pyatov

An international symposium on nuclear states with high spin was held in Stockholm from May 30 to June 3, 1972. The symposium was organized by the Institute of Physical Research. More than 130 scientists from 20 countries participated in it. Over 60 review papers and original communications, dealing with the problems of rotational motion in atomic nuclei, the properties of isomer states, nuclear moments, gigantic resonances, and polarization effects, were presented.

A considerable number of the papers were devoted to the discussion of the anomalous behavior of the moment of inertia of in even–even atomic nuclei, which was recently detected during the excitation of "long" rotational bands in reactions with heavy ions. For example, in rare earth nuclei with the values of the spin equal to 12-14 a sharp increase of the moment of inertia is observed as a function of the angular frequency of rotation; sometimes the growth is so rapid that in fact the angular frequency even decreases somewhat during the growth of the angular moment [1]. The most interesting experimental data were presented in the papers by A. Ionson (Sweden), R. Lider (FRG), and A. Sunyar (USA). In particular, A. Sunyar communicated the observation of rotational states with spin I = 20.22 in Dy^{158}, Er^{162}, and Hf^{170} nuclei.

Three possible reasons for the anomalous behavior of the moment of inertia were discussed: 1) a sharp change of the deformation of the nucleus; 2) a phase transition caused by the disruption of paired correlations for large angular moments; 3) the effect of decoupling when for large angular moments the scheme of coupling changes sharply for two or more nucleons (replacement of strong coupling by weak).

The theoretical investigations related to the first hypothesis are mainly of phenomenological nature and usually represent different modifications of the model with a variable moment of inertia or of Harris formula. Among these investigations the attempt of P. Tiberger (USA) to reconstruct the form of the potential energy as a function of the moment of inertia from the experimental energies of the rotational states is interesting. It was found that even a small departure of the behavior of the potential energy from the parabolic curve leads to an appreciable change of the moment of inertia as a function of the angular frequency of rotation. In the paper by Walborn (Sweden) a method was put forward for the description of the energies of the rotational states right up to high values of the spin with the use of polynomial expansion for the moment of inertia as a function of the angular moment (three-four parameters are usually used). The limitation of the phenomenological approaches is due to both the absence of a clear physical dynamics of the process of rotation and the impossibility (or highly vague possibility) of obtaining specific theoretical predictions.

The second hypothesis was developed in the framework of microscopic approaches in the papers by R. Sorensen (USA), K. Kumar (USA), Z. Shimanskii (Poland), and others. Using different mathematical methods the authors investigate the effect of phase transition of the nucleus from superfluidized state to the normal state for the value of the moment of inertia. At the point of the phase transition all the models predict a sharp jump of the moment of inertia, which is in qualitative agreement with the empirical results. The main difficulty of such an approach is the need for an accurate investigation of paired correlations near the point of phase transition. K. Kumar showed also that it is very important to investigate simultaneously the changes of the energy gap as well as the deformation of the nucleus. His computations for Dy^{160} nucleus showed that the deformation increases slowly up to a spin I = 16 (centrifugal stretching of the nucleus) and later decreases sharply during the phase transition. The root mean square radius decreases abruptly at the same time.

Translated from Atomnaya Énergiya, Vol. 33, No. 5, pp. 942-943, November, 1972.

© 1973 Consultants Bureau, a division of Plenum Publishing Corporation, 227 West 17th Street, New York, N. Y. 10011. All rights reserved. This article cannot be reproduced for any purpose whatsoever without permission of the publisher. A copy of this article is available from the publisher for $15.00.

Declassified and Approved For Release 2013/02/27 : CIA-RDP10-02196R000300110005-5

Declassified and Approved For Release 2013/02/27 : CIA-RDP10-02196R000300110005-5

An alternative model (third hypothesis) was put forward in the paper by F. Stevens (USA). Here the anomalous behavior of the moment of inertia is related to coriolis interaction of two rotational bands, the bands of the ground state and those of some two-quasiparticle excited state, in which the quasiparticles are weakly coupled with the frame. Physically such "decoupling" can occur at large angular moments ($I \approx 10$-12) [2]. We note that the behavior of the moment of inertia at large spins and the phase transitions in nuclei were earlier investigated by soviet scientists Yu. T. Grin and A. I. Larkin [3].

All the investigated hypotheses, qualitatively describing the energetics of the rotational bands, generally lead to different predictions of the values of the mean square radius, the magnetic moment, and the transition probabilities in the band for high values of spin; this opens up a wide range of possibilities for experimental verification.

For odd atomic nuclei also by now a large amount of experimental information on rotational states with large angular moment has accumulated. A review of these data was presented in the papers by S. Hors and T. Lindblad (Sweden), R. Diamond (USA), and Zh. Taglaferi (Italy). A phenomenological description of odd nuclei is often not possible because of strong nonadiabatic effects caused by the coupling of odd nucleon with the rotation and internal motion of the even–even frame. The theoretical problems of the description of the properties of the rotational states in odd nuclei were discussed in these papers and also in the paper by the author of the present article.

The review paper by L. Grodzins (Denmark) was of considerable interest; the possibilities of investigation of atomic nuclei with the use of heavy ion accelerator were investigated in it. It was noted that Coulomb excitation can be effectively used for the investigation of nuclear states with high spin, since the role of inelastic channels increases sharply with the increase of the mass of the charged ions. The use of very heavy ions permits to widen the range of life time of the excited states that can be measured by the Doppler shift method. New possibilities for the measurement of the charge density distribution and the multipole moments of the nuclei have been opened up. In reactions with heavy ions large superfine elemental fields appear in nuclei due to the ionization of the inner shells. This can be used for the investigation of magnetic moments of nuclei in excited states. Thus a magnetic field intensity of 10^{11} G permits to measure the magnetic moment of a nuclear state with life time of the order of a nsec.

The properties of spherical, almost-magical nuclei, and nuclei of transitional regions were discussed in the papers by G. Holm (Sweden), Z. Syuikovskii (Poland), T. Sujihara (USA), J. Verve (Belgium), F. Stari (JINR), K. Maier (FRG), and others. Here a large amount of experimental information has accumulated, whose description apparently requires considerable development of the existing nuclear models.

The papers of D. Ward (Canada), B. Bochev (JINR), and V. Andreichev (GDR) were devoted to the measurement of lifetimes of nuclear states and to their systematization.

The investigations of resonance states of nuclei and the effective charges connected with them were presented in the papers by I. Hamamoto (FRG), G. Astner (Sweden), Ya. Blomkvist (Sweden), T. Yamazaki (Japan), and T. Walcher (FRG). In the last paper the author communicated the observation of gigantic M1- and E2-resonances with energies of 8.7 and 12 MeV respectively in the process of inelastic backscattering of electrons in Ce, La, and Pr nuclei. Estimates of radiational and total widths of the resonance states were given.

The problems of polarizability of atomic nuclei and elementary particles were discussed by T. Erickson (CERN). The corresponding experimental data, obtained in the investigation of exotic atoms (atoms with displaced adrons in them or muon atoms) were presented by J. Backenshtoss (CERN), H. Bakke (FRG), and R. Engfer (CERN).

In the concluding session papers were presented by K. Kankeleit (FRG) on the construction of a new heavy ion accelerator in Darmstadt and by R. Diamond (USA) on the reconstruction of the heavy ion accelerator in Berkeley.

The symposium showed that reactions with heavy ions permit obtaining a wide and at the same time unique information on the structure of atomic nuclei; a significant growth of the volume and the quality of this information may be expected in the next few years. On the theoretical side the attention was mainly concentrated on the fundamental problem of microscopic description of rotation of atomic nuclei that would be valid for all angular moments.

Declassified and Approved For Release 2013/02/27 : CIA-RDP10-02196R000300110005-5

Declassified and Approved For Release 2013/02/27 : CIA-RDP10-02196R000300110005-5

The excellent and clear organization of the symposium was also worthy of note, which to a large extent led to its success.

LITERATURE CITED

1. A. Johnson et al., Nucl. Phys., A179, 753 (1972).
2. F. Stephens and R. Simon, Nucl. Phys., A183, 257 (1972).
3. Yu. T. Grin and A. I. Larkin, Yad. Fizika, 2, 40 (1965).

Declassified and Approved For Release 2013/02/27 : CIA-RDP10-02196R000300110005-5

Declassified and Approved For Release 2013/02/27 : CIA-RDP10-02196R000300110005-5

IV INTERNATIONAL CONFERENCE ON CRYOGENIC TECHNOLOGY

L. B. Golovanov

The IV International Conference on Cryogenic Technology was held in Eindhoven (Netherlands) at the end of May, 1972. These conferences are held once every two years; the first three were held in Japan, England, and West Berlin. About 400 specialists from over 30 countries took part in the conference. Over 100 papers covering all principal directions of development of cryogenic technology were presented. A large part of the papers was devoted to the investigation of different types of refrigerators, superconductivity, transmission of electric power over cryogenic cables, heat transfer under different conditions, cryogenic pumping, and properties of materials at low temperatures.

A refrigerator without moving parts (for low temperatures) capable of maintaining temperature at 90-100° K, developed by the Aerlikid firm (France), is worth noting. It operates on a gaseous mixture consisting of butane, ethane, methane, and nitrogen. The regenerator is made from tubes filled with metallic balls separated longitudinally by particles of an insulating material. The low power efficiency of this equipment (1-2 kW must be spent for obtaining 10 W at 100° K) is compensated for by its simplicity and reliability of operation. At present the firm is investigating the possibility of using such refrigerators in the traps of vacuum pumps and the cooling systems of infrared detectors.

In the case of large consumption of helium a problem connected with the recharging of the gas returning along the tubes appears. The Linde firm (Munich) has developed a helium liquefier which can operate for more than 120 h for 20% mixture of air. The output of the equipment is 24 liter/h.

A promising direction in liquefying technology is the development of refrigerators, in which ejectors are used as expansion device. The use of such liquefiers is especially advantageous at temperatures of 4.2 and 1.8° K. The papers of V. M. Brodyanskii, A. V. Martynov, A. I. Ageev (USSR), and J. Mulder (Netherlands) were devoted to cooling cycles with ejectors. In the first paper processes occurring in the ejector are analyzed and experimental dependences of the adiabatic indices on pressure and temperature are given, which can serve as the basis for the computation of cryogenic ejectors; in the second paper it is shown, in particular, that the ejector can be effectively used for obtaining temperature of 1.8° K, if the gas pressure behind it is lowered to 30 mm Hg.

A number of papers were devoted to the use of superconducting systems in accelerators and separators of elementary particles. At present a 60 MeV proton accelerator with a superconducting magnet is being set up in Karlsruhe (FRG); it is a prototype of a large accelerator. Cryogenic tests of the first four-meter section have been conducted at T = 1.8° K. A project of cryogenic systems for a 20 m long 1 mA and 60 MeV superconducting linear accelerator and a particle separator for CERN was also mentioned. The preliminary tests of the latter are to be conducted in Karlsruhe. The Linde firm (Munich) has made and tested a cryostat 4000 mm long and 600 mm in diameter, in which the separator of elementary particles with superconducting magnetic system will be placed. A 300 W refrigerator at T = 1.8° K will provide cooling. The difficulties appearing in the construction and testing of the cryostat are described in detail in the paper.

The paper by V. P. Peshkov (USSR) on obtaining extra-low temperatures in solution cryostats, presented at the plenary session, was paid considerable attention. The heat exchange in different parts of the equipment and other important problems pertaining to the attainment of extra-low temperatures and their measurements were discussed in detail in this paper. A special section was devoted to this system; in particular, the use of a solution cryostat for dynamic polarization of nuclei was communicated in this section.

Translated from Atomnaya Énergiya, Vol. 33, No. 5, pp. 943-944, November, 1972.

© 1973 Consultants Bureau, a division of Plenum Publishing Corporation, 227 West 17th Street, New York, N. Y. 10011. All rights reserved. This article cannot be reproduced for any purpose whatsoever without permission of the publisher. A copy of this article is available from the publisher for $15.00.

Declassified and Approved For Release 2013/02/27 : CIA-RDP10-02196R000300110005-5

Declassified and Approved For Release 2013/02/27 : CIA-RDP10-02196R000300110005-5

A large number of papers were connected with the investigation of superconducting materials and the use of superconductivity in technology. One of the main directions in the study of superconductivity is the investigation of losses in the conductors with alternating current and the development of cables with small losses for operation in variable fields. In this connection it is interesting to note the work done by the staff of the Imperial Metal Industries jointly with the Rutherford Laboratory. A cable has been made which has 13,255 separate wires of a superconducting material embedded into a matrix. The thickness of each wire is 5-10 μ. This cable is intended for the production of a variable magnetic field whose growth and decay occur in a period of a few seconds. The losses in this cable are insignificant. Interesting work on the use of superconducting systems in railroad transport has been done in Japan. A wagon with natural size for several passengers has already been constructed, which is held above the ground with the use of a magnetic field produced by a superconducting system.

The participants of the conference were offered the opportunity of visiting some cryogenic laboratories of the Philips firm. One of the innovations demonstrated by the firm was a refrigerator for obtaining a cold environment to the level of 20° K using a thermoadsorption compressor.

An exhibition of cryogenic equipment and instruments made by different foreign firms was organized in the building of Eindhoven Technological University, where the conference was held.

The proceedings of the conference will be published at the end of 1972.

Declassified and Approved For Release 2013/02/27 : CIA-RDP10-02196R000300110005-5

Declassified and Approved For Release 2013/02/27 : CIA-RDP10-02196R000300110005-5

breaking the language barrier

WITH COVER-TO-COVER ENGLISH TRANSLATIONS OF SOVIET JOURNALS

in mathematics and information science

Title	# of Issues	Subscription Price
Algebra and Logic *Algebra i logika*	6	$110.00
Automation and Remote Control *Avtomatika i telemekhanika*	24	$185.00
Cybernetics *Kibernetika*	6	$125.00
Differential Equations *Differentsial'nye uravneniya*	12	$150.00
Functional Analysis and Its Applications *Funktsional'nyi analiz i ego prilozheniya*	4	$ 95.00
Journal of Soviet Mathematics	6	$135.00
Mathematical Notes *Matematicheskie zametki*	12 (2 vols./yr. 6 issues ea.)	$175.00
Problems of Information Transmission *Problemy peredachi informatsii*	4	$100.00
Siberian Mathematical Journal of the Academy of Sciences of the USSR Novosibirski *Sibirskii matematicheskii zhurnal*	6	$185.00
Theoretical and Mathematical Physics *Teoreticheskaya i matematicheskaya fizika*	12 (4 vols./yr. 3 issues ea.)	$125.00
Ukrainian Mathematical Journal *Ukrainskii matematicheskii zhurnal*	6	$135.00

Back volumes are available.
For further information, please contact the Publishers.

SEND FOR YOUR FREE EXAMINATION COPIES

PLENUM PUBLISHING CORPORATION
Plenum Press • Consultants Bureau
• IFI/Plenum Data Corporation
227 WEST 17th STREET
NEW YORK, N. Y. 10011

In United Kingdom
Plenum Publishing Co. Ltd., Davis House (4th Floor)
8 Scrubs Lane, Harlesden, NW10 6SE, England

Declassified and Approved For Release 2013/02/27 : CIA-RDP10-02196R000300110005-5

Declassified and Approved For Release 2013/02/27 : CIA-RDP10-02196R000300110005-5

breaking the language barrier

WITH COVER-TO-COVER ENGLISH TRANSLATIONS OF SOVIET JOURNALS

in physics

Title	# of Issues	Subscription Price
Astrophysics *Astrofizika*	4	$100.00
Fluid Dynamics *Izvestiya Akademii Nauk SSSR mekhanika zhidkosti i gaza*	6	$160.00
High-Energy Chemistry *Khimiya vysokikh énergii*	6	$135.00
High Temperature *Teplofizika vysokikh temperatur*	6	$125.00
Journal of Applied Mechanics and Technical Physics *Zhurnal prikladnoi mekhaniki i tekhnicheskoi fiziki*	6	$150.00
Journal of Engineering Physics *Inzhenerno-fizicheskii zhurnal*	12 (2 vols./yr. 6 issues ea.)	$150.00
Magnetohydrodynamics *Magnitnaya gidrodinamika*	4	$100.00
Mathematical Notes *Matematicheskie zametki*	12 (2 vols./yr. 6 issues ea.)	$175.00
Polymer Mechanics *Mekhanika polimerov*	6	$120.00
Radiophysics and Quantum Electronics (Formerly Soviet Radiophysics) *Izvestiya VUZ. radiofizika*	12	$160.00
Solar System Research *Astronomicheskii vestnik*	4	$ 75.00
Soviet Applied Mechanics *Prikladnaya mekhanika*	12	$160.00
Soviet Atomic Energy *Atomnaya énergiya*	12 (2 vols./yr. 6 issues ea.)	$150.00
Soviet Physics Journal *Izvestiya VUZ. fizika*	12	$160.00
Soviet Radiochemistry *Radiokhimiya*	6	$145.00
Theoretical and Mathematical Physics *Teoreticheskaya i matematicheskaya fizika*	12 (4 vols./yr. 3 issues ea.)	$125.00

Back volumes are available. For further information, please contact the Publishers.

SEND FOR YOUR FREE EXAMINATION COPIES

PLENUM PUBLISHING CORPORATION
227 WEST 17th STREET
NEW YORK, N. Y. 10011
Plenum Press • Consultants Bureau
• IFI/Plenum Data Corporation

In United Kingdom,
Plenum Publishing Co. Ltd., Davis House (4th Floor)
8 Scrubs Lane, Harlesden, NW10 6SE, England

Declassified and Approved For Release 2013/02/27 : CIA-RDP10-02196R000300110005-5